UNIVERSITY OF NAPLES FEDERICO II

DEPARTMENT OF PHARMACY

SCHOOL OF MEDICINE AND SURGERY

Ph.D. THESIS IN

PHARMACEUTICAL SCIENCES

XXXIV CYCLE

ROLE OF THE ENDOCANNABINOIDOME – GUT MICROBIOME AXIS IN THE DEVELOPMENT OF INFLAMMATORY BOWEL DISEASE AND COLORECTAL CANCER

Tommaso Venneri

TUTOR:

PROF. FRANCESCA BORRELLI

COORDINATOR:

PROF. MARIA V. D'AURIA

A.Y. 2018-2022

Ai miei nonni

e alle mie nonne

TABLE OF CONTENTS

ABSTRACT

Background and aim: Inflammatory bowel disease (IBD) and colorectal cancer (CRC) are the two most important pathologies of the gastrointestinal tract. They affect millions of people around the world, with a higher incidence and prevalence in developed countries, and their prevention and treatment represent a global health concern. The recently discovered endocannabinoidome is a diverse and complex system of lipid mediators and their receptors and enzymes that has been reported to play a role in various physio-pathological processes such as inflammation, immune responses, and energy metabolism. The gut microbiota, which contains trillions of different microorganisms, plays a key role in gut immune homeostasis, and recent evidence suggests that an imbalance in its composition is involved in the onset and development of IBD and CRC. The endocannabinoidome (eCBome) and the microbiome (miBIome) are closely related and are thought to form the eCBome – miBIome axis. In this thesis, by modulating either the eCBome or the miBIome, we explore the possible role of this axis in the development of colon inflammation and tumorigenesis.

Materials and methods: We investigated the effect of the eCBome – miBIome axis on IBD and CRC, using receptor ligands, enzymatic inhibitors, genetic deletion of receptors and depletion of gut microbiota in chemically induced models of IBD and CRC. Firstly, we examined the effect of cannabidivarin, an agonist of TRPA1 (ion channel belonging to the eCBome) administered via oral gavage or intraperitoneal injection, either with or without a selective TRPA1 antagonist, in both DNBS- and DSS-induced models of IBD measuring inflammatory parameters, such as colon weight/colon length *ratio*, histological damage, myeloperoxidase (MPO) activity, intestinal permeability, inflammatory cytokines levels, TRPA1 expression levels and gut microbiota composition; in addition, we investigated the effect of CBDV treatment in biopsies from UC paediatric patients on IL-1β production.

Secondly, we investigated the synergistic effect of cannabidiol, an inhibitor of FAAH (a serine hydrolase responsible for the degradation of some eCBome mediators), and fish oil (FO, which contains n-3 PUFAs) administered by oral gavage in the DNBS- and DSS-induced ulcerative colitis models, measuring colon weight/colon length *ratio*, anxiety-like behaviour, disease activity index (DAI) score, MPO activity, intestinal permeability, inflammatory cytokines levels, gut microbiota composition and eCBome lipid mediator content.

Thirdly, we investigated the impact of genetic deletion of Trpm8 (member of the TRPs channel family belonging to eCBome) on colon carcinogenesis and associated changes in gut microbiota composition.

Finally, we investigated the effects of altering the gut microbiota using antibiotics or germfree conditions in the DNBS-induced models of IBD by assessing inflammatory parameters in the colon (colon weight/colon length *ratio*, DAI score, inflammatory cytokines, MPO activity) and associated changes in eCBome lipid mediator levels.

Results: Oral administration of cannabidivarin by gavage counteracted intestinal inflammation by reducing, in a TRPA1 dependent manner, signs of colitis induced by DNBS or DSS administration, such as colon weight/colon length *ratio*, MPO activity, intestinal permeability, histological damage and inflammatory cytokine production. It also alters the profile of the gut microbiota and reduces IL-1β in biopsies from paediatric patients with colitis.

Co-administration of per se inactive doses of FO and CBD produced anti-inflammatory effects in DSS-treated mice by decreasing colon weight/colon length *ratio*, MPO activity, DAI score, intestinal permeability, histological damage and inflammatory cytokines production increased by DSS. In contrast, no effect was observed on anxiety-like behaviour induced by DSS. An altered composition of the gut microbiota was demonstrated. The anti-inflammatory effect of co-administration of FO and CBD was also confirmed in the DNBS-

induced model. The synergistic effect was neither due to an increase in CBD bioavailability by FO nor to a change in eCBome mediator levels.

Mice with a genetic deletion of Trpm8 showed a lower susceptibility to colon cancer development. Deletion of Trpm8 alters the composition of the gut microbiota in both healthy and AOM-treated mice; in AOM treated mice, the deletion of Trpm8 increases the abundance of CRC-protecting families, such as *Ruminococcaceae*, *Lachnospiraceae* and *Lactobacillaceae*, while reducing the abundance of CRC-related families, such as *Burkholderiaceae*.

Finally, germfree conditions, but not antibiotic treatment, affected inflammatory parameters in DNBS-induced colitis by reducing colon weight/colon length *ratio* and the expression of inflammatory cytokines. This effect was accompanied by changes in eCBome mediators involved in inflammation, such as oleoylethanolamide, linoleoylethanolamide and docosahexaenoylethanolamide.

Conclusions: In conclusion, by studying the eCBome – miBIome axis in experimental colitis and colon cancer, we highlight the crucial role of this axis in the development of IBD and CRC and propose it as an innovative target for the treatment of these diseases.

List of abbreviations and acronyms

13-HODE	13-hydroxyoctadecadienoic acid
15-LOX	15-lipoxygenase
2-AG	2-arachidonoylglycerol
5-FU	5-fluorouracil
AA	Arachidonic acid
ABX	Antibiotic
ACF	Aberrant crypt foci
AEA	Anandamide or N-arachidonoylethanolamide
ANOVA	Analysis of variance
AOM	Azoxymethane
CAC	Colitis-associated colorectal cancer
CB_1	Cannabinoid receptor 1
CB_2	Cannabinoid receptor 2
CBC	Cannabichromene
CBD	Cannabidiol
CBDV	Cannabidivarin
CBG	Cannabigerol
CBN	Cannabinol
CBRs	Cannabinoid receptors
CD	Crohn's disease
CMC	Carboxymethylcellulose
CNS	Central nervous system
COX2	Cyclooxygenase 2
CR	Conventionally raised
CRC	Colorectal cancer
CSS	Cumulative sum scaled
DAGL	Diacylglycerol lipase
DAI	Disease activity index score
DHEA	Docosahexaenolylethanolamide
DSS	Dextran sulphate sodium salt

eCBome	Endocannabinoidome
eCBs	Endocannabinoids
eCBS	Endocannabinoid system
EGFR	Epidermal growth factor receptor
ELISA	Enzyme-linked immunosorbent assay
ETBF	*Enterobacteroides fragilis*
FAP	Familial adenomatous polyposis
FBS	Fetal bovine serum
FITC	Fluorescein isothiocyanate
FO	Fish oil
GF	Germfree
GM	Gut microbiota
GPCRs	G-protein coupled receptors
GPR110	G-protein coupled receptor 110
GPR119	G-protein coupled receptor 119
GPR18	G-protein coupled receptor 18
GPR55	G-protein coupled receptor 55
HPLC	High performance liquid chromatography
HPRT	Hypoxanthine-guanine phosphoribosyltransferase
IBD	Inflammatory bowel disease
IFNγ	Interferon γ
IL-10	Interleukin 10
IL-1β	Interleukin 1β
IL-6	Interleukin 6
IT-TOF	Ion trap time of flight mass spectrometry
LEA	Linoleoylethanolamide
MAGL	Monoacylglycerol lipase
mBIome	Microbiome
MCP-1	monocyte chemoattractant protein 1
MPO	Myeloperoxidase
NAEs	N-acylethanolamines
NAPE	N-arachidonoyl phosphatidylethanolamine

NAPE-PLD	N-arachidonoyl phosphatidylethanolamine Phospholipase D
N-ArPE	N-arachidonoylethanolamine
NAT	N-acyltransferase
NOR	Novel object recognition
OEA	Oleoylethanolamide
OTUs	Operational taxonomic units
PBS	Phosphate buffered saline solution
PCoA	Principal coordinate analysis
PE	Phosphatidylethanolamine
PEA	Palmitoylethanolamide
PI	Phosphatidylinositol
PLC	Phospholipase C
PPARα	peroxisome proliferator-activated receptor α
PPARγ	peroxisome proliferator-activated receptor γ
PUFAs	Polyunsaturated fatty acids
qPCR	Quantitative polymerase chain reaction
ROS	Reactive oxygens species
SCFAs	Short chain fatty acids
SEM	Standard error of mean
TGFβ	Transforming growth factor β
THCV	Tetrahydrocannabivarin
TNFα	Tumour necrosis factor α
TRPA1	Transient receptor potential ankyrin type 1
TRPM8	Transient receptor potential melastatin type 8
TRPs	Transient receptor potential channels
TRPV1	Transient receptor potential vanilloid type 1
TRPV2	Transient receptor potential vanilloid type 2
UC	Ulcerative colitis
VEGF	Vascular endothelial growth factor
Δ^9-THC	Δ^9-tetrahydrocannabinol

Chemical names

DNBS	2,4-dinitrobenzensulfonic acid
HC030031	2-(1,3-dimethyl-2,6-dioxo-1,2,3,6-tetrahydro-7H-purin-7-yl)-N-(4-isopropylphenyl)acetamide
HTAB	hexadecyltrimethylammonium bromide
MOPS	3-(N-morpholino)propanesulfonic acid

INTRODUCTION

1. The endocannabinoid system

1.1 Cannabis and phytocannabinoids

The plant *Cannabis sativa* is considered one of the oldest sources of textile fibre (ElSohly et al., 2017); it was used as a medicinal plant in ancient China as early as the sixth century BC, but its use in European medicine was not established until much later, in the 19th century.

The effects of *Cannabis sativa* have long been known, with its resin being used extensively in India as a medicine. Numerous efforts have been made to identify the active components of *Cannabis sativa* (Mechoulam, 2000). To date, at least 500 phytochemicals have been isolated from the plant, of which more than one hundred are terpenophenolic compounds known as phytocannabinoids (Izzo et al., 2009; Gulck and Moller, 2020). The first phytocannabinoid isolated from *C. sativa* was cannabinol (CBN) from a red oil extract produced in the late 19th century. Its structure was elucidated by R.S. Cahn in the early 1930s and its chemical synthesis was achieved in 1940. Cannabidiol (CBD; Figure 1) was isolated from *Cannabis* by Adams and colleagues in 1940, while Δ^9-tetrahydrocannabinol (Δ^9-THC) was extracted by Wollner, Matchett, Levine and Loewe in 1942. The structures and stereochemistry of CBD and Δ^9-THC were elucidated by Raphael Mechoulam in 1963 and 1964, respectively, and both compounds were synthesised in Mechoulam's laboratory in 1965 (Pertwee, 2006).

Chemically, these compounds are meroterpenoids with a resorcinyl core, usually with a para-isoprenyl, -alkyl or -aralkyl substituent. They occur naturally in plants such as *C. sativa*, the best known and best studied plant, but not the only one capable of producing phytocannabinoids; indeed, several *Rhododendron* species, *Helichrysum umbraculigerum* Less. (*Asteraceae*), the edible roots of

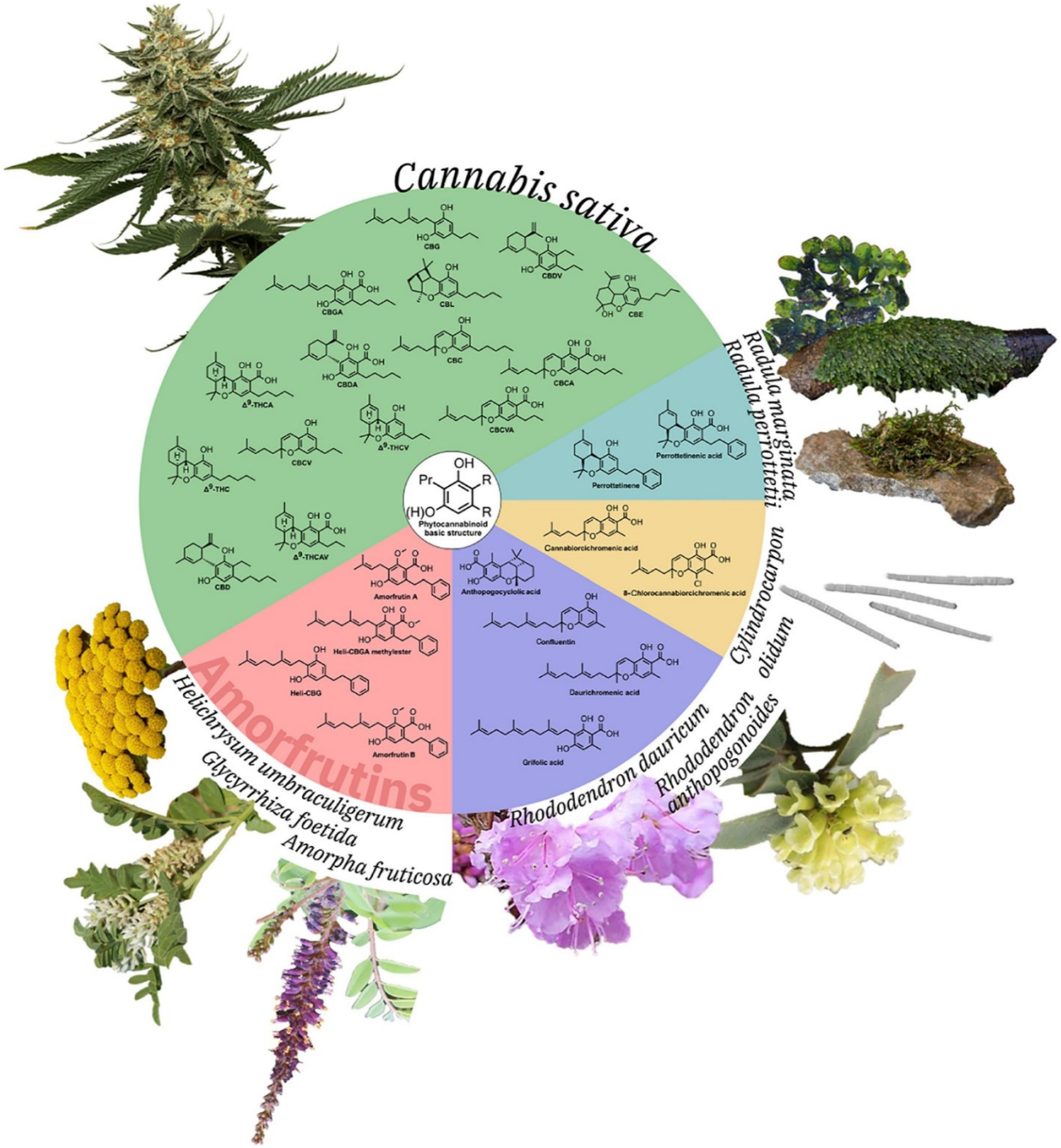

Figure 1. Pytocannabinoids: structures and natural sources (Gulck and Moller, 2020)
Abbreviations: CBC, cannabichromene; CBCA, cannabichromenic acid; CBCV, cannabichromevarine; CBCVA, cannabichromevarinic acid; CBD, cannabidiol; CBDA, cannabidiolic acid; CBDV, cannabidivarine; CBE, cannabielsoin; CBG, cannabigerol; CBGA, cannabigerolic acid; CBL, cannabicyclol; Δ^9-THC, Δ^9-tetrahydrocannabinol; Δ^9-THCA, Δ^9-tetrahydrocannabinolic acid; Δ^9-THCAV, Δ^9-tetrahydrocannabivarinic acid; Δ^9-THCV, Δ^9-tetrahydrocannabivarine.

Glycyrrhiza foetida Desf. (*Fabaceae*), *Radula perrottetii* and *R. marginata* (*Radulaceae*), *Cylindrocarpon olidum* (*Nectriaceae*) and *Amorpha fruticosa* L. (*Fabaceae*) are able to produce compounds with a cannabinoid backbone (Figure 1).

Based on their chemical structure, they differ into cannabigerol (CBG), cannabichromene (CBC), cannabidiol (CBD), Δ^9-trans-tetrahydrocannabinol (Δ^9-THC), Δ^8-trans-tetrahydrocannabinol (Δ^8-THC), cannabicyclol (CBL), cannabielsoin (CBE), cannabinol (CBN), cannabinodiol (CBND), cannabitriol (CBT); in the plant *C. sativa*. the most abundant pythocannabinoids are trans-Δ^9-THC, CBD, CBC, and CBG (Elsohly and Slade, 2005; Gulck and Moller, 2020). These compounds are present in *Cannabis* mainly as acids that are decarboxylated when the plant is dried.

Since the discovery of the Δ^9-THC structure, research into the pharmacology of cannabinoids has increased significantly, largely due to the recreational use of *Cannabis* in the UK and other Western countries. Preclinical and clinical studies, focusing mainly on the psychoactive properties of *Cannabis* rather than its therapeutic uses, showed that Δ^9-THC is the main contributor to the psychotropic properties of the plant (Pertwee, 2006). By contrast, CBD, CBG, CBC, CBDV are non-euphoric cannabinoids.

1.2 Cannabinoid receptors

As phytocannabinoids are highly lipophilic molecules, it was initially assumed that these compounds exert their various biological effects through non-specific disruption of cell membranes (Zou and Kumar, 2018). Later, the existence of a specific receptor was proposed, as the pharmacological activity of psychotropic cannabinoids was significantly influenced by chemical structure and stereoselectivity due to the presence of chiral centres (Howlett et al., 2002). In the mid-1980s, the discovery of the ability of phytocannabinoids to act via a $G_{i/0}$ protein to inhibit adenylate cyclase (Howlett and Fleming, 1984) and the

presence of high-affinity binding sites for cannabinoids in rat brain membranes (Johnson et al., 1988) provided definitive evidence for the existence of cannabinoid receptors. Further confirmation of the existence of this receptor came in 1990 with the cloning of cannabinoid receptor-1 (CB_1) first in the rat (Matsuda et al., 1990) and then in humans (Gerard et al., 1991) and cannabinoid receptor-2 (CB_2) in 1993 (Munro et al., 1993).

Both CB_1 and CB_2 receptors are G protein-coupled receptors (GPCRs) that contain seven transmembrane spanning domains (Figure 2). Activation of these receptors inhibits adenylyl cyclase activity, inhibits various calcium channels, activates potassium influx, reduces cell excitability and alters responses to various neurotransmitters by reducing their release.

CB_1 was first discovered in the brain and is highly expressed in most regions of the central nervous system (CNS) (Zou and Kumar, 2018). In particular, CB_1 is strongly expressed in the cerebral cortex, basal ganglia, periaqueductal grey, hypothalamus, amygdala and cerebellum (Herkenham et al., 1991). As expected, CB_1 receptor expression is low in brain regions not affected by cannabinoids, such as the respiratory centres of the medulla, but high in the medullary nuclei of the brainstem, where it acts in the primary integrative centres for the cardiovascular system and vomiting (nucleus of the solitary tract and area postrema, respectively) (Haspula and Clark, 2020). CB_1 is moderately expressed in the spinal cord; here, it regulates nociception of afferent nerve fibres such as the trigeminal ganglion, dorsal root ganglion and dermic nerve terminals of primary sensory neurons (Zou and Kumar, 2018).

Neuroanatomical studies have found that CB_1 is mainly expressed in presynaptic terminals of different neuronal circuits (GABAergic, glutamatergic, dopaminergic, cholinergic, noradrenergic and serotonergic neurons), where it mediates retrograde signaling of endocannabinoids (the endogenous ligand for CB receptors, see next) (Zou and Kumar, 2018; Haspula and Clark, 2020).

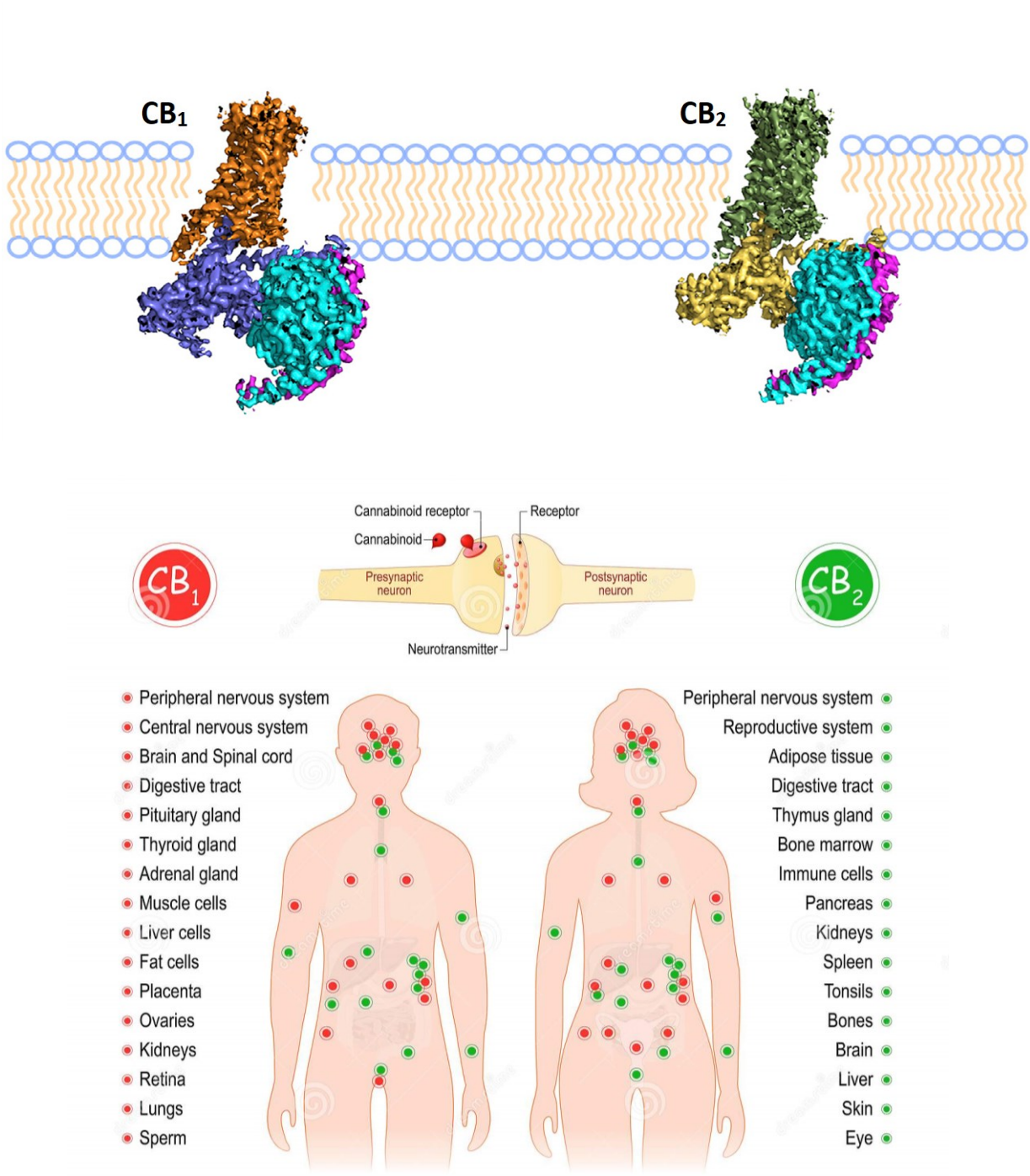

Figure 2. Cannabinoid receptors: structure (Hua et al., 2020) and locations (An et al., 2020)
Abbreviations: CB_1, cannabinoid receptor-1; CB_2, cannabinoid receptor-2.

CB_1 is also abundantly expressed in the peripheral nervous system (PNS) as well as in peripheral tissues in a region-specific manner; CB_1 receptor expression has been found in fat (adipocytes), liver, pancreas and skeletal muscle (Mackie, 2008). CB_1 is also expressed in the enteric nervous system and in non-neuronal cells of the intestinal mucosa, including enteroendocrine cells, immune cells and enterocytes; here, CB_1 modulates gastrointestinal tract mobility, secretion and permeability (Izzo and Sharkey, 2010).

In contrast, CB_2 receptor expression in the CNS is very low under physiological conditions, although neuroinflammatory conditions have been shown to lead to upregulation of CB_2 in glial cells. CB_2 is mainly expressed in immune cells and lymphoid tissue; indeed, high levels of CB_2 are found in cells involved in both innate and adaptive immune responses, such as spleen, thymus and peripheral blood mononuclear cells (Haspula and Clark, 2020).

1.3 Endocannabinoids

After the successful discovery of cannabinoid receptors (CBRs), questions have arisen regarding endogenous cannabinoids-like substances capable of binding CBRs at the same site as Δ^9-THC. This led to the discovery of the first endocannabinoid (eCB) N-arachidonoylethanolamide (AEA), or "anandamide", from the Sanskrit word "*ānanda*", literally meaning "bliss", and amide (Devane et al., 1992). Anandamide, a derivative of arachidonic acid first identified in pig brain, can act as a partial agonist of CB_1 with very high affinity, but with lower activity towards CB_2 (Pertwee, 2015). The fact that AEA cannot fully reproduce the effect induced by Δ^9-THC led to the discovery in 1995 of another eCB, 2-arachidonoylglycerol (2-AG) (Mechoulam et al., 1995; Sugiura et al., 1995). While AEA is mildly selective for CB_1 receptors, 2-AG has moderate affinity and is a full agonist for both CB_1 and CB_2 receptors (Di Marzo and De Petrocellis, 2012).

Unlike many neurotransmitters, which are stored in intracellular deposits and then released following cell stimulation, eCBs are produced "on demand" from membrane phospholipids in response to specific stimuli (Di Marzo and De Petrocellis, 2012); the biosynthetic pathway differs between AEA, an acylethanolamine (NAE), and 2-AG, an acylglycerol (Figure 3).

The best studied biosynthetic pathway of NAEs is the transacylation phosphodiesterase reaction, which can be divided into two steps: (i) N-acylation of phosphatidylethanolamine (PE) to produce N-acylphosphatidylethanolamine (NAPE) by N-acyltransferase (NAT) activity and (ii) hydrolysis of NAPE to give NAE by the enzyme N-acylphosphatidylethanolamine (NAPE)-hydrolysing phospholipase D (NAPE-PLD). This pathway was confirmed for AEA biosynthesis in 1994, having N-arachidonoylphosphatidylethanolamine (NArPE) as a precursor (Figure 3) (Di Marzo et al., 1994).

The major pathway of 2-AG biosynthesis involves the sequential action of phospholipase-C (PLC) on phosphatidic acid (PA) or phosphatidylinositol (PI) via a diacylglycerol intermediate and then diacylglycerol lipase (DAGL) with the formation of 2-AG (Figure 3) (Ueda et al., 2013).

Endocannabinoids are metabolised by two different pathways: hydrolysis and oxidation. Two hydrolases are involved in the hydrolysis of AEA: fatty acid amide hydrolase (FAAH) and N-acylethanolamine-hydrolysing acid amidase (NAAA). While the first is more specific for AEA and is bound in the cytosol to the membrane of mitochondria and endoplasmic reticulum (Gulyas et al., 2004), the second is more specific for other NAEs (such as palmitoylethanolamide) and is localised near acidic organelles such as lysosomes (Tsuboi et al., 2007); on the other hand, 2-AG is hydrolysed mainly by the selective enzyme monoacylglycerol lipase (MAGL).

Other enzymes are involved in the oxidation pathways: in particular, lipoxygenases (LOXs) and cyloxygenase-2 (COX-2), which oxidise arachidonic

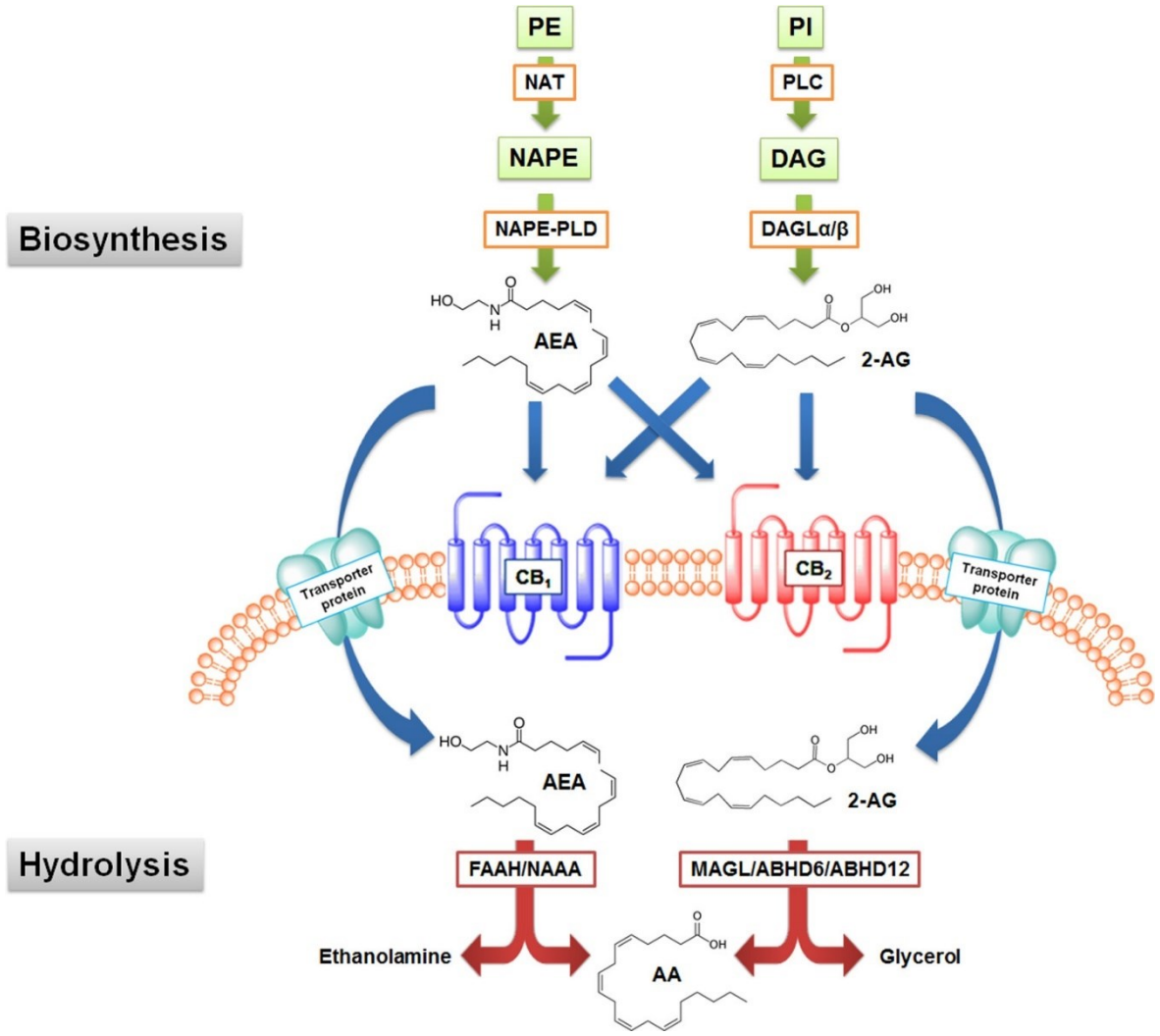

Figure 3. Biosynthetic and degradation pathways of anandamide (AEA) and 2-arachidonoylglycerol (2-AG) (Lee et al., 2016)

Abbreviations: 2-AG, 2-arachidonoylglycerol; AA, arachidonic acid; ABHD-6/12, α,β-hydrolase-6/12; AEA, N-arachidonoylethanolamine or anandamide; DAG, diacylglycerol; DAGLα/β, diacylglycerol lipase α/β; FAAH, fatty acid amide hydrolase; MAGL, monoacylglycerol lipase; NAAA, N-acylethanolamine-hydrolyzing acid amidase; NAPE, N-acylphosphatidylethanolamine; NAPE-PLD, NAPE-phospholipase D; NAT, N-acyltransferase (NAT); PE, phosphatidylethanolamine; PI, phosphatidylinositol; PLC, phospholipase C.

acid (AA) as a component of AEA and 2-AG; in addition, AEA can also be oxidised by cytochrome P450 (Rouzer and Marnett, 2011).

Therefore, the endocannabinoid system (eCBS) has been defined as an endogenous system consisting of two GPCRs (CB_1 and CB_2), two lipid mediators that can bind and activate these receptors (AEA and 2-AG), and the enzymes responsible for their production and degradation (mainly FAAH, NAAA and MAGL).

1.4 The expanded endocannabinoid system: "endocannabinoidome"

As described before, with the discovery of cannabinoid receptors and the endogenous lipid mediators that can activate them, a new endogenous signalling pathway was discovered: the endocannabinoid system. At the beginning of the century, it was defined as a system comprising two GPCRs (CB_1 and CB_2), two lipid mediators (AEA and 2-AG) and five enzymes responsible for their production and inactivation (NAPE-PLD, DAGL, FAAH, NAAA and MAGL) (Di Marzo and Piscitelli, 2015); but the picture was still incomplete.

First of all, among all the phytocannabinoids found in *C. sativa*, only THC and THCV are able to bind with high affinity CB_1 and CB_2, while the other cannabinoids are able to bind other receptors, such as GPR18, GPR55 and GPR119, thermosensitive ion channels belonging to the Transient Receptor Potential (TRP) channels superfamily, such as TRPV1-4, TRPM8 and TRPA1 and PPARs receptors (De Petrocellis and Di Marzo, 2010; Martinez et al., 2020); secondly, AEA and 2-AG were found to be quite promiscuous in their pharmacological activity and able to interact with these other targets at higher concentrations than required for CB_1 and CB_2 activation, (Di Marzo and Silvestri, 2019; Martinez et al., 2020). Finally, these targets have been found to be readily activated by other lipids chemically correlated with AEA and 2-AG: long chain N-acylethanolamines (NAEs) and 2-monoacylglycerols (2-MAGs); the discovery

of these lipid mediators led to the definition of the “expanded endocannabinoid system” known as the “endocannabinoidome” (eCBome) (Figure 4).

The eCBome includes the congeners of anandamide (the N-acylethanolamines, NAEs) and 2-AG (the 2-acylglycerols, 2-AcGs), the N-acyl-aminoacids (glycine, taurine), acylated neurotransmitters such as the N-acyl-dopamines and N-acyl-serotonins, and the primary fatty acid amides as well as their receptors and biosynthetic and metabolizing enzymes. These lipid mediators are often produced or metabolised via the same pathway as AEA and 2-AG, but not necessarily. These congeners of AEA and 2-AG act on several targets, including thermosensitive transient receptor potential (TRP) channels, such as TRPV1-4 and TRPM8, some orphan GPCRs, such as GPR18, GPR55, GPR110 or GPR119 and peroxisome proliferator-activated receptor-α and -γ (PPARα and PPARɣ) (Di Marzo and Piscitelli, 2015). Therefore, this expanded eCBS includes more than 100 lipid mediators, 20 enzymes, and 20 receptors (Di Marzo, 2020).

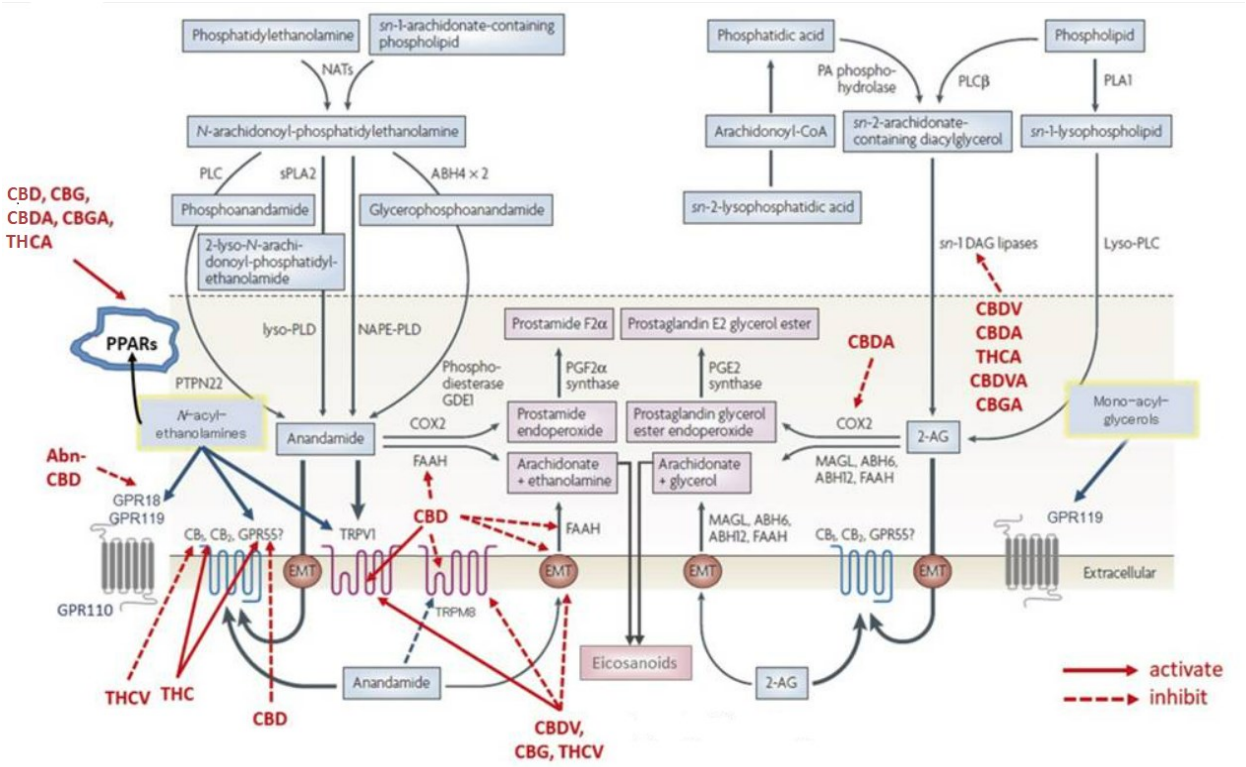

Figure 4. Endocannabinoidome (mediators, targets, enzymes) and its interactions with phytocannabinoids (Di Marzo, 2020)

Abbreviations: 2-AG, 2-arachydonoylglycerol; ABH2, α,β-hydrolase-2; ABH4, α,β-hydrolase-4; ABH6, α,β-hydrolase-6; Abn-CBD, abnormal cannabidiol; CB_1, cannabinoid receptor-1; CB_2, cannabinoid receptor-2; CBD, cannabidiol; CBDA, cannabidiolic acid; CBDV, cannabidivarin; CBDVA, cannabidivarinic acid; CBG, cannabigerol; CBGA, cannabigerolic acid; CoA, coenzyme A; COX2, cyclooxygenase-2; DAG, diacylglycerol; EMT, endocannabinoid membrane transporter; FAAH, fatty acid amide hydrolase; GDE1, glycerophosphodiester phosphodiesterase-1; GPR110, G protein-coupled receptor-110; GPR119, G protein-coupled receptor-119; GPR18, G protein-coupled receptor-18; GPR55, G protein-coupled receptor-55; lyso-PLC, lyso phospholipase C; MAGL, monoacylglycerol lipase; NAPE-PLD, N-acylphosphatidylethanolamine-phospholipase D; NAT, N-acyltransferase; PGE2, prostaglandin E2; PGF2α, prostaglandin F2α; PLA1, phospholipase A1; PLA2, phospholipase A2; PLC, phospholipase C; PLCβ, phospholipase Cβ; PPARs, peroxisome proliferator-activated receptors; PTPN22, tyrosine-protein phosphatase nonreceptor type 22; sn-1-DAG lipase, sn-1-specific diacylglycerol lipase; sPLA2, secretory phospholipase A2; THC, Δ9-tetrahydrocannabinol; THCA, Δ9-tetrahydrocannabivarinic acid; THCV, Δ^9-tetrahydrocannabivarin; TRPM8, transient receptor potential melastatin type 8; TRPV1, transient receptor potential vanilloid type 1.

2. Gut microbiome

2.1 Gut microbiota composition

The human gut (200-300 m^2 of mucosa) is home to ten trillion different symbionts (50 bacterial phyla and about 1000 bacterial species), collectively known as the 'microbiota'. With the term “gut microbiome” we refer to the intestinal microbiota, with its warehouse of genes, proteins and small molecules (Qin et al., 2010). In an adult human, 150-170 bacterial species predominate, colonising the gastrointestinal tract and establishing themselves as host commensals (Adak and Khan, 2019).

The human gut microbiota consists of bacteria, archaea, eukaryotes, viruses and parasites (Lozupone et al., 2012); bacteria are the most abundant in this environment and are divided into seven phyla: *Firmicutes*, *Bacteroidetes*, *Actinobacteria*, *Fusobacteria*, *Proteobacteria*, *Verrucomicrobia* and *Cyanobacteria*, with *Bacteroidetes* and *Firmicutes* being the most abundant with a relative abundance of over 90% (Backhed et al., 2005). Although the relative abundance of bacterial phyla can vary greatly among different individuals, some are present in almost every human gut and are defined as the "core microbiota", while others vary and act more like a "flexible pool". Among the "core bacteria" we find *Faecalibacterium prausnitzii*, *Roseburia intestinalis* and *Bacteroides uniformis* (< 0.5% relative abundance) (Adak and Khan, 2019).

The different environment in the different parts of the gastrointestinal tract allows specific bacteria to grow and creates a physiochemical barrier between the different areas (Figure 5). It was previously thought that the very low pH, thick mucus layer and gastric peristalsis of the stomach were impervious to bacterial growth. However, several bacteria that originated in the mouth are present in all parts of the gut, including the stomach, such as *Firmicutes*, *Bacteroidetes*, *Actinobacteria*, *Fusobacteria* and *Proteobacteria*, as well as the bacterial genera

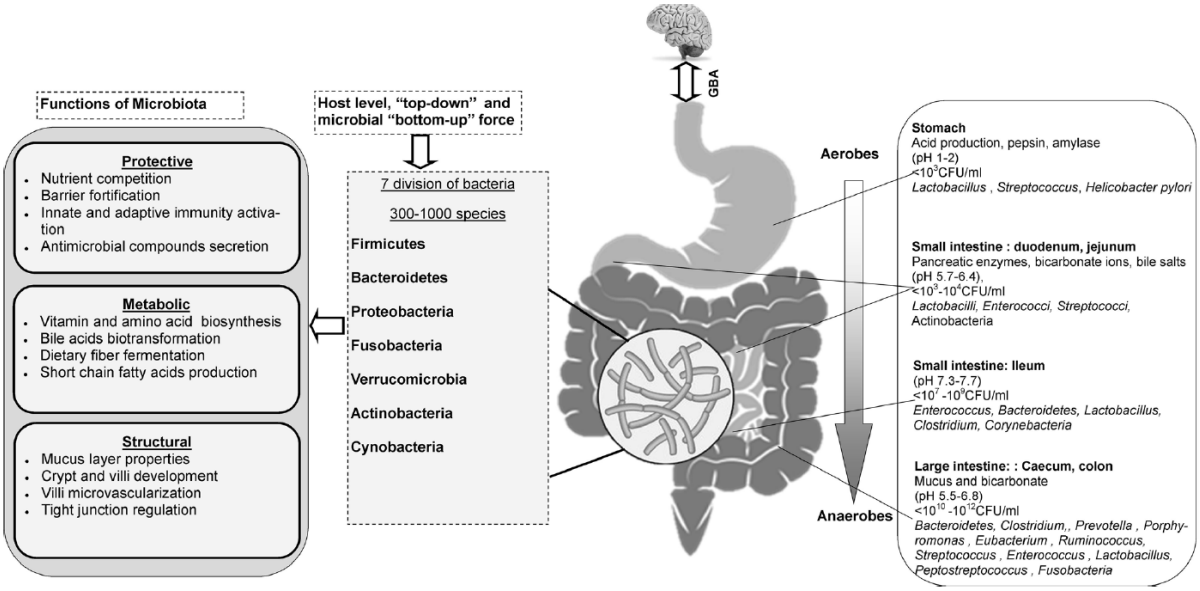

Figure 5. Composition of gut microbiota in different parts of intestine and its functional role (Adak and Khan, 2019)

Prevotella, *Streptococcus*, *Veillonella*, *Rothia* and *Haemophilus* (Nardone and Compare, 2015).The small intestine, where digestion and absorption of food takes place, is divided into three parts: duodenum, jejunum and ileum. *Firmicutes* and *Actinobacteria* are the predominant phyla in the duodenum; in the jejunum we find mainly Gram-positive aerobes and facultative anaerobes, including *Lactobacilli*, *Enterococci* and *Streptococci*, while in the ileum aerobic species predominate in the first tract and Gram-negative bacteria in the distal part (El Aidy et al., 2015).

The large intestine, consisting of cecum and the ascending, transverse and descending colon, is the predominant site of water absorption and fermentation of undigested food; here, we find 1000 times more anaerobes than aerobes because of the anaerobic conditions. The bacterial community is mainly composed of *Firmicutes* and *Bacteroidetes* (Eckburg et al., 2005). The *ratio* of these two bacterial phyla changes at different stages of life and is also a predictive marker for health and disease status (Mariat et al., 2009).

The microbiota is acquired at birth and develops in parallel with the host, which plays a crucial role in adulthood until death. During birth, a baby acquires microbes from the mother's vagina. In contrast, a baby born by caesarean section acquires microbes from the mother's skin, resulting in lower microbial diversity and delayed colonisation of *Bacteroidetes*, making the baby vulnerable to disease (Adak and Khan, 2019). After birth, breastfed infants absorb more complex oligosaccharides through breast milk than formula-fed infants, resulting in a higher abundance of *Bifidobacterium* and *Lactobacillus* sp., while formula-fed infants are dominated by *Clostridium*, *Granulicatella*, *Citrobacter*, *Enterobacter* and *Bilophila* (Pacheco et al., 2015).

Subsequently, at 3-5 years of age, the composition of the gut microbiota begins to differentiate and resembles that of an adult (Backhed et al., 2005). From here on, the composition remains the same if long-term dietary habits, antibiotic treatment, stress and pathophysiology do not change in adulthood (Adak and

Khan, 2019). In older people, a decline in the abundance of 'core bacteria' (*Ruminococcaceae*, *Lachnospiraceae* and *Bacteroidaceae*) has been reported; high abundance of *Akkermansia*, *Bifidobacterium* and *Christensenella* has been associated with healthy ageing and longevity (Biagi et al., 2016).

In the gastrointestinal tract, approximately 85% of carbohydrates, 66-95% of proteins and all fats are digested; in the colon, the gut microbiota utilises 10-30% of energy from food (Adak and Khan, 2019). Dietary fibres are resistant to digestion by host enzymes, but the gut microbiota has a range of enzymes that can metabolise these carbohydrates. In particular, bacteria belonging to the phyla *Bacteroidetes* and *Firmicutes* have the largest set of enzymes for utilising various polysaccharides as an energy source (Louis and Flint, 2009). Fermentation of dietary fibres in the colon leads to the release of gases (methane, hydrogen and carbon dioxide), short-chain fatty acids (SCFAs, formate, acetate, propionate, butyrate, valerate, isovalerate and hexanoate), small amounts of organic acids (lactate and succinate) and alcohols (methanol and ethanol) (Adak and Khan, 2019).

Intestinal microbial species such as *Roseburia spp*, *Eubacterium rectale* and *Faecalibacterium prausnitzii*, as well as the *Clostridium groups IV* and *XIVa* are the main producers of SCFAs (Louis and Flint, 2009). Among SCFAs, acetate, propionate and butyrate are predominant; about 90-95% of them are absorbed in the colon and used by the human body as an energy source (Duncan et al., 2007). Acetate serves as an energy source for peripheral tissues, lipogenesis and cholesterol biosynthesis in the liver; butyrate serves as an energy source for colonocytes and produces ketone bodies, while propionate is transported to the liver where it acts as an acetate (Donohoe et al., 2011).

Apart from their energetic functions, SCFAs play a key role in regulating gut homeostasis: specifically, butyrate, which binds to GPR43, can activate the production of anti-inflammatory cytokines in immune cells such as TGFβ and IL-10, inhibits histone deacetylase activity and down-regulates the nuclear factor-

κβ; acetate has a greater binding affinity to GPR43 than butyrate and stimulates the secretion of IgA in the gut. Indeed, GPR43 knockout mice showed increased susceptibility to dextran sodium sulphate-induced colitis by increasing neutrophil chemotaxis and inflammatory gene expression (Adak and Khan, 2019). Propionate and butyrate in combination are also effective in inhibiting LPS-induced inflammation by activating immune cells and reducing the production of inflammatory cytokines such as IL-6 and IL-12 (Morrison and Preston, 2016).

2.2 The endocannabinoidome-gut microbiome axis

Recently, it has been reported the existence of an interaction between the eCBome and the gut microbiome (mBIome) named eCBome-mBIome axis (Shen et al., 2021). As discussed before, the gut microbiota produces a plethora of metabolites, that influence intestinal homeostasis (Adak and Khan, 2019). Some of these molecules are structurally similar to lipid mediators belonging the eCBome (Sihag and Di Marzo, 2022); therefore, is not a surprise that eCBome and microbiome mutually influence each other, playing a role in several physiological and physio-pathological functions including energy intake and processing (Sihag and Di Marzo, 2022). Moreover, it has also been reported that the gut microbiota i) strongly and directly affects small intestinal eCBome signaling and ii) exploits eCBome signaling to exert some of its physio-pathological functions (Manca et al., 2020).

3. Inflammatory bowel disease (IBD)

3.1 Physiopathology and statistics

Inflammatory bowel disease (IBD) is a recurrent and lifelong condition characterised by chronic inflammation of the gastrointestinal tract. It represents a global health burden affecting millions of people, with increasing incidence and prevalence worldwide (Figure 6) (Kaplan and Ng, 2017). IBD affects both sexes with equal frequency, with a clinical onset usually between 15 and 45 years of age; globally, IBD has a higher incidence and prevalence in developed countries such as North America, Europe and Australia (Mak et al., 2020). In terms of prevalence, IBD affects 2 million people in North America, 3.2 million in Europe and millions more worldwide (Ananthakrishnan et al., 2020). There are two main forms of IBD: ulcerative colitis (UC) and Crohn's disease (CD). In Europe, the incidence of CD in Northern Europe is 6.3 compared to only 3.6 in Southern Europe, and the incidence of UC in Northern and Southern Europe is 11.4 and 8.0 respectively (per 100,000 people-year) (Mak et al., 2020).

IBD is an idiopathic disease characterised by periods of inflammation, remission and relapse that destabilise patients psychologically, emotionally and symptomatically. Both are characterised by chronic inflammation of the gastrointestinal tract, but while ulcerative colitis is limited to the colon, Crohn's disease can affect any part of the gastrointestinal tract from the mouth to the anus (Figure 7); in addition, ulcerative colitis usually affects the mucosal layer of the colon, whereas Crohn's disease affects the entire thickness of the gastrointestinal tract, often causing internal fistulas or strictures characterised by fibro-stenotic inflammation (Flynn and Eisenstein, 2019).

There are several risk factors for IBD: genetics, environment, immune response and gut microbiota dysbiosis (Ananthakrishnan, 2015). The most credible hypothesis is an abnormal immune system response to antigens in the

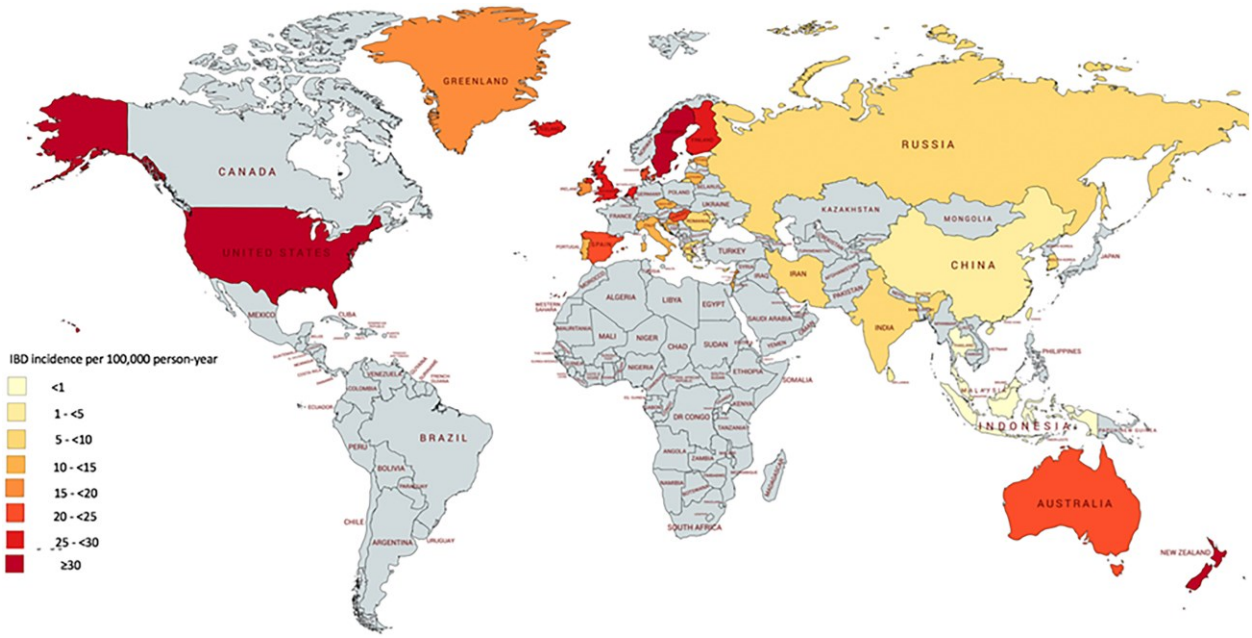

Figure 6. Global incidence of IBD according to population-based studies from 2010 to 2019 (Mak et al., 2020)

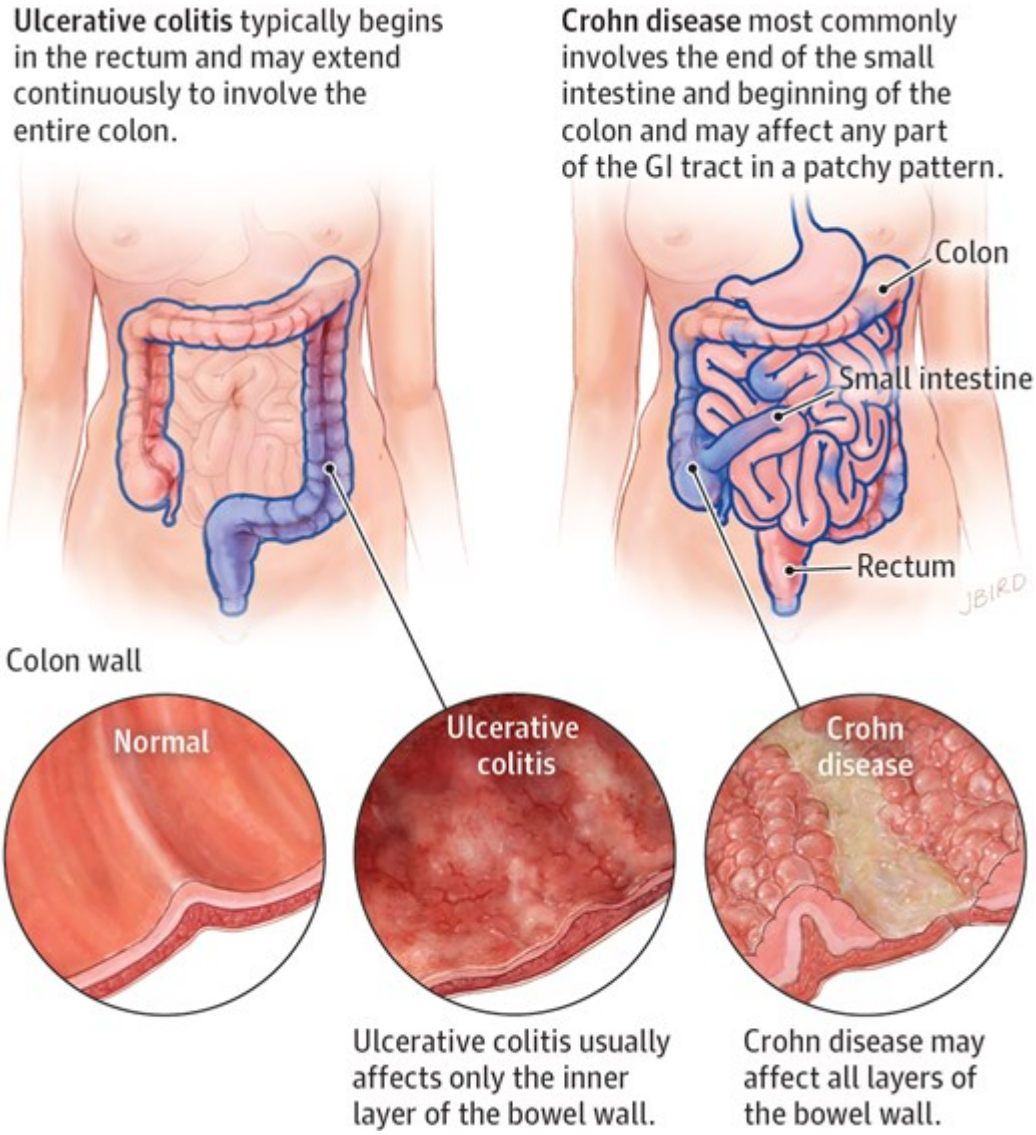

Figure 7. Pathological differences between the two main forms of IBD: Ulcerative Colitis and Croh's disease. From (Jin, 2014)

presence of a predisposing gut microbiota capable of triggering a vigorous immune response, sometimes amplified by risk factors such as host genetic predisposition. There is not one single risk factor that is sufficient alone to cause IBD, but there is a complex interaction between the individual factors (Ananthakrishnan, 2015). Gene mutations have been associated with increased risk of developing IBD. Among these, we find mutation of genes involved in IL-10 and IL-23/Th17 signalling, bacteria recognition pathways, such as NOD2, ATG16L1 and IRGM (all correlated with CD development) and mutations in genes involved in barrier function such as HNF4A, LAMB1, CDH1 and GNA12 (all correlated with the development of UC (Lees et al., 2011). Other risk factors for IBD identified in a recent umbrella review of meta-analyses, include smoking (CD), urban living (CD and IBD), appendectomy (CD), tonsillectomy (CD), antibiotic exposure (IBD), oral contraceptive use (IBD), soft drink consumption (UC), vitamin D deficiency (IBD) and non–*Helicobacter pylori*–like enterohepatic *Helicobacter* species (IBD); factors that reduce the risk of IBD include physical activity (CD), breastfeeding (IBD), bed sharing (CD), tea consumption (UC), high folate levels (IBD), high vitamin D levels (CD) and *H. pylori* infection (IBD) (Piovani et al., 2019).

Conventional treatment of IBD focuses on alleviating symptoms during the active phases of the disease and inducing remission; in the case of remission, the main goal is to maintain remission (Pithadia and Jain, 2011). Pharmacological treatment in UC includes the use of amino-salicylates alone (mild UC) or in combination with corticosteroids (severe UC); immunosuppressants such as azathioprine, cyclosporine and infliximab are used in steroid-resistant UC (Zhu et al., 2012). CD treatment includes the use of corticosteroids during relapsing phases and combination with immunosuppressants in severe CD (Pithadia and Jain, 2011). Alternative therapies include the use of metronidazole and broad-spectrum antibiotics, cholestyramine, sodium cromoglycate, bismuth and arsenic salts and methotrexate (Jeong et al., 2019a).

3.2 Endocannabinoidome and IBD

Manipulation of the endocannabinoid system has been shown to be of great benefit in attenuating inflammation in mouse models of colitis. Specifically, the use of CB receptor agonists and eCB hydrolysis inhibitors has been shown to reduce inflammation in chemically induced models of UC by decreasing inflammatory cell recruitment, reactive oxygen species production and proinflammatory cytokine release, and increasing the production of anti-inflammatory cytokines (Ambrose and Simmons, 2019). It has also been demonstrated that endocannabinoids (especially AEA and 2-AG) can modulate the functions of inflammatory cells not only by activating the CB receptors, but also by producing a variety of bioactive lipids with anti-inflammatory effects through their hydrolysis (Figure 8) (Turcotte et al., 2015).

Several receptors, as well as lipid mediators belonging to the endocannabinoidome have also been studied in preclinical models of IBD. Pharmacological or genetic modulation of TRPV1, TRPA1, PPARα, and GPR55, showed significant anti-inflammatory effects in mouse models of colitis (Stancic et al., 2015; Wlodarczyk et al., 2017; Cseko et al., 2019; Duo et al., 2020; Yao et al., 2021). Furthermore, lipids such as oleoylethanolamide (OEA) and palmitoylethanolamide (PEA) showed anti-inflammatory effects in preclinical models of ulcerative colitis (Esposito et al., 2014; Otagiri et al., 2020; Esposito et al., 2021). Finally, pharmacological blockade of MAGL, FAAH and NAAA, enzymes that metabolise the endocannabinoidome mediators, reduces inflammation in experimental models of IBD by increasing levels of endocannabinoidome mediators (Alhouayek et al., 2011; Alhouayek et al., 2015; Shamran et al., 2017).

Over the last two decades, several studies have investigated the anti-inflammatory effects of *Cannabis* compounds, namely CBD, CBG and CBC in

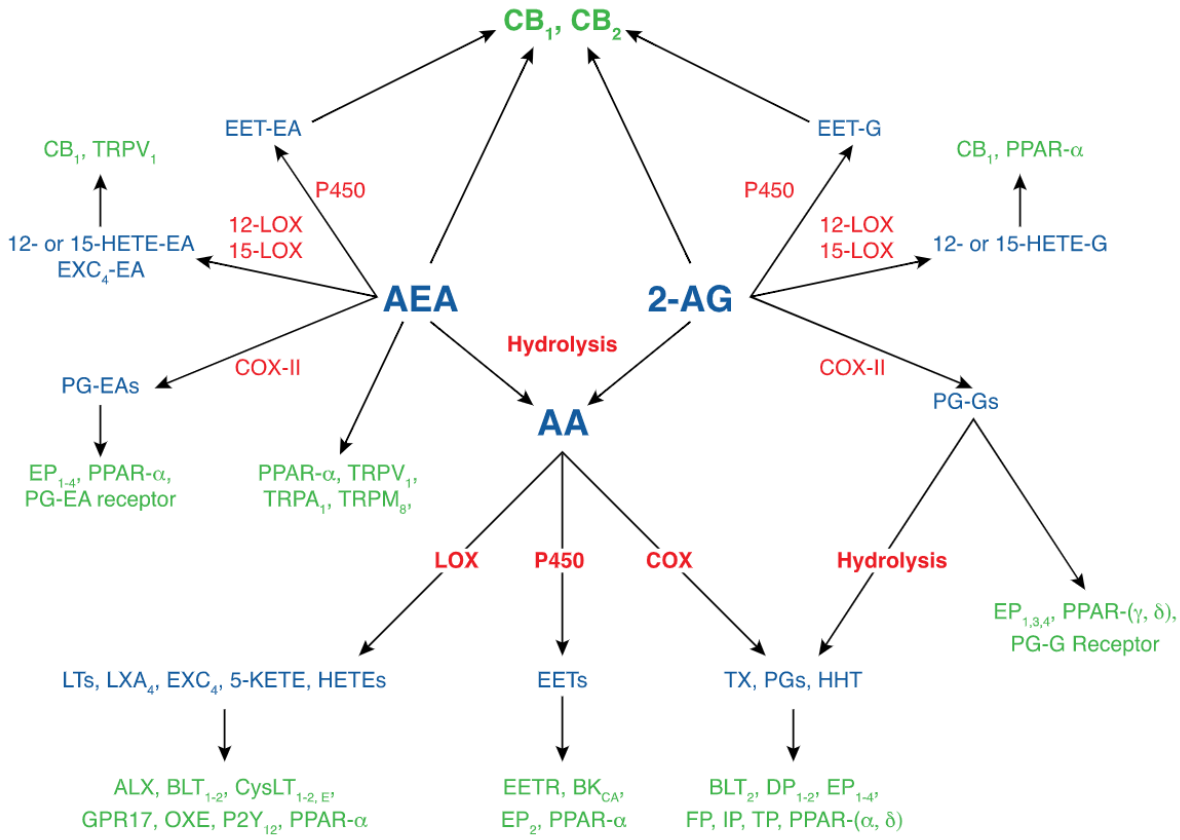

Figure 8. Anandamide (AEA) and 2-arachydonoylglycerol (2-AG) interactions with inflammatory pathways (Turcotte et al., 2015). AEA and 2-AG actions are exerted through cannabinoid receptors. However, enzymes involved in eicosanoids production (red) can metabolize AEA, 2-AG and their main product of enzymatic degradation (arachidonic acid, AA), producing bioactive lipid mediators which can interact with other receptors (green).

Abbreviations: 12/15-HETE-EA, 12/15-hydroxyeicosatetraenoylethanolamide; 12/15-HETE-G, 12/15-hydroxyeicosatetraenoylglycerol; 2-AG, 2-arachydonylglycerol; 5-KETE, 5-oxo-eicosatetraenoic acid; AA, arachydonic acid; AEA, anandamide; ALX, lipoxin-A4; BKCa, big potassium calcium-activated channels; BLT, leukotriene B4 receptor; BLT1-2, leukotriene B4 receptor-1/2; CB_1, cannabinoid receptor-1; CB_2, cannabinoid receptor-2; COX, cyclooxygenase; CysLT1-2, leukotriene D4 receptor-1/2; DP, prostaglandin D2 receptor; EETR, epoxyeicosatrienoic acid receptor; EETs, epoxyeicosatrienoic acids; EP, prostaglandin E2 receptor; EP1-4, prostaglandin E2 receptor 1-4; EXC4, exocin-C4; EXC4-EA, exocin-C4-ethanolamide; FP, prostaglandin F2 receptor; GPR17, G protein-coupled receptor-17; HETEs, hydroxyeicosatetraenoic acids; IP, prostaglandin I2 receptor; LOX, lypooxygenase; LTs, leukotrienes; LXA4, lipoxin; OXE, oxoeicosanoid receptor 1; P2Y12, adenosine diphosphate receptor; P450, cytochromes P450; PG-EAs, prostaglandin-ethanolamides; PG-Gs, prostaglandin-glycerols; PPARα/γ/δ, peroxisome proliferator-activated receptor-α/ γ/δ; TP, tromboxane receptor; TRPA1, transient receptor potential ankyrin type-1; TRPM8, transient receptor potential melastatine type-8; TRPV1, transient receptor potential vanilloid-1.

different models of intestinal inflammation in mice and rats (Borrelli et al., 2009; De Filippis et al., 2011; Borrelli et al., 2013; Romano et al., 2013; Pagano et al., 2016).

CBD intraperitoneal administration has been reported to improve disease parameters, reduce epithelial damage and decrease the production of cytokines, chemokines and oxidative stress markers (De Filippis et al., 2011; Esposito et al., 2013; Pagano et al., 2016). Some of these effects have also been confirmed in *in vitro* models, where CBD reduced reactive oxygen species production (ROS) and lipid peroxidation (Borrelli et al., 2009) and counteracted LPS/interferon gamma (IFNγ)-induced inflammatory-like responses in cultured human colon biopsies from UC patients (De Filippis et al., 2011). Similar results were also reported for CBG and CBC, which showed significant anti-inflammatory effects in *in vivo* and *in vitro* models of intestinal inflammation (Borrelli et al., 2013; Romano et al., 2013).

Anecdotal reports suggest that *Cannabis* exerts a positive anti-inflammatory effect in patients with IBD. Despite these reports and the large number of preclinical studies, evidence for the positive effect of *Cannabis* in IBD patients is lacking. Two recent Cochrane meta-analyses evaluating the safety and efficacy of *Cannabis*/*Cannabis*-derived products to induce and maintain remission in patients with CD or UC reached inconclusive conclusions (Kafil et al., 2018b; Kafil et al., 2018a). A more recent clinical trial, which was not included in the meta-analysis, showed that a high-CBD *Cannabis* extract improves quality of life but does not reduce inflammatory markers or endoscopic scores in patients with IBD (Naftali et al., 2021).

3.3 Gut microbiota and IBD

The intestinal microbiome plays a crucial role in the pathogenesis of IBD (Sultan et al., 2021). Indeed, dysbiosis (changes in the composition of the intestinal microbiota) has been found in individuals with IBD (Kostic et al., 2014). In

addition, exposure to pathogenic bacteria in childhood may impair immune system development and reduce tolerance to environmental factors, which could contribute to an increased risk of IBD later in life (Gensollen et al., 2016).

Dysbiosis of the gut microbiota in IBD is characterised by reduced diversity, lower abundance of short-chain fatty acids (SCFAs) producers (such as *Roseburia hominis* and *Faecalibacterium prausnitzii*) and enrichment of proinflammatory microbes such as adherent/invasive *Escherichia coli*, *Fusobacterium* and *Proteus* (Kostic et al., 2014; Kaplan and Ng, 2017; Sultan et al., 2021). In addition, microbial dysbiosis in IBD has been shown to have a potential impact on colonocyte metabolism and this may underlie disease progression. Crohn's disease patients have been reported to have increased intestinal abundance of *Enterobacteriaceae* and decreased *Clades IV and XIVa Clostridia* (Gevers et al., 2014). All these findings have highlighted gut microbiota as a target for a possible therapeutic approach for IBD.

4. Colorectal cancer (CRC)

4.1 Physiopathology and statistics

Colorectal cancer (CRC) is the most common malignancy of the gastrointestinal tract with high incidence and prevalence worldwide (Wong et al., 2021). It is estimated to be the third leading cause of death from neoplastic disease in the USA in 2021, with an estimated number of deaths and new cancer cases of 52,980 and 149,500, respectively (Figure 9) (Siegel et al., 2021). One of the most recent statistics on European cancer mortality estimates that CRC will be the second leading cause of death from neoplasia in 2021, with a total of 155,200 deaths in both men and women (Carioli et al., 2021). In Italy, CRC is the second most common cancer after breast cancer, with an estimated 43,700 cases in 2020, accounting for 14% and 13% of cancers diagnosed in men and women, respectively, with an estimated number of deaths of 21,700 in 2021 (AIOM and AIRTUM, 2021).

CRC develops as a result of a sequential accumulation of genetic changes and epigenetic modulations (Lao and Grady, 2011). These are the result of mutations in genes that regulate cell growth, such as APC, Smad4 and p53 (tumour suppressor genes), and K-Ras, c-myc, c-neu, c-src (oncogenes) (Koveitypour et al., 2019). This multistep process develops over 10 to 15 years and offers an opportunity for prevention.

In the sporadic form, colorectal carcinogenesis begins with the appearance of preneoplastic lesions known as aberrant crypt foci (ACF) and progresses to adenoma and then adenocarcinoma via the formation of polyps with high-grade dysplasia; this process, known as "adenoma-carcinoma sequence", represents the process by which most, if not all, colorectal carcinomas develop (Figure 10) (West et al., 2015). Lifestyle and environmental factors are considered important risk factors for CRC, in particular consumption of red meat, flour and refined

Estimated New Cases

Males				Females		
Prostate	248,530	26%		Breast	281,550	30%
Lung & bronchus	119,100	12%		Lung & bronchus	116,660	13%
Colon & rectum	79,520	8%		Colon & rectum	69,980	8%
Urinary bladder	64,280	7%		Uterine corpus	66,570	7%
Melanoma of the skin	62,260	6%		Melanoma of the skin	43,850	5%
Kidney & renal pelvis	48,780	5%		Non-Hodgkin lymphoma	35,930	4%
Non-Hodgkin lymphoma	45,630	5%		Thyroid	32,130	3%
Oral cavity & pharynx	38,800	4%		Pancreas	28,480	3%
Leukemia	35,530	4%		Kidney & renal pelvis	27,300	3%
Pancreas	31,950	3%		Leukemia	25,560	3%
All Sites	**970,250**	**100%**		**All Sites**	**927,910**	**100%**

Estimated Deaths

Males				Females		
Lung & bronchus	69,410	22%		Lung & bronchus	62,470	22%
Prostate	34,130	11%		Breast	43,600	15%
Colon & rectum	28,520	9%		Colon & rectum	24,460	8%
Pancreas	25,270	8%		Pancreas	22,950	8%
Liver & intrahepatic bile duct	20,300	6%		Ovary	22,950	5%
Leukemia	13,900	4%		Uterine corpus	12,940	4%
Esophagus	12,410	4%		Liver & intrahepatic bile duct	9,930	3%
Urinary bladder	12,260	4%		Leukemia	9,760	3%
Non-Hodgkin lymphoma	12,170	4%		Non-Hodgkin lymphoma	8,550	3%
Brain & other nervous system	10,500	3%		Brain & other nervous system	8,100	3%
All Sites	**319,420**	**100%**		**All Sites**	**289,150**	**100%**

Figure 9. Ten leading cancer types for the estimated new cancer cases and deaths by sex, United States, 2021 (Siegel et al., 2021)

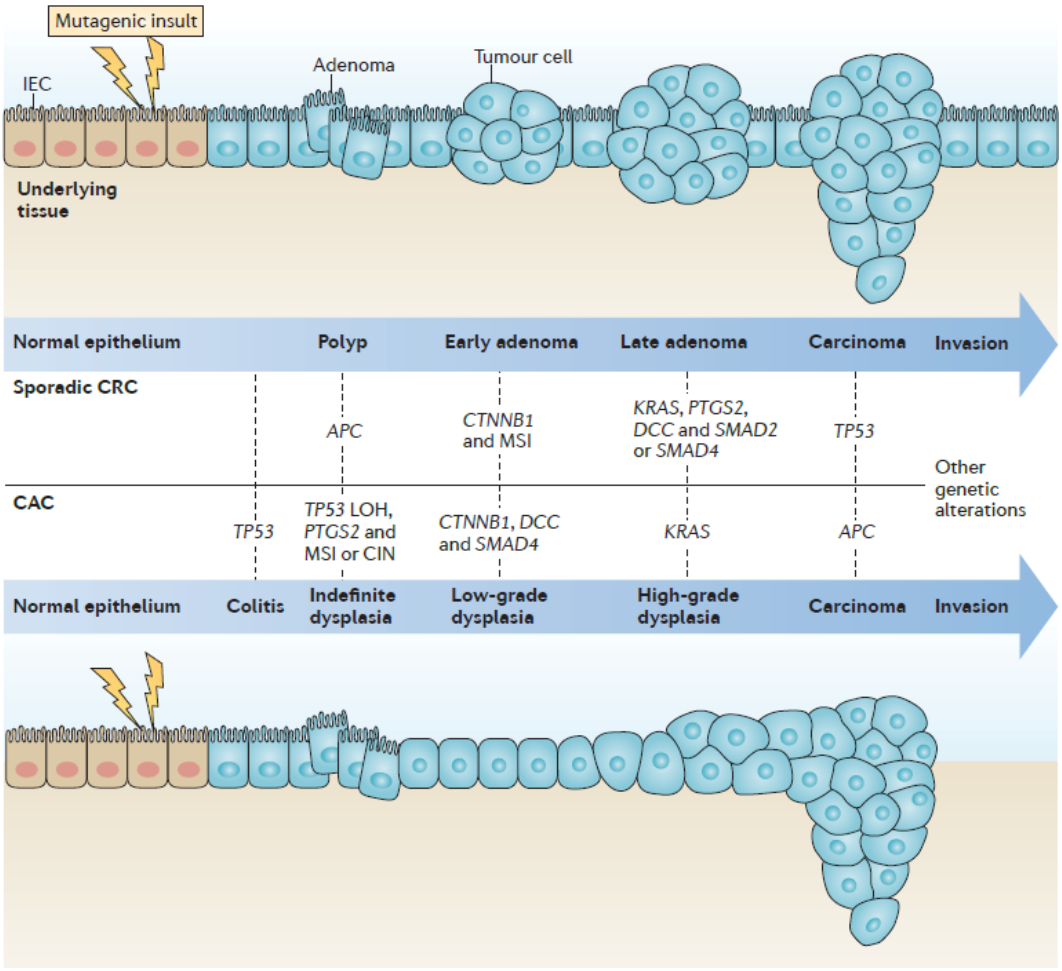

Figure 10. Canonical mechanisms of sporadic colorectal cancer (CRC) and colitis-associated cancer (CAC) development (West et al., 2015). CRC and CAC share similarities in their developmental pathways, including microsatellite instability (MSI), activation of the oncogene KRAS, activation of cyclooxygenase 2 (COX2; encoded by PTGS2), and mutation and eventual loss of heterozygosity (LOH) of TP53, adenomatous polyposis coli (APC), deleted in colon cancer (DCC) and SMAD4. However, the frequency and sequence of these events differs between the cancers. For example, mutation in APC is one of the first events in CRC, whereas it occurs at later stages in CAC. By contrast, TP53 mutations usually occur early in CAC but at a later stage in the progression of CRC. Although CRC shows a clear progression of morphological changes, from polyp to carcinoma, CAC progression involves increasing histological grades of dysplasia that culminate in an invasive carcinoma.

sugar, obesity, reduced physical activity, smoking and excessive alcohol consumption appear to significantly increase the incidence of CRC (Brenner et al., 2014); in contrast, proper lifestyle habits such as regular physical activity, reduced alcohol consumption and a healthy diet with consumption of fruits, vegetables, fibre, fish and dairy products are associated with low CRC risk (Thanikachalam and Khan, 2019).

There is also a strong association between IBD and the likelihood of developing colorectal cancer; this type of CRC is defined as colitis-associated colorectal cancer (CAC, Figure 10) (Grivennikov and Cominelli, 2016). Ten years after UC diagnosis, the risk of developing CRC is 1.6% and increases to 8.3% and 18.4% after 20 and 30 years, respectively (Bernstein et al., 2001). Furthermore, patients with UC who develop CRC have a worse prognosis than CRC patients without UC, even when cases with the same tumour stage are compared (Watanabe et al., 2011).

Finally, about 10% of colorectal cancers are the result of well-defined hereditary syndromes. The hereditary mutation of the adenomatous polyposis coli (APC) gene, which causes familial adenomatous polyposis (FAP), may increase the likelihood of developing CRC in carriers before the age of 40 (Rustgi, 2007). Lynch syndrome or Hereditary Non-Polyposis Colorectal Carcinoma (HNPCC) is another risk factor caused by a mutation in one of the genes involved in the DNA mismatch repair mechanism (Lynch and de la Chapelle, 2003).

The most effective therapeutic approach remains surgical resection of the affected area, followed by neoadjuvant radiotherapy (for patients with rectal cancer) and adjuvant chemotherapy (for patients with stage III /IV and high-risk stage II colon cancer) (Marley and Nan, 2016). The most widely used chemotherapeutic agent is 5-fluorouracil (5-FU), which is used in CRC advanced patients in several poly-chemotherapy regimens such as FOLFOX (fluorouracil/leucovorin and oxaliplatin) and FOLFIRI (fluorouracil/leucovorin

and irinotecan) (Gustavsson et al., 2015). However, intrinsic or acquired resistance to 5 FU may occur (Ahn et al., 2015).

In recent years it has been shown that the tumour microenvironment plays a key role in the growth and especially the spread of the neoplasm. In particular, the importance of angiogenesis in the development of solid tumours has been widely documented, as tumour spread requires the growth of new blood vessels (Mody et al., 2018). Considering this assumption, conventional drugs are used in combination with new anti-angiogenic drugs in the treatment of metastatic CRC. In particular, bevacizumab, a monoclonal antibody (mAb) targeting vascular endothelial growth factor (VEGF), a potent proangiogenic factor, and cetuximab, a mAb targeting epidermal growth factor receptor (EGFR), another proangiogenic factor, are used. The combination of anti-angiogenic therapy with the other chemotherapy regimens has been shown to significantly increase survival in patients with metastatic colorectal cancer (Kirstein et al., 2014).
Despite the obvious advances in understanding the pathophysiology of colorectal cancer, current therapeutic interventions cannot prevent or stop the progression of the disease to metastasis. Therefore, it is crucial to identify new molecular agents that play an important role in CRC oncogenesis.

4.2 Endocannabinoidome and CRC

Significant alterations in the ECS have been described in colorectal cancer. In particular, increased endocannabinoid levels, downregulation of CB_1 receptors and upregulation of CB_2 receptors were observed in intestinal samples from CRC patients (Grill et al., 2019; Tutino et al., 2019). These observations support the possible role of cannabinoids in regulating cancer progression.

The potential effect of cannabinoids on colorectal carcinogenesis has been studied in CRC epithelial cells and experimental models of colorectal cancer (Izzo and Sharkey, 2010; Velasco et al., 2012; Daris et al., 2019). Regarding their mechanism of action, cannabinoids could exert protective effects by directly

activating cannabinoid receptors or indirectly by modulating endocannabinoid levels via inhibition of metabolising enzymes. Indeed, activation of cannabinoid receptors has been associated with antiproliferative effects, promotion of apoptosis, inhibition of tumour cell migration and/or inhibition of angiogenesis (Martinez et al., 2020).

Several receptors, as well as lipid mediators belonging to the endocannabinoidome have also been investigated in preclinical models of CRC. In particular, GPR55, PPARγ, TRPV1 and TRPM8 have been implicated in the development of CRC (Aviello et al., 2012; Kargl et al., 2016); specifically, GPR55 has been reported to be involved in the migration of HCT116 colon cancer cells and appears to play an important role in preventing metastasis (Kargl et al., 2016). Activation of TRPV1 and PPARγ has also been reported to reduce cell proliferation in colorectal adenocarcinoma cell lines (Aviello et al., 2012), while the use of a TRPM8 antagonist reduces the growth of colorectal cancer cells (Borrelli et al., 2013).

PEA has been reported to have antitumour activity in *in vitro* and *in vivo* models of colon cancer by reducing cell proliferation and tumour development (Pagano et al., 2021). Finally, among the enzymes that metabolise the endocannabinoidome, NAAA, FAAH and MAGL have been associated with colorectal cancer progression, and their pharmacological blockade attenuates experimental carcinogenesis by increasing NAEs and MAGs levels (Pagano et al., 2017; Wasilewski et al., 2017; Romano et al., 2021).

As with IBD, most studies conducted on *Cannabis* compounds have focused on CBD, due to its main mechanism of action (CBD can increase endocannabinoid levels by inhibiting their enzymatic degradation) and pharmacological effects (antioxidant and anti-inflammatory activity) (Kis et al., 2019); secondly, CBD has already been reported to be able to inhibit Noxa activation, mTOR/cyclin D1 and G-protein-coupled receptor/mitogen-activated protein kinase (GPR/MAPK) signalling pathway in various cancers such as

pancreatic cancer, glioblastoma, leukaemia and breast cancer (Martinez et al., 2020); thirdly, CBD may target GPR55 and produce the effects on cell migration described above (Kargl et al., 2016); finally, the synthetic CBD analogue O-1602 is able to reduce the viability of colon cancer cell lines and induce apoptosis, as well as reduce tumour size and incidence in a colitis-associated colon cancer mouse model (Kargl et al., 2013).

In vitro studies have shown that CBD is able to protect DNA from damage, increase endocannabinoid levels and decrease cell proliferation in colorectal adenocarcinoma cell lines (Caco-2 and HCT116) (through activation of the CB_1 receptor, TRPV1 channel and PPARγ) (Aviello et al., 2012); CBD also showed a proapoptotic effect in HCT116, colo205 and DLD-1 cell lines in a Noxa- and ROS-dependent manner (Jeong et al., 2019b; Jeong et al., 2019c).

The effect of CBD has also been studied in *in vivo* models of colorectal cancer. In azoxymethane (AOM)-induced colorectal tumorigenesis in mice, a CBD-enriched plant extract or pure CBD was able to reduce preneoplastic lesions, polyps and tumour formation and attenuate the upregulation of phospho-Akt and downregulation of caspase-3 (Romano et al., 2014).

Other phytocannabinoids have also been tested in CRC. In particular, CBG was reported to be able to reduce the growth of CRC cells (Caco-2 and HTC 116) via a ROS-mediated pro-apoptotic mechanism, and to counteract the development and growth of colon carcinogenesis in *in vivo* models of CRC (AOM-induced and xenograft model), effect mediated by TRPM8 (Borrelli et al., 2014).

4.3 Gut microbiota and CRC

The gut microbiota plays an important role in maintaining intestinal homeostasis through various mechanisms and a link between its alteration and the development of gastrointestinal diseases such as colorectal cancer has been demonstrated (Gao et al., 2017). Recent studies have shown that the occurrence

of CRC is related both to changes in the composition of the gut microbiota and to infections caused by certain bacteria. To better understand the relationship between the microbiota and CRC, some hypotheses have been proposed, such as the alpha-bug hypothesis and the driver-passenger model (Cheng et al., 2020).
The alpha-bug hypothesis assumes that certain bacteria, known as alpha-bugs, are pro-oncogenic in nature and can induce mutations in epithelial cells (Yu and Fang, 2015). This hypothesis stems from a series of studies conducted with a putative alpha-bug bacterium, the enterotoxigenic *Bacteroides fragilis* (ETBF) (Sears and Pardoll, 2011). ETBF acts in the early phase of CRC, producing a toxin that not only has a direct genotoxic effect, but also stimulates intestinal epithelial cell loss and E-cadherin-gamma-secretase-dependent cleavage, increases intestinal wall permeability and triggers β-catenin/Wnt signal transduction in intestinal epithelial cells; thus ETBF contributes to the proliferation and pathogenic transformation of CRC (Yu and Fang, 2015).

The driver-passenger model suggests that there are "driver" bacteria involved in the early stages of colorectal cancer development, and that these bacteria are then later replaced by "passenger" bacteria (Yu and Fang, 2015). Driver bacteria are intestinal bacteria with pro-carcinogenic properties that can trigger the development of CRC. Possible driver bacteria include *Enterococcus faecalis* and *Escherichia coli* (Tjalsma et al., 2012). Passenger bacteria are intestinal bacteria that are relatively uncolonized in a healthy person but have a competitive advantage in the tumour microenvironment that allows them to outcompete the driver bacteria (Tjalsma et al., 2012).

Studies in animal models of CRC (genetically or chemically induced) have shown greater tumour development in animals with a normal gut microbiota compared to those without (germfree), confirming that the gut microbiota plays an important role in the development of CRC (Lucas et al., 2017). CRC is often associated with dysbiosis (Tilg et al., 2018), which is partly characterised by the expansion of the bacterial taxon: quantitative changes in the components of the

gut microbiota can promote the development of chronic inflammation and the production of carcinogenic metabolites, contributing to the development of neoplasia (Song et al., 2020).

AIM

As mentioned above, inflammatory bowel disease (IBD) and colorectal cancer (CRC) are the most important pathologies of the gastrointestinal tract worldwide. Recently, the endocannabinoidome (eCBome), a complex system of lipid mediators, enzymes involved in their biosynthesis and degradation, and receptors/channels, has been shown to be involved in the regulation of gut homeostasis and immune system. The gut microbiome (miBIome), composed of trillions of different microorganisms, has also been reported to play a key role in gut homeostasis, and imbalance of this microbiome is implicated in the onset and development of IBD and CRC. Recently, a link between eCBome and miBIome has been described. Given these assumptions, the general aim of this work is to investigate whether the interaction between the eCBome and the gut microbiome has an impact on the development of IBD and CRC. This aim was achieved by manipulating the eCBome and gut microbiota using naturally derived receptor ligands and enzymatic inhibitors, genetic deletion of the receptors and depletion of the gut microbiota.

In particular, we achieve this goal by:

a. activation of TRPA1 (Transient Receptor Potential Ankyrin type-1, part of the eCBome) by using its natural agonist cannabidivarin; the effect of cannabidivarin on colon inflammation (in two mouse models of ulcerative colitis and in biopsies from human patients with ulcerative colitis) and its possible effect on the gut microbiota were evaluated;
b. inhibition of FAAH (fatty acid amide hydrolase, enzyme responsible for the degradation of some mediators of eCBome) by the natural inhibitor cannabidiol in combination with fish oil (FO, fish oil); the effect of this combination on inflammatory parameters in two mouse models of ulcerative colitis and its possible influence on the composition of the gut microbiota were evaluated;

c. genetic deletion of Trpm8 (Transient receptor potential melastatin type-8, also part of the eCBome). Specifically, using a model of chemically induced sporadic colorectal cancer in mice Trpm8$^{-/-}$, we investigated the development of colon carcinogenesis and the resulting changes in the composition of the gut microbiota.
d. modification of the gut microbiota (using antibiotic-treated mice or germfree mice). The effect of this depletion on chemically induced ulcerative colitis and changes in eCBome mediator levels was investigated.

In few words, the ultimate goal of my PhD thesis is to understand the possible role of the endocannabinoidome – gut microbiome axis in the pathogenesis of IBD and CRC.

MATERIALS AND METHODS

1.1 Drugs and reagents

2,4-dinitrobenzenesulfonic acid (DNBS), azoxymethane (AOM), myeloperoxidase (MPO) from human leucocytes, and fluorescein isothiocyanate (FITC)-conjugated dextran (molecular mass 3–5 kDa) were purchased from Sigma Aldrich S.r.l. (Milan, Italy); dextran sulfate sodium salt (DSS, molecular weight 36,000–50,000) was purchased from MP Biomedical (Illkirch, France). All the reagents for DNA extraction and library preparation were purchased from FisherScientific (Canada) and Qiagen (Hilden, Germany); 16S DNA sequencing reagents were purchased from Illumina (CA, USA).

CBD and CBDV [purity by high-performance liquid chromatography (HPLC) 99.5% and 99.0% respectively], were kindly supplied by GW Research Ltd (Cambridge, UK). CBD was dissolved in sesame oil (90 µL/mouse). CBDV was dissolved in ethanol-Tween20-saline (1:1:8) for intraperitoneal (i.p.) injection (60 µL/mouse) and in carboxymethylcellulose (CMC 1%, 150 µL/mouse) for oral gavage administration. The vehicles had no significant effects on the responses under study. Fish oil (FO; Marco Viti Farmaceutici, Mozzate, CO, Italy) and sesame oil (Il fiore di Loto S.r.l., Orbassano TO, Italy) were obtained from a local pharmacy. All chemicals and reagents employed in this study were of analytical grade.

1.2 Animals

Male adult CD1 (25–30 g) and C57BL6/J mice (wild type, 6 weeks old) were purchased from Charles River Laboratories (Calco, Lecco, Italy) and Jackson Laboratory, respectively. C57BL6/J Trpm8$^{-/-}$ mice, purchased from Jackson Laboratory, were bred in our colony in the Animal Facility of the Department of Pharmacy, University of Naples, Federico II; 6 weeks old male mice were used in our experiments. CD1, C57BL6/J and C57BL6/J Trpm8$^{-/-}$ mice were maintained in the animal care facility at the University of Naples in

polycarbonate cages under controlled temperature (23 ± 2 °C), constant humidity (60%) and with a 12-h light, 12-h dark cycle. The animals were acclimatised to their environment at least 1 week under standard conditions, with free access to water and standard rodent diet.

Conventionally Raised (CR) and Germ free (GF) Balb/c mice (6-8 weeks old) were purchased from Taconic (Taconic Bioscience, NY, USA) and maintained in the animal facility of the Institut Universitaire de Cardiologie et Pneumologie de Québec (IUCPQ, QC, Canada). Mice were housed in single cage under a 12h:12h light dark cycle with *ad libitum* access to NIH-31 Open Formula Autoclavable Diet (Zeigler, PA, USA) and water. GF mice were housed in axenic status and fecal samples as well as litter samples from each cage were tested to ensure that the GF condition was maintained throughout the whole experiment. Both GF and CR mice were acclimatized for at least one week prior to start with the procedures.

All mice were fasted overnight before the intracolonic injection of DNBS and for 2 h before the oral gavage of the drugs. Mice were randomly allocated to different experimental groups and outcome assessments were performed in single blind.

All animal procedures performed in Italy were approved by the Institutional Animal Ethics Committee for the use of experimental animals and were carried out in accordance with the Italian D.L. no. 116 of January 27, 1992 and associated guidelines in the European Communities Council (86/609/ECC and 2010/63/UE). Animal procedures performed in Québec (QC, Canada), were validated by the approved by Laval University animal ethics committee (CPAUL). Animal studies are reported in compliance with the ARRIVE guidelines (Kilkenny et al., 2010; McGrath and Lilley, 2015). G*Power was used for sample size calculation (Faul et al., 2007).

1.3 Patients

Human studies were approved by Ethical Committee of the University of Trieste, Department of Medicine (protocol number 111/ 2015). Human colon samples were obtained by colonoscopy as previous described (Lazzerini et al., 2017) from pediatric patients with a well-established diagnosis of ulcerative colitis (UC); patients were clinically scored using the Geboes score which classifies UC in six grades of severity: grade 0, architectural changes; grade 1, chronic inflammatory infiltrate; grade 2, lamina propria neutrophils and eosinophils; grade 3, neutrophils in epithelium; grade 4, crypt destruction; grade 5, erosions or ulcerations (Geboes et al., 2000).

1.4 Human tissue culture

Colonic biopsies of inflamed areas were collected from pediatric patients with active UC; as a paired control, biopsies of non-inflamed areas were collected from areas proximal to the inflamed ones. Colonic biopsies were washed with cold phosphate buffer saline (PBS), divided in two pieces and cultured in a 0.95 cm^2 plate with or without CBDV (10 μM) in RPMI-1640 medium [supplemented with 10% foetal bovine serum (FBS), 100 U/mL penicillin and 100 μg/mL streptomycin and 2 mM L-glutamine] (Petito et al., 2016). The concentration of CBDV was selected on the basis of *in vitro* studies previously reported (Hill et al., 2012). After 18 h, supernatants were collected and stored at −80 °C for interleukin- (IL-) 1β detection.

1.5 Induction of experimental colitis and pharmacological treatments

1.5.1 Dinitrobenzenesulfonic acid (DNBS)-induced colitis

DNBS (150 mg/kg for CD1 and 120 mg/kg for Balb/c mice) was dissolved in 50% or 30% ethanol for CD1 and Balb/c mice (150 μL/mouse), respectively. DNBS was administrated into the rectum by a polyethylene catheter (1 mm in diameter) inserted approximately 4.5 or 3.0 cm proximal to the anus respectively

for CD1 and Balb/c mice (Morampudi et al., 2014; Pagano et al., 2016). In preliminary experiments this dose of DNBS was found to induce remarkable colonic damage associated with high reproducibility and low mortality. After 3 days, when intestinal inflammation can be assessed, all mice were euthanized by asphyxiation with CO_2 or by cardiac puncture during isoflurane anaesthesia, the mice abdomen was opened by a midline incision and the colon removed, isolated from surrounding tissues, length measured, rinsed, weighed and then processed (Borrelli et al., 2013). Mice body weight was measured every day during the treatment period. For biochemical analysis, tissues were kept at −80 °C until the use, while for histopathological analysis the colons were fixed in 10% formaldehyde.

In the preventive protocol, CBDV was given intraperitoneally (0.3–10 mg/kg) or by oral gavage (0.3–30 mg/kg) once a day for seven consecutive days starting three days before DNBS administration, while in the curative protocol CBDV, at the same doses, was given for three consecutive days starting 24-h after DNBS administration. In particular mice were killed 1 hour (for intraperitoneal administration) or 2 hours (for oral gavage) after the last administration of CBDV; the dose-range was selected on the basis of other phytocannabinoids previously evaluated in experimental colitis (Borrelli et al., 2013; Pagano et al., 2016). TRPA1 antagonist, HC030031, was dissolved in DMSO/Tween20/saline (1:1:8) and administered intraperitoneally (30 mg/kg) alone or 30 min before CBDV administration. The dose of HC030031 was selected on the basis of preliminary experiments showing that the antagonist, at 30 mg/kg dose, did not affect, per se, DNBS-induced intestinal inflammation. A higher dose of HC030031 (i.e., 50 mg/kg) reduced, per se, DNBS-induced colitis (data not shown).

Fish oil (FO), cannabidiol (CBD) and their combination (CBD+FO) were also tested in this model. In particular we tested a dose of FO of 75 mg/mouse that was active in the DSS model (see later), daily by oral gavage starting from the

same day of DNBS administration. CBD was tested in a dose range of 0.3-30 mg/kg by oral gavage starting from the day after the DNBS administration, either alone or in combination with FO 75 mg/kg.

Antibiotic treatment

To eliminate the gut microflora, mice were treated with a mix of ampicillin (1 mg/mL), streptomycin (1 mg/mL) and clindamycin (1 mg/mL) in their drinking water (Guida et al., 2018). After two weeks of antibiotic treatment, mice started the DNBS-induced colitis protocol as reported before.

1.5.2 Dextran sulfate sodium (DSS)-induced colitis

CD1 mice received 4% dextran sulfate sodium (DSS, molecular weight 36,000–50,000; MP Biomedical, Illkirch, France) in drinking water ad libitum for five days; after that, the DSS solution was replaced with normal drinking water for additional three days (Chassaing et al., 2014); control mice received drinking water throughout the study. CBDV was administered by oral gavage [at dose of 3 mg/kg (dose found to be the most effective in the DNBS model of colitis)] once a day for six consecutive days starting three days after the start of DSS administration. The last administration of CBDV was given 2 h before the euthanasia. At day eight all mice were euthanized, the abdomen was opened by a midline incision, the colon removed, isolated from surrounding tissues, length measured, rinsed and weighed (to measure colon weight/colon length *ratio*) and the spleen was collected and weighed. The DSS dose (4% w/v) and the time points (5-day treatment and sacrifice at day 8) were selected on the basis of our preliminary experiments showing a remarkable colonic damage associated to high reproducibility and low mortality.

FO was administered once a day starting two days after DSS and continued every day until day 8 or day 14. In preliminary experiments FO was given either simultaneously or one day before CBD; results showed a greater beneficial effect of CBD, dissolved in sesame oil, when it was given by oral gavage one day after

FO (data not shown), therefore, all the experiments were carried out according to this schedule of administration [i.e., CBD was administered once a day starting one day after the administration of FO (i.e., 3 days after DSS), and continued every day until euthanasia on day 8 or day 14]. All animals were euthanized by asphyxiation with CO_2. Four experiments were carried out: Experiment 1) a dose-response curve for FO (20–50 mg/mouse each mouse weighing 28 – 30 g), to find the highest inactive dose of FO; Experiment 2) a dose-response curve for CBD (0.3–10 mg/kg by gavage in sesame oil) in the presence or absence of FO (20 mg/mouse), to find the highest inactive dose of CBD; Experiment 3) a co-administration of an inactive dose of FO (20 mg/mouse) with an inactive dose of CBD (1 mg/kg), to assess the potential stronger anti-inflammatory effects of a combination treatment in the acute and remission phases (RP) of DSS-induced colitis; and Experiment 4) a co-administration of FO at a dose of 75 mg/ mouse with different doses (0.3 – 30 mg/kg) of CBD, to determine even potentially stronger effects on markers of inflammation through the combination of non-inactive doses. In the first, second and fourth experiments, animals were sacrificed at d8, and in the third at both d8 (immediately after behavioral tests) and d14 (i.e., RP). In the third set of experiments, intestinal inflammatory parameters were evaluated at both d8 and d14, whereas behavioral tests were performed at d8 only. In the other experiments, only intestinal inflammatory parameters were evaluated at d8.

Stools were collected within 1 h directly from mice previously kept in clean separate cages at d0, d8 and d14 (immediately before the sacrifice) and quickly stored at −80°C. Body weight, food, and water consumption were measured daily throughout the experiment. Stool consistency and visible blood in faeces were also examined to determine the Disease Activity Index (DAI) score (Nishiyama et al., 2012). At the time of sacrifice, colons were removed and colon weight/colon length *ratio* was measured. Colons were then snap frozen at −80°C for determination of myeloperoxidase (MPO) activity and interleukin (IL) levels.

1.6 Induction of experimental sporadic colorectal cancer

1.6.1 Azoxymethane (AOM)-induced sporadic colorectal cancer

Mice were randomly divided into four groups (5 animals/group): group 1 (control, wild type) and group 3 (control, Trpm8$^{-/-}$) were treated with vehicles (NaCl 0.9% w/v solution); group 2 (AOM, wild type) and 4 (AOM, Trpm8$^{-/-}$) were treated with azoxymethane (AOM) at the single dose of 10 mg/kg at the beginning of the first, second, third and fourth week (40 mg/kg in total). All animals were euthanized by asphyxiation with CO_2 three months after the first injection of AOM. Based on our laboratory experience, this time (at the used dose of AOM) is associated with the occurrence of a significant number of aberrant crypt foci (ACF), polyps and tumors. In particular, mice develop pre-neoplastic lesions (ACF) 4 weeks after the first AOM administration; subsequently, they develop polyps after 8 weeks and tumors after 12 weeks (Borrelli et al., 2014). The total number of tumors was assessed on isolated colons as follows: colons were excised from the whole gastrointestinal tract, washed with cold PBS, opened along the antimesenteric border and the epithelium was quickly observed in the whole area under a stereo microscope.

1.7 Behavioral Tests

Novel object recognition (NOR) task to evaluate recognition memory and Light/Dark box test to evaluate anxiety (Guida et al., 2017; Zhu et al., 2018) were performed at day 8 in animals treated with DSS (See the third experiment in the DSS model of colitis).

1.7.1 Novel object recognition task

Novel object recognition (NOR) task was done as described previously with some modifications (Zhu et al., 2018) . Each mouse was placed in a cage (40 cm × 25 cm × 18 cm) in the presence of two identical objects (training phase) and filmed for 10 minutes. Successively, one object was replaced with a new object and mice were placed again in the cage for 10 min (testing phase). The tests were

automatically detected by a video camera coupled with video-tracking software (Any-maze, Stoelting Co., Wood Dale, IL, USA). Video clips were analyzed considering the number of explorations of the new object and the meters traveled in the cage (spontaneous locomotion). Mice with cognition disorders spend less time with the new object. After each trial, the cages and the objects were cleaned with 70% ethanol in order to remove odor cues.

1.7.2 Light/dark box test

Light/Dark box was performed as previously reported (Guida et al., 2017). Mice, one at a time, were placed for 10 min in a light and dark box apparatus, i.e., a box (60 cm × 30 cm × 30 cm) divided in a dark area and a light area (equally sized compartments, 30 x 30 cm each). Mice were placed in the light area and allowed to move freely. Time spent in dark side (mice with anxiety spent more time in dark) and number of transitions between light side and dark side (in order to observe mouse movements) were evaluated.

1.8 *In vivo* intestinal permeability

In vivo intestinal permeability was measured using a FITC-labelled dextran method, as previously described (Borrelli et al., 2015). Mice were administered with 600 mg/kg of FITC-conjugated dextran (molecular mass 3 – 5 kDa) by oral gavage 24h before the sacrifice. After 24 h, the blood was collected by cardiac puncture and the serum was immediately analysed for FITC-derived fluorescence (fluorescent microplate reader with 2104 EnVision Multilabel Plate Readers, PerkinElmer Instruments, Walthan, MA, USA) with an excitation wavelength of 485 ± 14 nm and emission wavelength of 520 ± 25 nm. Serial dilution of FITC dextran was made to generate a standard curve. Intestinal permeability was expressed as the concentrations of FITC (μM) detected in the serum.

1.9 Histology

Following euthanasia, a subset of three mice colons, randomly selected from each group, was fixed in 10% buffered formaldehyde for 24 h at room temperature and then dehydrated, paraffin embedded, 4 μm cut and mounted on glass slides. Slides were stained with Hematoxylin & Eosin using standard protocols and observed on light microscopy (LEICA DM1000, Leica Microsystem, Milan, Italy). Microscopic damage was evaluated and scored in blind by two independent pathologists according to Geboes score.

1.10 Measurements of myeloperoxidase activity

MPO activity, a peroxidase enzyme used to quantify the neutrophil infiltration in whole-tissue colons, was determined as previously described (Krawisz et al., 1984; Pagano et al., 2016). Full-thickness colons were mechanically homogenized in 0.5% w/v hexadecyltrimethylammonium bromide (HTAB) in 10 mM 3-(N-morpholino)-propanesulfonic acid (MOPS), using a *ratio* of 50 mg tissue/mL MOPS. The homogenates were centrifuged for 20 min at 15,000×g at 4 °C and an aliquot of the supernatant was incubated with sodium phosphate buffer (NaPP pH 5.5) and a 16 mM 3,3′,5,5′-tetramethylbenzidine solution in DMSO. After 5 min, hydrogen peroxide (10 mM in NaPP) was added and the reaction was stopped with acetic acid (2 M). The rate of change in absorbance was measured by a spectrophotometer at 650 nm. Different dilutions of human MPO enzyme of known concentration were used to obtain a standard curve. MPO activity was expressed as U/mg of tissue.

1.11 Gene expression analysis by quantitative PCR

Total RNA from murine and human tissues was purified, quantified, characterized and retrotranscribed. Final preparation of RNA was considered DNA- and protein-free if the integrity number (Bionalyzer 2100, Agilent) was greater than 8 in a 0–10 scale. Quantitative real-time PCR was carried out in an

iCycleriQ5 system (Biorad, MI, Italy) by use of SYBR Green detection. Selective primers were either purchased from Integrated DNA Technologies (Iowa, USA) or designed using Allele-Id software version 7.0 (Biosoft International, Palo Alto, CA, USA) and synthesized by MWG-Biotech (HPLC purification grade) (Table 1). Each sample was amplified simultaneously in a quadruplicate in one-assay run (maximum ΔCt of replicate samples <0.5), and a standard curve from consecutive fivefold dilutions (100–0.16 ng) of a cDNA pool representative of all samples was included for PCR efficiency determination. Data normalization was performed by using as a control the Ct from S16 and/or HPRT, both constitutively expressed proteins; differences in mRNA content between groups were calculated as normalized values by use of the $2^{-\Delta\Delta Ct}$ formula.

1.12 Enzyme-linked immunosorbent assay

Interleukin (IL)-1β, IL-10 and IL-6 concentrations in homogenate obtained from full-thickness mice colonic tissues or from human mucosal colonic biopsies were determined using commercial ELISA kits (ThermoFisher Scientific, Milano) according to manufacturer's instructions.

1.13 HPLC-MS/MS analysis for quantification of lipid mediators and phytocannabinoids

Lipid extraction was performed following the Bligh and Dyer method (Bligh and Dyer, 1959). Briefly, approximately 10 mg of colon tissues were homogenized in 1 mL of Tris-HCl 50 mM pH 7 and methanol (1/1) using a tissue grinder; 200 µL of the mixture were transferred in a new tube and then added 800 µL (1:5 dilution) of the same Tris-HCl/methanol solution containing 0.1 M acetic acid and 5 ng of deuterated standards. An organic phase extraction with chloroform was performed on each sample by adding 1 mL of chloroform in the mixture, vortexing for 30 seconds and centrifuging at 3000 g for 5 minutes. This was repeated three times for a total of 3 mL of chloroform. The organic phases

Table 1. List of primers used in RT-PCR analysis

Gene name	**Forward (5'-3')**	**Reverse (5'-3')**
Murine IL-1β	TATACCTGTCCTGTGTAAA	TTGACTTCTATCTTGTTG
Murine IL-10	TTATTACCTCTGATAATCT	CCATCATATAATATAATCTCC
Murine IL-6	CCTGGAGTACATGAAGAA	TGGTTGAAGATATGAATTAGAGT
Murine MCP1-α	TTGTATTTGTGACTATTTATTCT	GGCATATTTATTACTTCTCTG
Murine TNFα	GGTGCCTATGTCTCAGCCTCTT	GCCATAGAACTGATCAGAGGGAG
Murine TRPA1	GGAGATATGTGTAGATTAGAAGAC	TCGGAGGTTTGGATTTGC
Murine TRPV1	CTACCTCGTGTTCTTGTT	AGGCAGTGAGTTATTCTTC
Murine TRPV2	AACAAAGGAAAGAATGAG	GGTAGTTGAGATTCACTTT
Murine TRPV3	AACACCAACATTGATAAC	AGAAGGACAAGAAGAAC
Murine TRPV4	AAAGACTTGTTCACGAAG	CACAGAGTAGATGAAGTAGAG
Murine β-actin	CCAGGCATTGCTGACAGG	TGGAAGGTGGACAGTGAGG
Murine HPRT	TTGACACTGGTAAAACAATGC	GCCTG TATCCAACACTTCG
Human TRPA1	ACCCAAATCTCCGAAACTTCAAC	CTCAAGCAAGACCTTCATCACC
Human S16	TCGGACGCAAGAAGACAGCGA	AGCGTGCGCGGCTCAATCAT

were then collected and evaporated under a nitrogen flow and dissolved in 50 µL of mobile phase containing 50% of solvent A (water + 1mM ammonium acetate + 0,05% acetic acid) and 50% of solvent B (acetonitrile/water 95/5 + 1 mM ammonium acetate + 0.05% acetic acid).

After that, 40 µL of each sample were injected into an HPLC column (Kinetex C8, 150 × 2.1 mm, 2.6 µm, Phenomenex) and eluted at a flow rate of 400 µL/min using a discontinuous gradient of solvent A and solvent B. Quantification of lipid mediators was carried out by using an HPLC system interfaced with the electrospray source of a Shimadzu 8050 triple quadrupole mass spectrometer and using multiple reaction monitoring in positive ion mode the compounds of interest and their deuterated homologs (Manca et al., 2020).

CBD levels in mice colons were measured by using an LC20AB coupled to a hybrid detector IT-TOF (Shimadzu Corporation, Kyoto, Japan) equipped with an electrospray ionization interface as previously described (Piscitelli et al., 2017).

1.14 Metagenomic analysis by 16S rRNA gene sequencing

Fecal microbiota was analyzed from fecal samples that were collected at different time points: T0 (before the induction of the colitis) and T3 (three days after the induction of colitis by DNBS) for the DNBS-induced colitis; T0 (before the first DSS administration); T8 (after 8 days, in the acute phase) and T14 (after 14 days, in the remission phase) in the DSS-induced colitis; in the AOM-induced colorectal cancer model, taking in account the time dependent development of preneoplastic lesions, polyps and tumors, we collected fecal samples at the beginning of the protocol and at the fifth, ninth and thirteenth week. All the fecal samples were collected using a clean single cage per each mouse, and then immediately frozen at -80 °C.

DNA form AOM-treated mice and the corresponding control group was extracted from faeces using the QIAmp PowerFecal DNA kit (Qiagen, Hilden, Germany) according to the manufacturers' instructions. The DNA concentrations

of the extracts were measured fluorometrically with the Quant-iT PicoGreen dsDNA Kit (Thermo Fisher Scientific, MA, USA) and the DNAs were stored at −20 °C until 16S rDNA library preparation. Briefly, 1 ng of DNA was used as template and the V3-V4 region of the 16S rRNA gene was amplified by polymerase chain reaction (PCR) using the QIAseq 16S Region Panel protocol in conjunction with the QIAseq 16S/ITS 384- Index I (Sets A, B, C, D) kit (Qiagen, Hilden, Germany) (Rausch et al., 2019). The 16S metagenomic libraries were eluted in 30 μL of nuclease-free water and 1 μL was qualified with a Bioanalyzer DNA 1000 Chip (Agilent, CA, USA) to verify the amplicon size (expected size ~600 bp) and quantified with a Qubit (Thermo Fisher Scientific, MA, USA). Libraries were then normalized and pooled to 2 nM, denatured and diluted to a final concentration of 6 pM and supplemented with 5% PhiX control (Illumina, CA, USA). Sequencing (2 × 275 bp paired-end) was performed using the MiSeq Reagent Kit V3 (600 cycles) on an Illumina MiSeq System. Sequencing reads were generated in less than 65 h. Image analysis and base calling were carried out directly on the MiSeq.

For CBDV fecal samples, V3-V4 16S rDNA FASTQ paired-end reads were pre-processed with PEAR (Zhang and Li, 2014) in order to assemble reads with an overlap of at least 40 nucleotides, and to retain high quality sequences (PHRED score ≥ 33) that were comprised between 400 and 500 bp. These reads were then processed with PRINSEQ (Schmieder and Edwards, 2011) in order to obtain FASTA and QUAL files for further analyses. Pick of operational taxonomic units (OTUs), taxonomic assignment and diversity analyses were conducted using Quantitative Insights Into Microbial Ecology (QIIME, version 1.8.0) (Caporaso et al., 2010). A closed reference-based OTU picking method was employed to obtain OTUs at 97% sequence similarity from Greengenes 16S gene database (GG; May 2013 version) (DeSantis et al., 2006). The GG database was used to taxonomically classify the identified OTUs and to compute their distribution across different taxonomic levels. To avoid sample size biases in

subsequent analyses, samples were normalized to 18,871 sequences/sample using a sequence rarefaction procedure. Species heterogeneity in each sample was assessed by employing two Alpha diversity metrics (the number Observed species and the Shannon entropy) and compared using a two-sample permutation t-test, using 999 Monte Carlo permutations to compute p-values. Unweighted and weighted Unifrac distances were calculated to analyze OTUs diversity among sample communities (beta diversity). Species and *Clostridium* cluster classification was performed using SPecies level IdentificatioN of metaGenOmic amplicons package (SPINGO version 1.3) with default parameters on a representative sequence of each OUT (Allard et al., 2015).

For the other fecal samples, FASTQ files were processed using the DADA2 pipeline and taxonomic assignation with reference to the RDP database (Callahan et al., 2016). All sequences were cumulative sum scaled (CSS) (Paulson et al., 2013).

1.15 Statistical analysis

Statistical analysis was performed using GraphPad Prism version 8.1.2. Data are expressed as the mean ± SEM of *n* experiments, or as median interquartile range (IQR) with bars showing the minimum and maximum values. Outliers were identified by ROUT test.

Normal data were compared via Student's *t* test (for comparing a single treatment mean with a control mean) or one-way analysis of variance (ANOVA) with Dunnett's or Tukey's post hoc test and non-normal data were compared via Kruskal–Wallis with Dunn's test. $p<0.05$ was considered to be significant.

Statistical analysis of parameters measured in ABX-treated or germfree mice, compared to conventionally-raised mice, was performed using two-way ANOVA followed by Fisher's Least Significant Difference (LSD) test.

Statistical analysis of microbiota composition analyzed with Principal Coordinate Analysis (PCoA), using the Bray-Curtis dissimilarity indexes to estimate beta-

diversity, was carried out using the PERMANOVA test. Cumulative Sum Scale (CSS) graphs were analysed using Student's *t* test or Two-way ANOVA followed by Tukey test for multiple comparison post-hoc analysis. $p<0.05$ was considered to be significant.

RESULTS

Part I – Cannabidivarin (CBDV) counteracts chemically-induced ulcerative colitis and microbiota dysbiosis in mice via TRPA1 activation

1.1 DNBS administration induces ulcerative colitis

Intracolonic administration of DNBS, either in the preventive or curative protocols (Figure 11), caused inflammatory signs such as increased colon weight/colon length *ratio* and intestinal permeability, neutrophil infiltration (measured by MPO activity), histological damage, production of pro-inflammatory cytokines and a decrease in the anti-inflammatory cytokine IL-10 (Figures 12-14).

1.2 CBDV reduces colon weight/colon length ratio in DNBS-induced ulcerative colitis

Oral or intraperitoneal administration of CBDV (0.3-10 mg/kg) resulted in a significant reduction in the *ratio* of colon weight/colon length increased by DNBS administration in both the preventive and curative protocols (Figure 12). Specifically, intraperitoneal administration of CBDV resulted in a statistically significant reduction from 3 mg/kg dose in the preventive protocol and from 10 mg/kg dose in the curative protocol (Figures 12A and 12B). A statistically significant reduction in the colon weight/colon length was achieved by oral gavage administration of CBDV starting from a 1 mg/kg dose in the preventive protocol and 3 mg/kg dose in the curative protocol (Figures 12C and 12D). As the aim of pharmacological treatment of IBD is to reduce the inflammatory status in the relapsing phases of the disease, further studies have been conducted using the curative protocol.

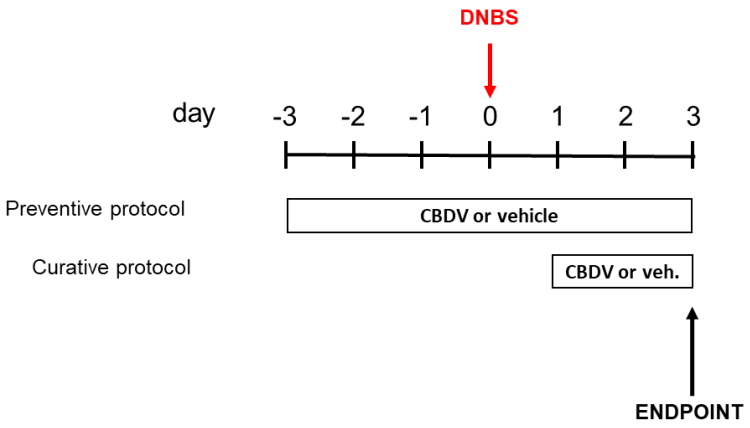

Figure 11. Schematic representation of administration protocols of CBDV in DNBS-induced colitis. DNBS was injected in mice colon at the dose of 150 mg/kg. CBDV was administered once a day either by oral gavage or intraperitoneal injection in a dose range of 0.3-30 mg/kg. CBDV treatment started three days before DNBS administration in the preventive protocol and one day after DNBS administration in the curative protocol; mice were killed three days after the DNBS administration. Feces were collected in the curative protocol the day before DNBS administration and at the endpoint for gut microbiota analysis.

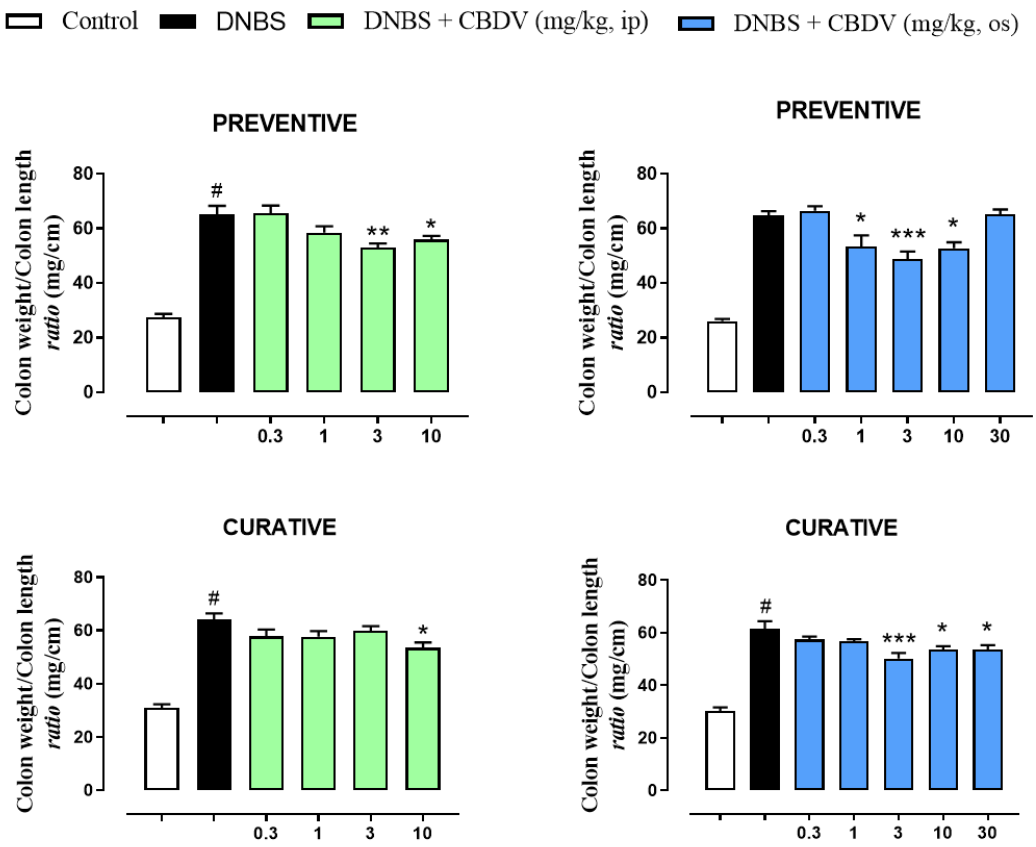

Figure 12. Preventive and curative effect of cannabidivarin (CBDV) on colon weight/colon length *ratio* in DNBS-induced colitis in mice. DNBS was injected in mice colon at the dose of 150 mg/kg. CBDV was administered once a day either by oral gavage or intraperitoneal injection in a dose range of 0.3-30 mg/kg. CBDV treatment started three days before DNBS administration in the preventive model (A, C) and one day after DNBS administration in the curative model (B, D); mice were killed three days after the DNBS administration. Data are expressed as mean ± SEM of 7 mice for each experimental group. Data were statistically analyzed using one-way ANOVA followed by the Dunnett's multiple comparisons test. #p<0.001 *vs* control, *p<0.05, **p<0.01 and ***p<0.001 *vs* DNBS alone.

1.3 CBDV decreases neutrophil infiltration and intestinal permeability in DNBS-induced ulcerative colitis

The curative effect of CBDV at the dose of 10 mg/kg (i.p.) and 3 mg/kg (o.s.) on DNBS-induced colitis was further confirmed by analysis of other parameters of intestinal inflammation. Neutrophil infiltration was determined by measuring MPO activity. As expected, DNBS administration increased MPO activity, which was significantly reduced by CBDV treatment in both the 10 mg/kg i.p. and 3 mg/kg o.s. treated groups (Figures 13A and 13B). Experimental and clinical colitis are known to cause abnormal gut permeability (Atreya and Neurath, 2015). To measure the change in gut barrier permeability, we measured serum levels of FITC-dextran after its oral administration. DNBS-treated mice had higher serum FITC-dextran concentrations than the control group. Administration of CBDV reduced the increase in FITC-dextran when administered both intraperitoneally and via oral gavage (Figures 13C and 13D). Since a significant anti-inflammatory effect of CBDV (as measured by colon weight/colon length *ratio*, MPO activity and barrier function) was obtained at the lower dose of 3 mg/kg after oral administration than after i.p. injection, and since the oral route of administration is more clinically relevant, we next focused our attention on the effect of CBDV administered by oral gavage.

1.4 CBDV lessens histological damage and pro-inflammatory cytokines production in DNBS-induced ulcerative colitis

Histological analysis of H&E-stained colon sections showed that DNBS administration induced acute inflammation of the colon mucosa characterised by erosions, ulceration, edema, hyperplasia, loss of goblet cells, disruption of crypt integrity and massive infiltration of inflammatory cells (Figure 14A). Administration of CBDV (3 mg/kg, o.s.) resulted in a reduction in damage, mucosal ulceration and mononuclear cell infiltration (Figure 14A). Mice treated

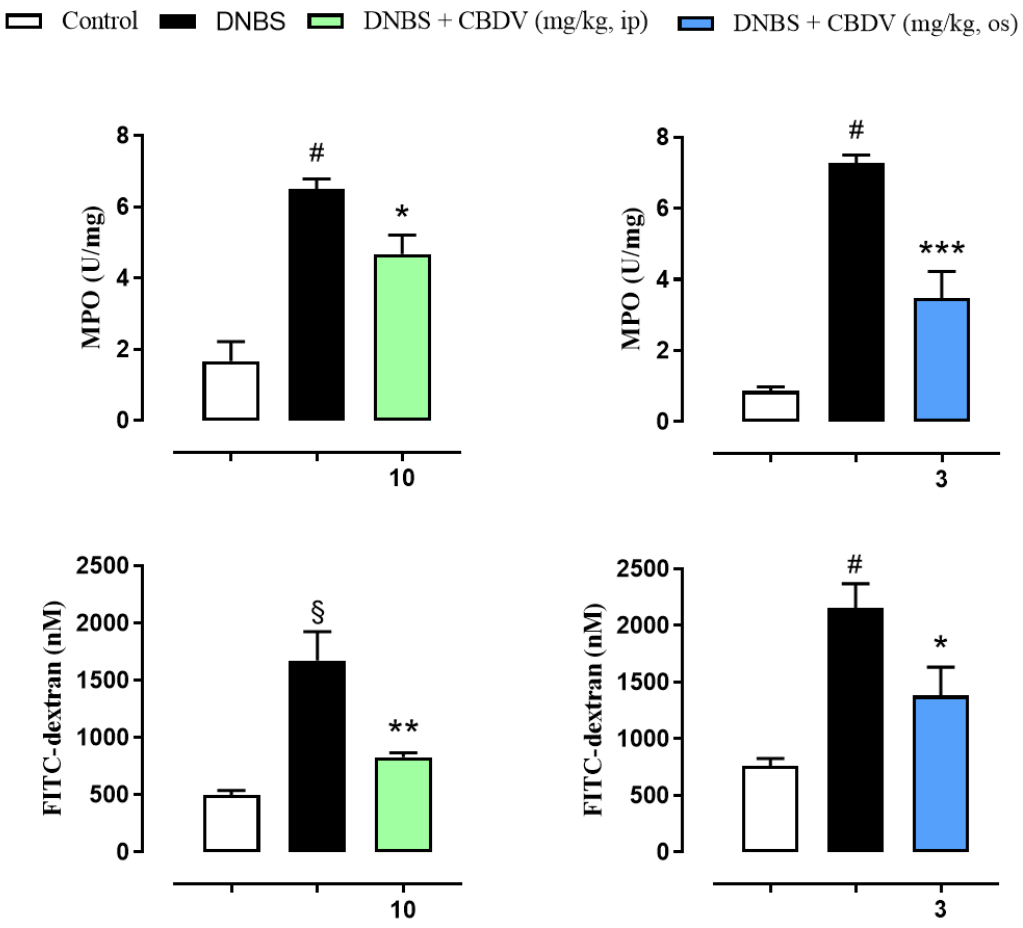

Figure 13. Therapeutic effect of cannabidivarin (CBDV) on inflammatory parameters in DNBS-induced colitis. DNBS was injected in mice colon at the dose of 150 mg/kg. CBDV was administered once a day, either by oral gavage (3 mg/kg) or intraperitoneal injection (10 mg/kg), starting one day after DNBS administration; mice were killed three days after the DNBS administration and inflammation was evaluated on myeloperoxidase (MPO) activity (A and B) and intestinal permeability (C and D). Data are expressed as mean ± SEM of 6 mice for each experimental group. Data were statistically analyzed using one-way ANOVA followed by the Dunnett's multiple comparisons test. §$p<0.01$ and #$p<0.001$ *vs* control, *$p<0.05$, **$p<0.01$ and ***$p<0.001$ *vs* DNBS alone.

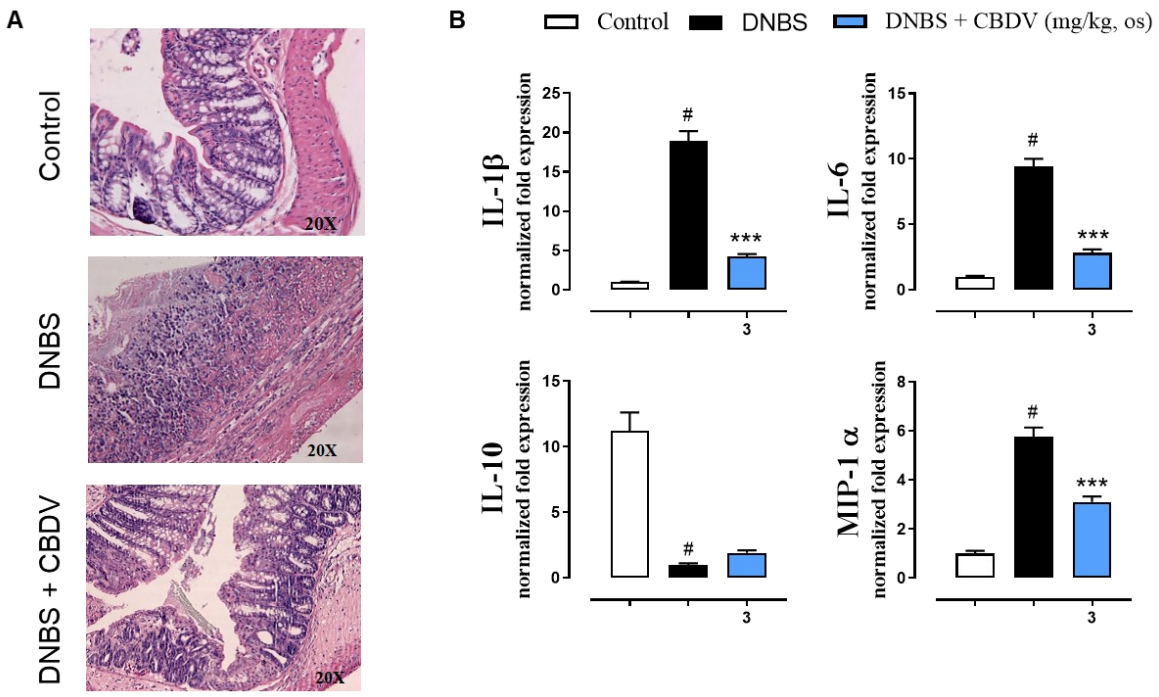

Figure 14. Therapeutic effect of cannabidivarin (CBDV) on histological damage and inflammation-related proteins in DNBS-induced acute colitis. DNBS was injected in mice colon at the dose of 150 mg/kg. CBDV was administered once a day by oral gavage (3 mg/kg) starting one day after DNBS administration; mice were killed three days after the DNBS administration. A) Representative H&E-stained colon cross-sections of mice treated with vehicle, DNBS and DNBS plus CBDV (3 mg/kg, o.s.). B) IL-1β, IL-6, MCP-1α and IL-10 colonic expression, evaluated by qPCR analysis, in vehicle, DNBS or DNBS plus CBDV-treated mice (B). Data are expressed as mean ± SEM of 3 mice for each experimental group. Data were statistically analyzed using one-way ANOVA followed by the Dunnett's multiple comparisons test. #p<0.001 *vs* control, ***p<0.001 *vs* DNBS alone.

with CBDV without DNBS showed no histological signs of colitis (data not shown). The effect of CBDV was also confirmed by quantification of a panel of cytokines dysregulated by DNBS administration, as determined by quantitative (q)-PCR. Administration of CBDV (3 mg/kg, o.s.) decreased mRNA levels of pro-inflammatory cytokines in the colon (i.e., IL-1β and IL-6), but did not alter levels of IL-10, the major anti-inflammatory cytokine (Figure 14B). In addition, CBDV (3 mg/kg, o.s.) decreased colonic mRNA expression of monocyte chemoattractant protein-1 (MCP-1), a chemokine responsible for macrophage migration into inflamed tissue (Figure 14B).

Since IL-1β levels showed a higher increase (about 19-fold increase) compared to the other cytokines, we also measured its expression by ELISA. Consistent with the mRNA expression data, CBDV decreased IL-1β protein levels in the colon of DNBS-treated mice by 78% [IL-1β (pg/mL): control, 1283.2±50.1; DNBS, 2828.3 ± 404.7#; DNBS+CBDV 3 mg/kg p.o., 1618.1 ± 128.3*; #p<0.01 *vs* control and *p<0.01 *vs* DNBS alone; mean ± SEM, n=6].

1.5 CBDV reduces alterations in gut microbiota composition induced by DNBS administration

Amplicon sequencing of the 16S rRNA gene (regions V3-V4) was performed on a subset of animals randomly selected from each group (control, DNBS and DNBS plus CBDV at time points T0 and T3). The sequencing process yielded 1,139,314 high-quality sequences from 18 fecal samples assigned to a total of 2968 operational taxonomic units (OTUs). A sequencing depth of 18,871 sequences/sample, with a good's coverage greater than 98%, was considered for describing and comparing the composition of the gut microbiota (GM) between the groups studied. The total number of OTUs observed at sequencing depth was 2261. Alpha diversity revealed no significant differences between groups and showed no significant variation in species richness and distribution after treatment (Table 2). To analyse phylogenetic distances between all groups at T0

and T3, we used unweighted beta diversity (OTUs presence or absence) and weighted beta diversity (abundance of all common OTUs); both analyses showed significant differences in gut microbiota composition between groups at T3 (Figures 15A and 15B). In particular, the faecal microbial composition showed a significant increase in phylogenetic distance compared to control samples after DNBS administration (T3), indicating a shift in species type and a strong change in the relative abundances of shared species (Figures 15A and 15B), demonstrating the presence of strong dysbiosis in the DNBS-treated groups. Co-administration of CBDV showed a trend towards a reduction in UniFrac abundance in terms of type and relative abundance of species compared to DNBS-treated mice, resulting in a microbiota profile closer to that of the control group (Figures 15A and 15B). Profiling and comparison of GM between the different groups was performed at the phyla level at time T3 (Figure 15C). *Firmicutes* and *Bacteroidetes* were the most abundant phyla detected in all groups. There was a marked increase of *Proteobacteria* in DNBS-treated mice compared to control mice. Co-administration of CBDV showed a trend towards restoring the abundance of this phylum to control levels; furthermore, CBDV administration resulted in a decrease in the relative abundance of *Firmicutes* compared to DNBS (Figure 15C).

To find changes at the species level, Greengene's taxonomic classification of bacterial genera was implemented using the SPINGO package (Table 3). Among the significant genera, the U.g. of *Bacteroidales* was significantly increased by CBDV in DNBS-induced colitis (Table 3). We found that several bacterial species assigned to *Clostridium cluster* XIVa and IV decreased by DNBS treatment. Among these, *Clostridium aldenense*, was increased and partially restored to control levels by oral CBDV treatment (Table 3).

Table 2. Alpha diversity for 16S rRNA gene sequences at 97% similarity from NGS analysis. Alpha diversity indexes are reported as mean ± SD.

Group	Observed species	Shannon entropy	Good's coverage (%)
CTRL T0	713.00 ± 8.04	6.48 ± 0.24	98.70 ± 0.03
DNBS T0	653.97 ± 53.27	6.30 ± 0.24	98.78 ± 0.07
DNBS + CBDV T0	751.00 ± 25.96	6.85 ± 0.09	98.74 ± 0.04
CTRL T3	695.30 ± 64.21	6.36 ± 0.21	98.72 ± 0.17
DNBS T3	548.67 ± 106.93	5.74 ± 0.67	98.99 ± 0.19
DNBS + CBDV T3	695.30 ± 64.21	6.48 ± 0.24	98.93 ± 0.13

T0: before DNBS administration; T3: three days after DNBS administration (endpoint)

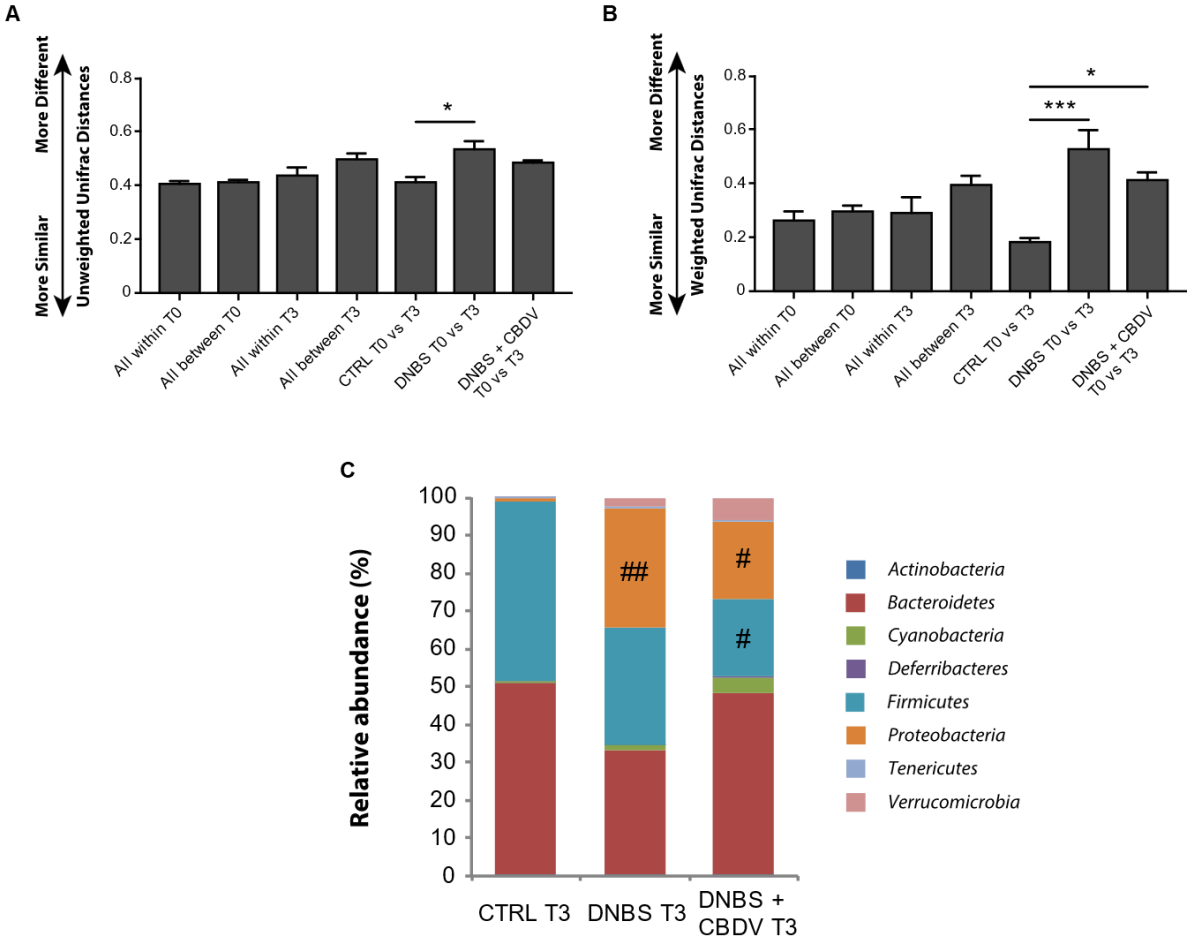

Figure 15. Differences in fecal microbiota composition before (at time points T0) or three days after (at time point T3) the induction of colitis, in presence or absence of CBDV administration. DNBS was injected in mice colon at the dose of 150 mg/kg. CBDV was administered once a day by oral gavage (3 mg/kg) starting one day after DNBS administration; mice were killed three days after the DNBS administration. Comparison of A) unweighted and B) weighted Unifrac phylogenetic distances; C) percentage distribution of all bacterial phyla identified with 16S rRNA gene sequencing at time point T3 (three day after the induction of colitis and CBDV treatment. Data are expressed as mean ± SEM (A, B) or % of relative abundance (C). Data were statistically analyzed using one-way ANOVA followed by the Dunnett's multiple comparisons test. *$p<0.05$ and ***$p<0.001$; #$p<0.05$ and ##$p<0.01$ *vs* Control T3 (CTRL T3) (n=3 mice for each experimental group).

Table 3. Significant bacterial species belonging to key genera discriminating T3 groups.

Significant genera	Species	Control (T3)	DNBS (T3)	DNBS + CBDV (T3)
U.g. Bacteroidales	*Cytophaga fermentaris (ambiguous)*	0.04 ± 0.03	0.05 ± 0.03	0.70 ± 0.26*
U.g. Clostridiales	*AMBIGUOUS*	2.37 ± 0.51	0.31 ± 0.18*	0.32 ± 0.22*
	Anaerosporobacter mobilis	0.08 ± 0.03	0.00 ± 0.00*	0.00 ± 0.00*
	Clostridium aldense	3.30 ± 0.32	0.25 ± 0.14*	1.20 ± 0.87
	Clostridium asparagiforme	2.81 ± 0.80	0.01 ± 0.01*	0.05 ± 0.04*
	Clostridium celerecrescens	1.19 ± 0.40	0.05 ± 0.03*	0.05 ± 0.04*
	Clostridium hylemonae	0.11 ± 0.03	0.01 ± 0.01*	0.01 ± 0.00*
	Clostridium saccharolyticum	2.89 ± 0.37	0.18 ± 0.10***	0.39 ± 0.16***
	Filifactor villosus	0.22 ± 0.08	0.01 ± 0.01*	0.01 ± 0.00*
	Oscillibacter valericigenes	0.12 ± 0.03	0.02 ± 0.01*	0.02 ± 0.01*
	Oscillospira guilliermondii	0.13 ± 0.02	0.05 ± 0.02*	0.02 ± 0.01*
U.g. Lachnospiraceae	*Clostridium Asparagiforme*	0.36 ± 0.08	3.5E-05 ± 1.8E-05**	0.02 ± 0.01**
U.g. Ruminococcaceae	*Butyricicoccus pullicaecorum*	0.69 ± 0.20	0.13 ± 0.05*	0.07 ± 0.04*
	Flavonifracotr plautii	0.25 ± 0.06	0.04 ± 0.02*	0.05 ± 0.03*
	Intestinimonas butyriciproducens	0.22 ± 0.04	0.03 ± 0.01**	0.02 ± 0.01**
	Oscillibacter valericigenes	3.51 ± 0.65	0.65 ± 0.35**	0.62 ± 0.16**
	Oscillospira guilliermondii	0.17 ± 0.02	0.02 ± 0.01**	0.03 ± 0.01**

SPINGO classification of significant bacterial species according to Ribosomal Database Project taxonomy (80% minimum bootstrap cutoff). Bacterial species with relative abundance > 0.1% in at least one of the 3 groups are shown (mean ± SEM). Variations in species' relative abundances among control T3, DNBS T3 and DNBS plus CBDV T3 and groups were assessed by one-way ANOVA followed by Tukey's multiple comparison post-hoc test (*p<0.05, **p<0.01 and ***p<0.001 *vs* control T3).

1.6 CBDV decreases TRPA1 upregulation in DNBS-induced ulcerative colitis

Since CBDV is able to potently activate (EC_{50} = 0.42 ± 0.01 μM,) and subsequently desensitise (IC_{50} = 1.29 ± 0.38 μM) the TRPA1 channel (De Petrocellis et al., 2011) we focused on the possible involvement of TRPA1 to understand the mode of action of CBDV; therefore, we first investigated the effect of CBDV on TRPA1 expression during experimental acute colitis.

Consistent with previous studies (Engel et al., 2011), DNBS-induced intestinal inflammation caused a significant upregulation of the TRPA1 channel. Interestingly, oral administration of CBDV completely counteracted the DNBS-induced increase in TRPA1 expression (Figure 16A). To understand whether the effect of CBDV was selective for TRPA1, we also measured the expression of TRPV1 and TRPV2, two other members of the TRPs channel family known to be targeted by higher concentrations of CBDV and dysregulated in ulcerative colitis (De Petrocellis et al., 2011; De Petrocellis et al., 2012; Bertin et al., 2014; Issa et al., 2014). Administration of DNBS significantly downregulated TRPV1 without altering TRPV2 expression, whereas treatment with CBDV did not alter TRPV1 or TRPV2 expression in DNBS-treated mice (Figures 16B and 16C).

1.7 TRPA1 is involved in CBDV mechanism of action

To further confirm the possible involvement of TRPA1 in the anti-inflammatory effect of CBDV in the gut, we tested it in the presence of HC030031, a selective TRPA1 antagonist. Co-administration of HC030031 decreased the anti-inflammatory effect of CBDV, as shown by MPO activity and by colon weight/colon length *ratio* (Figures 16D and 16E). The TRPA1 antagonist HC030031 did not alter, *per se*, DNBS-induced colitis at the dose used in this study (30 mg/kg) [MPO (U/mg tissue) DNBS 7.03 ± 0.72; HC030031 (30 mg/kg) 6.85 ± 0.97; mean ± SEM, n=6].

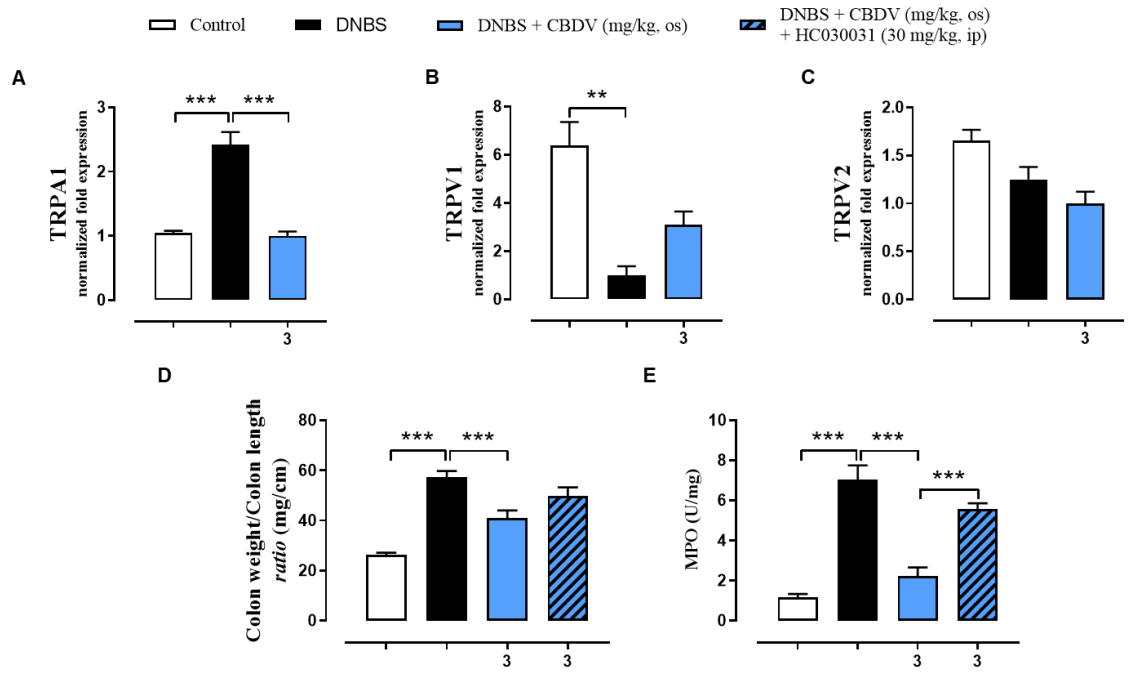

Figure 16. Involvement of TRPA1 in the anti-inflammatory effect of cannabidivarin (CBDV) in DNBS-treated mice. DNBS was injected in mice colon at the dose of 150 mg/kg. CBDV was administered once a day by oral gavage (3 mg/kg) starting one day after DNBS administration; mice were killed three days after the DNBS administration. Expression (by qPCR) of TRPA1 (A) and, for comparison, of TRPV1 (B) and TRPV2 (C) in mice colon treated with vehicle, DNBS or DNBS plus CBDV. D) Effect of CBDV alone or in the presence of the TRPA1 receptor antagonist HC030031 (30 mg/kg, i.p.) on MPO activity and E) colon weight/colon length *ratio* in mice with experimental colitis induced by DNBS. Data are expressed as mean ± SEM of 6 mice for each experimental group. Data were statistically analyzed using one-way ANOVA followed by the Tuckey's multiple comparisons test. **p<0.01 and ***p<0.001.

1.8 TRPA1 is overexpressed in UC paediatric patients

While the role of TRPA1 in visceral pain in adult IBD patients is well established (Kun et al., 2014), its expression in paediatric IBD patients has not been studied. Consistent with the results obtained in colitis samples from mice (see above), TRPA1 was found to be overexpressed in the inflamed colon of children with active UC compared to non-inflamed tissue (Figure 17A).

1.9 CBDV reduces IL-1β levels in biopsies from UC paediatric patients

To verify the potential anti-inflammatory effect of CBDV in humans, we investigated its effect in colonic mucosal biopsies obtained from children with active UC. Patients were clinically assessed using the Geboes score. IL-1β levels, assessed by ELISA in the supernatant collected from human colon tissues treated with CBDV (10 μM) were lower compared to inflamed untreated biopsies (Figure 17B).

1.10 CBDV attenuates intestinal inflammation in DSS-induced ulcerative colitis

In the model of DSS-induced colitis (Figure 18), CBDV (3 mg/kg, o.s.) exerted anti-inflammatory effects reducing colon weight/colon length *ratio* as well as DSS-induced splenomegaly (Figures 19A and 19B). In addition, CBDV treatment significantly reduced MPO activity and IL-1β levels in the colon of DSS-treated mice and caused a complete, although not statistically significant, reduction in IL-6 levels (Figures 19C and 19D). According to the DNBS model, CBDV had no effect on the expression of the anti-inflammatory cytokine IL-10 (Figure 19D).

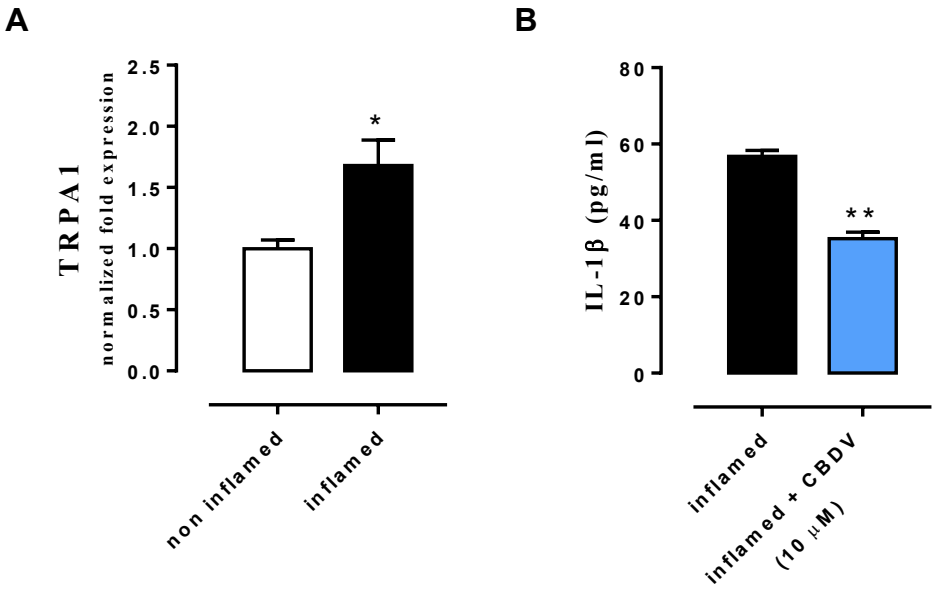

Figure 17. Effect of cannabidivarin (CBDV) on the colonic mucosa of paediatric patients with active UC. A) Expression of TRPA1 in colonic mucosa collected from non-inflamed and inflamed area of paediatric patients with active UC. B) Effect of CBDV (10 μM) was evaluated on IL-1β production in inflamed colonic biopsies. * Data are expressed as mean ± SEM of 4 tissues for each experimental group. Data were statistically analyzed Student's *t* test. * < 0.05 *vs* non inflamed tissues and **p<0.01 *vs* untreated inflamed tissues

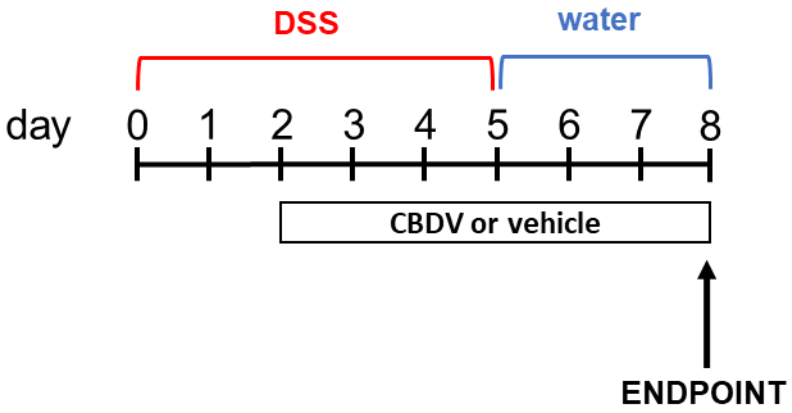

Figure 18. Schematic representation of administration protocols of CBDV in DSS-induced colitis. DSS, dissolved in drinking water at 4% w/v, was given for five consecutive days and then replaced with normal drinking water. CBDV (3 mg/kg) was administered once a day by oral gavage starting two days after the start of DSS administration. Mice were killed on the peak of inflammation, i.e., seven days after the beginning of DSS administration (on day 8).

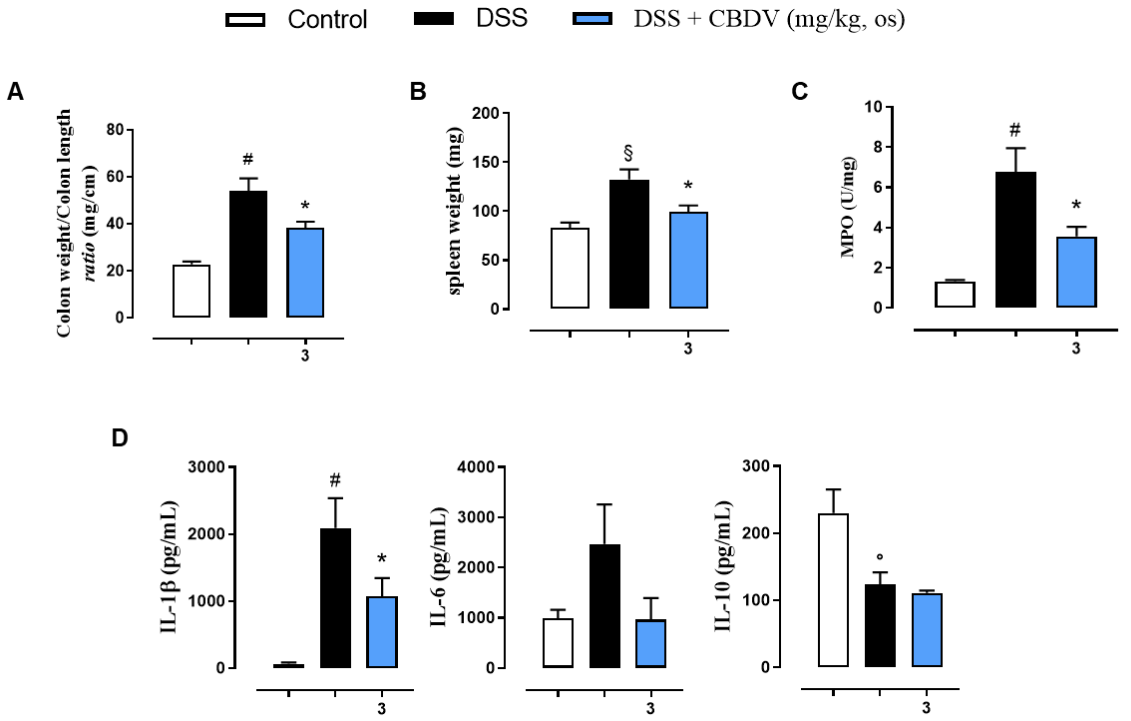

Figure 19. Therapeutic effect of cannabidivarin (CBDV) on colon weight/colon length *ratio* and splenomegaly in DSS-induced colitis. DSS was dissolved in drinking water at 4% w/v and given to mice for five days; then DSS was replaced with normal drinking water. CBDV was administered once a day by oral gavage at the dose of 3 mg/kg (previously found to be the more effective dose) starting two days after the beginning of DSS administration; mice were killed seven days after the beginning of DSS administration and colons and spleens were collected. A) colon weight/colon length *ratio*; B) spleen weight; C) MPO colonic activity; D) IL-1β, IL-6, and IL-10 colonic levels were evaluated in vehicle, DSS or DSS plus CBDV-treated mice. Data are expressed as mean ± SEM of 7 mice for each experimental group. Data were statistically analyzed using one-way ANOVA followed by the Dunnett's multiple comparisons test. °$p<0.05$, §$p<0.01$ and #$p<0.001$ *vs* control, *$p<0.05$ *vs* DSS alone.

Part II – Combined administration of cannabidiol (CBD) and fish oil (FO) counteracts chemically-induced ulcerative colitis and microbiota dysbiosis in mice

2.1 DSS consumption induces ulcerative colitis

In the first three sets of experiments (Figure 20), DSS consumption caused colon inflammation, as revealed by DAI score, colon weight/colon length *ratio*, MPO activity, intestinal permeability, cytokines production and appearance of stress and anxiety related behaviours (Figure 21-24).

2.2 FO administration reduces DSS-induced ulcerative colitis in a dose-dependent manner

Fish oil administration, by oral gavage (20, 35 and 50 mg/mouse) to DSS-treated mice, significantly and in a dose-dependent manner, decreased colon weight/colon length *ratio* (Figure 21A), DAI score (Figure 21B) and MPO activity (Figure 21D); in contrast, DSS-induced body weight loss was not affected by any of the FO doses (Figure 21C).

2.3 Combined administration of CBD and FO, at per se ineffective doses, reduces colon inflammation in DSS-induced ulcerative colitis

Oral gavage administration of CBD (0.3-10 mg/kg) had no effect on DSS-induced intestinal inflammation for any of the four endpoints measured (Figure 22). However, co-administration of a *per se* inactive dose of FO (20 mg/mouse) with CBD, reduced inflammatory parameters such as colon weight/colon length *ratio* (Figure 22A), DAI score (Figure 22B) and MPO activity (Figure 22D), but not body weight loss (Figure 22C), compared to DSS-treated mice. CBD 1 mg/kg was the most effective dose and was therefore, selected for the following experiment.

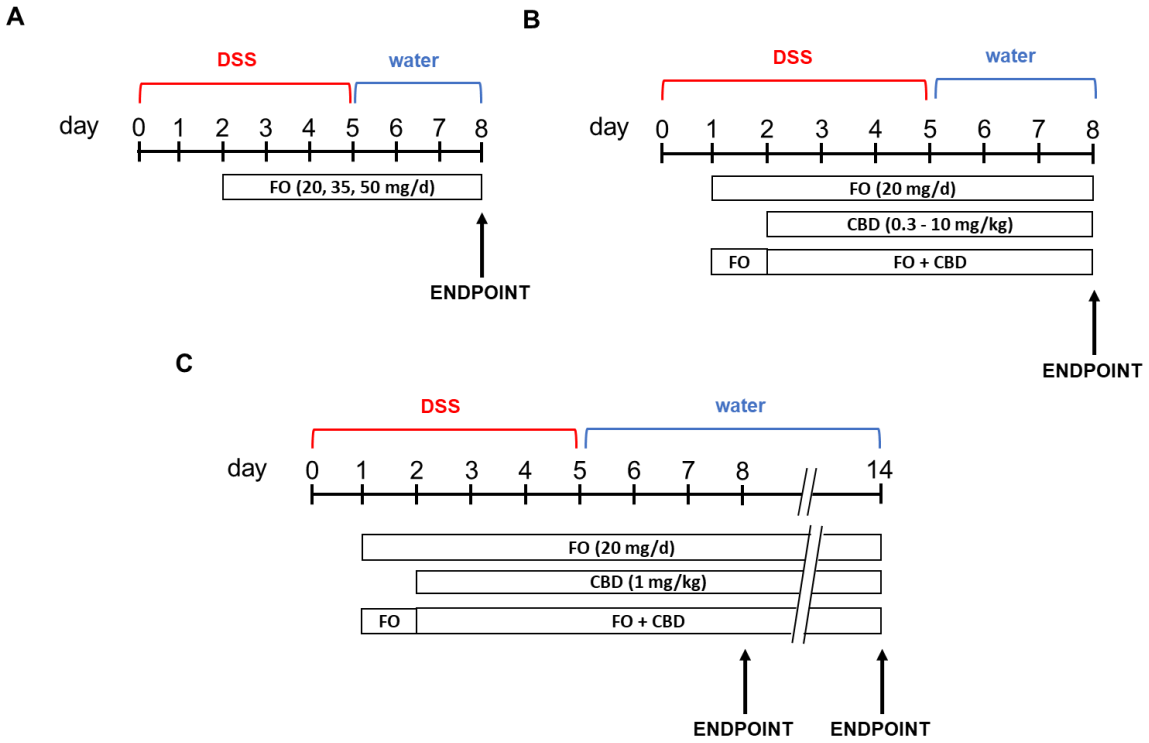

Figure 20. Schematic representation of different combination of CBD and FO on DSS-induced ulcerative colitis. A) dose response of FO given alone; B) inactive dose of FO in combination with a dose range of CBD; C) co-administration of ineffective doses of CBD and FO. DSS, dissolved in drinking water at 4% w/v, was given for five consecutive days and then replaced with normal drinking water. Mice were killed on the peak of inflammation, i.e., eight days after the beginning of DSS administration (on day 8, in A, B and C) or in the resolving period, i.e., fourteen days after the beginning of DSS administration (on day 14, in C). Feces were collected at different timepoints (day 1, day 8 and day 14) for gut microbiota analysis; behavioural tests were performed on day 8.

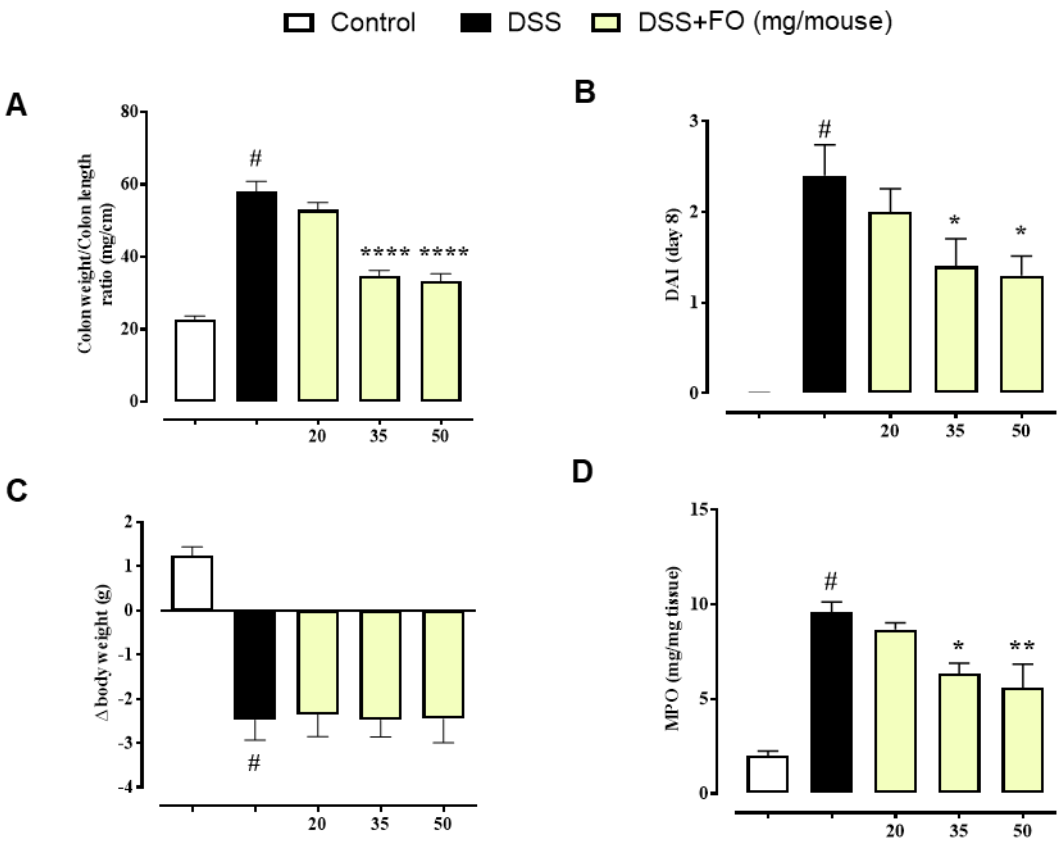

Figure 21. Effect of fish oil (FO) on inflammatory parameters in DSS-treated mice. Effect of FO (20, 35, and 50 mg/mouse, by oral gavage) on colon weight/colon length *ratio* (A), disease activity index (DAI) score (B), body weight (C), and MPO activity (D) in DSS-treated mice (weighing 28–30 g). DSS (4% w/v) was given for five consecutive days and then replaced with normal drinking water; FO was administered once a day by oral gavage starting the day after the beginning of DSS administration; mice were killed on Data are expressed as mean ± SEM of 10 mice for each experimental group. Data were statistically analyzed using one-way ANOVA followed by the Dunnett's multiple comparisons test. #$p<0.0001$ *vs* control; *$p<0.05$, **$p<0.01$, and ****$p<0.0001$ *vs* DSS.

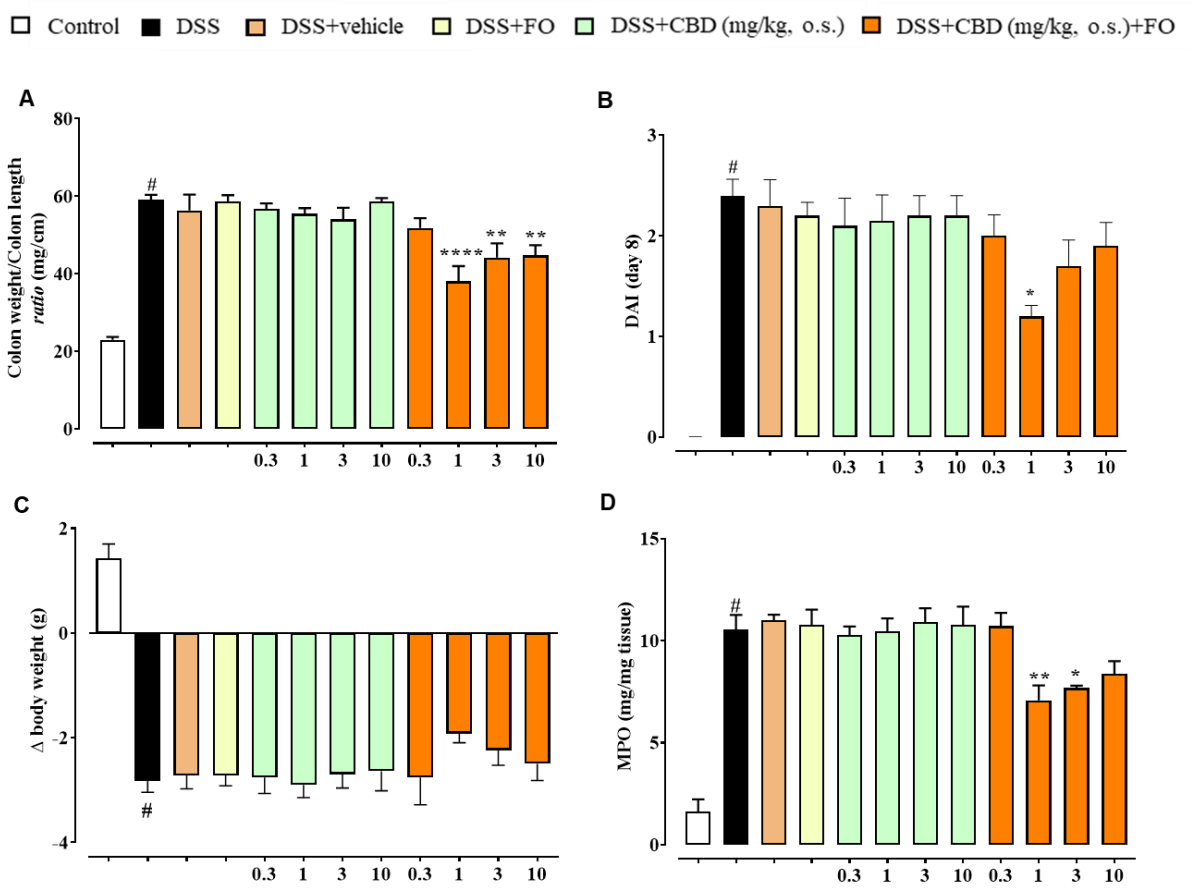

Figure 22. Effect of fish oil (FO, 20 mg/mouse) and cannabidiol (CBD, 0.3–10 mg/kg), both alone and in combination, on colon weight/colon length *ratio* (A), disease activity index (DAI) score (B), colon weight/colon length *ratio* (C), and MPO activity (D) in DSS-treated mice. DSS (4% w/v) was given for five consecutive days and then replaced with normal drinking water; FO was administered once a day by oral gavage starting the day after the beginning of DSS administration; CBD was administered daily in a dose range of 0.3-10 mg/kg mice starting two days after the beginning of DSS administration. Mice were killed on the peak of inflammation, i.e., seven days after the beginning of DSS administration. Data are expressed as mean ± SEM of 10 mice for each experimental group. Data were statistically analyzed using one-way ANOVA followed by the Dunnett's multiple comparisons test. #p<0.0001 *vs* control, *p<0.05, **p<0.01, and ****p<0.0001 *vs* DSS + FO.

2.4 Combined administration of CBD and FO, at per se ineffective doses, reduces intestinal permeability but not behaviour impairments in DSS-induced ulcerative colitis

As expected from the previous results, FO (20 mg/ mouse) or CBD (1 mg/kg) given alone by oral gavage, had no effect on DSS-induced intestinal inflammation (Figure 23). However, the combined treatment with CBD (1 mg/kg) and FO (20 mg/mouse) significantly reduced the increase in inflammatory parameters induced by DSS administration on day 8 (d8, acute phase) such as colon weight/colon length *ratio* (Figure 23A), DAI score (Figure 23B), MPO activity (Figure 23D), IL-1β and IL-6 (Figures 24A and 24B) and intestinal permeability (Figure 24D). Moreover, the combination of drugs at d8 was also able to increase IL-10 levels which were reduced by administration of DSS (Figure 24C). No effect on body weight loss was observed (Figure 23C). At day 14 (d14, remission phase) the overall degree of inflammation was lower in the DSS-treated mice than at d8 (Figures 23E-H). At this time point, the combination of CBD (1 mg/kg) with FO (20 mg/mouse) completely restored almost all the measured parameters to control levels. In particular, co-administration of CBD and FO significantly reduced the DSS-induced increase in colon weight/colon length *ratio* (Figure 23E), IL-1β levels (Figure 24E) and intestinal permeability (Figure 24H).

As expected, DSS administration induced behavioural changes in the mice as measured by the light-dark box (anxiety test) and NOR (cognitive ability test) on d8 (Figure 25). CBD (1 mg/kg) and FO (20 mg/mouse), either given alone or in combination, did not affect the DSS-induced behavioural changes (Figure 25).

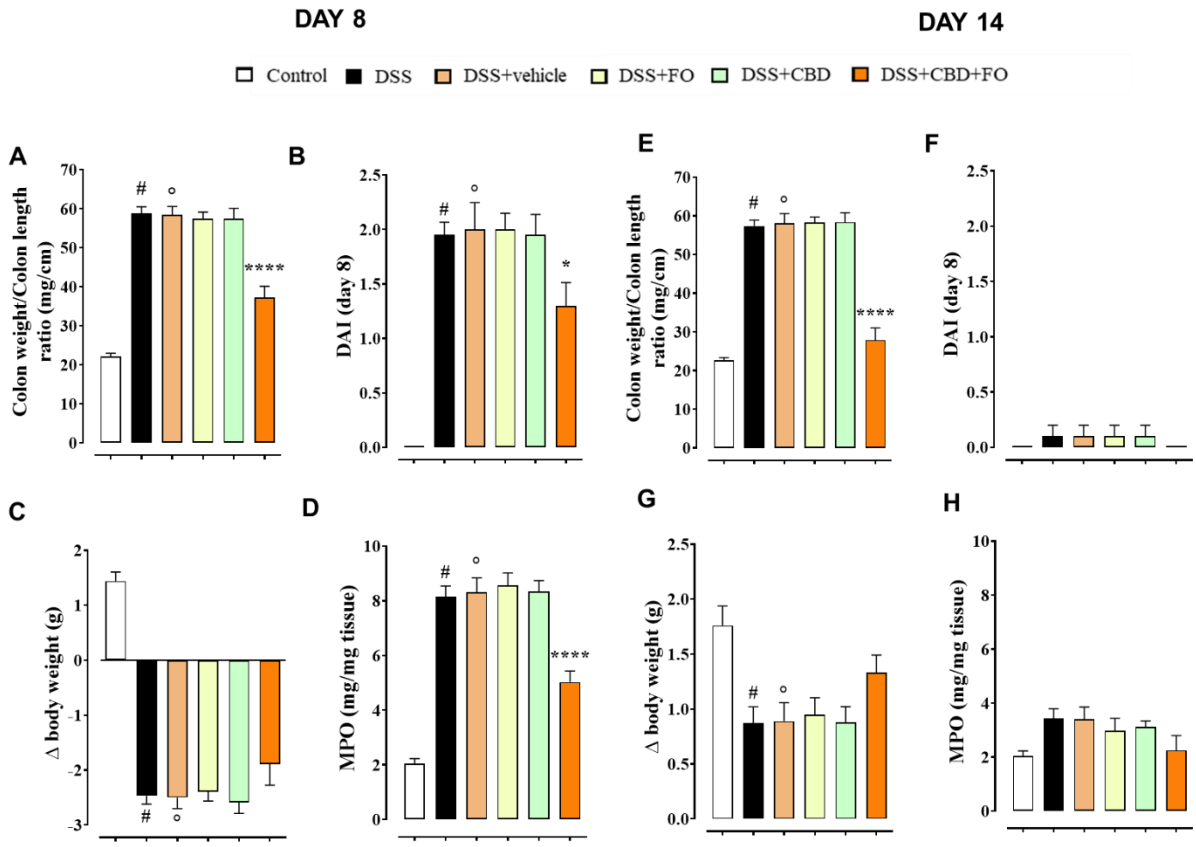

Figure 23. Effect of fish oil (FO, 20 mg/mouse, by oral gavage), cannabidiol (CBD, 1 mg/kg, by oral gavage) and FO + CBD on colon weight/colon length *ratio* (A, E), disease activity index (DAI) score (B, F), body weight (C, G) and MPO activity (D, H) either in control mice (without DSS treatment) or animals with colitis at day 8 (A–D) or day 14 (E–H) of DSS-induced ulcerative colitis. DSS (4% w/v) was given for five consecutive days and then replaced with normal drinking water; FO was administered once a day by oral gavage starting the day after the beginning of DSS administration; CBD was administered daily starting two days after the beginning of DSS administration. Mice were killed on the peak of inflammation, i.e., seven days after the beginning of DSS administration. Data are expressed as mean ± SEM of 10 mice for each experimental group. Data were statistically analyzed using one-way ANOVA followed by the Tuckey's multiple comparisons test. #$p<0.0001$ (A–D, F) or $p<0.01$ (H) *vs* control; °$p<0.0001$ (A–D, F) or $p<0.01$ (H) *vs* vehicle; *$p<0.05$ and ****$p<0.0001$ *vs* DSS + vehicle and DSS + FO and DSS + CBD.

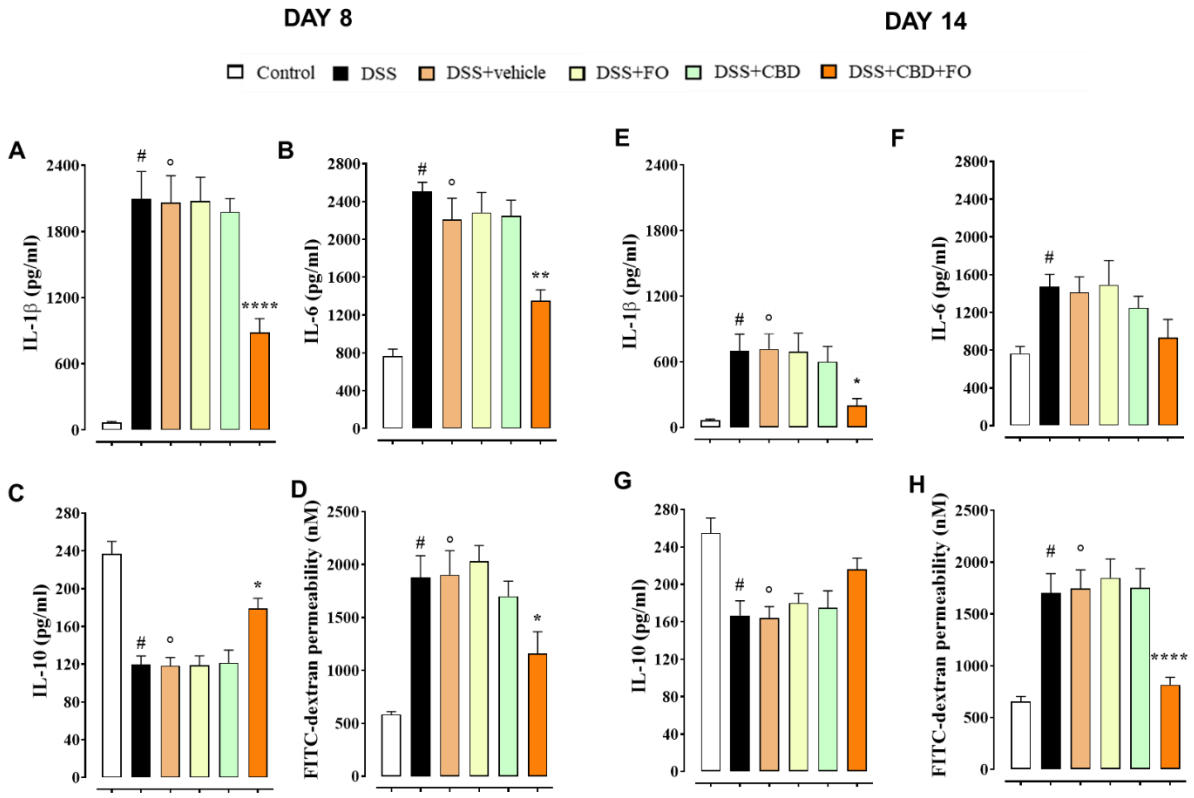

Figure 24. Effect of fish oil (FO, 20 mg/mouse, by oral gavage), cannabidiol (CBD, 1 mg/kg, by oral gavage) and FO + CBD on IL-1β (A, E), IL-6 (B, F), IL-10 (C, G) and intestinal permeability (D, H) in control and DSS-treated mice at day 8 (A–D) and day 14 (E–H) from the beginning of DSS administration. DSS (4% w/v) was given for five consecutive days and then replaced with normal drinking water; FO was administered once a day by oral gavage starting the day after the beginning of DSS administration; CBD was administered daily starting two days after the beginning of DSS administration. Mice were killed on the peak of inflammation, i.e., seven days after the beginning of DSS administration. Data are expressed as mean ± SEM of 5 mice for each experimental group. Data were statistically analyzed using one-way ANOVA followed by the Tuckey's multiple comparisons test. #$p<0.05$ (F) or $p<0.01$ (E, G) or $p<0.0001$ *vs* control (Ctrl) (A–D, H); °$p<0.05$ (G), 0.001 (E), or $p<0.0001$ (A–D, H) *vs* vehicle; *$p<0.05$, **$p<0.01$, and ****$p<0.0001$ *vs* DSS + vehicle or DSS + FO or DSS + CBD.

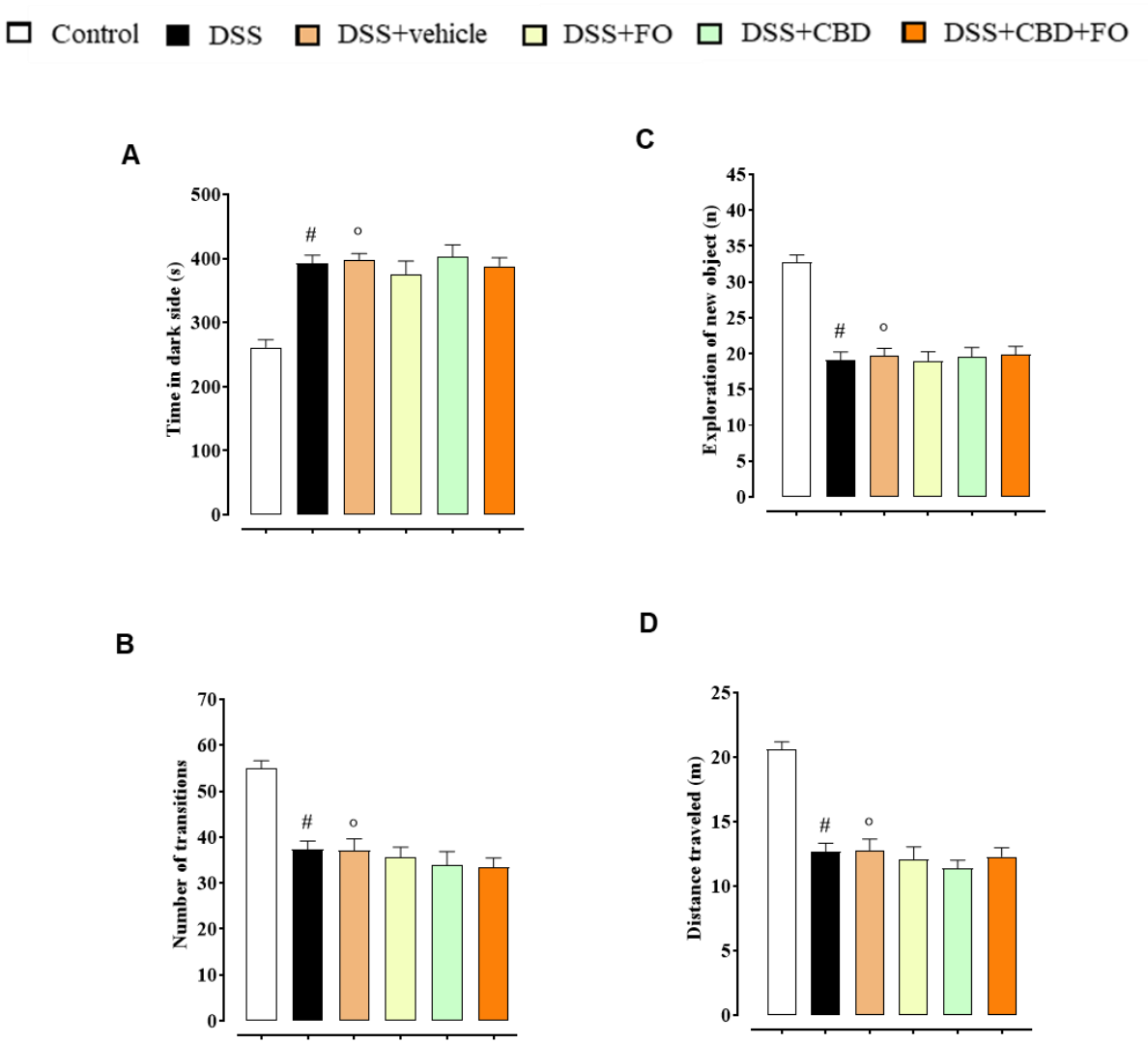

Figure 25. Effect of fish oil (FO, 20 mg/mouse) and cannabidiol (CBD, 1 mg/kg), both alone and in combination, on DSS-induced behaviour (Experiment 3). For the light/dark box test, the effect on time in dark side (seconds) (A) and the transitions (B) was assessed. For the novel object recognition test, the effect on number of entries on new object (C) and movements (D) was assessed. DSS (4% w/v) was given for five consecutive days and then replaced with normal drinking water; FO was administered once a day by oral gavage starting the day after the beginning of DSS administration; CBD was administered daily starting two days after the beginning of DSS administration. Data are expressed as mean ± SEM of 10 mice for each experimental group. Data were statistically analyzed using one-way ANOVA followed by the Tuckey's multiple comparisons test. #$p<0.0001$ *vs* control (Ctrl) and °$p<0.0001$ *vs* vehicle.

2.5 Combined administration of CBD and FO, at per se ineffective doses, induces changes in gut microbiota in DSS-induced ulcerative colitis

Neither DSS nor CBD or FO treatments, or their combination with DSS, affected the Shannon diversity of the faecal microbiome of the mice in a statistically significant manner (data not shown). The DSS treatment resulted in an increase in the *Firmicutes*:*Bacteroidetes ratio*, that was statistically significant only at the RP (d14). All treatments (i.e., CBD, FO, and CBD + FO) prevented this time-related increase (Figure 26A), no statistically significant difference was observed between treatments at either d8 or d14.

Hierarchical clustering of sequencing counts at the family level revealed that all d0 and vehicle-alone groups (irrespective of day) clustered together as did the DSS and DSS + Veh groups at d8 (i.e., during the inflammatory peak; Figure 26B). Moreover, all DSS-treated groups clustered independently at d14 (i.e., the RP) but within a larger cluster than the experimental treatments (CBD, FO, and CBD + FO) at d8.

DSS treatment affected several bacterial families, genera and species but mainly in the RP (d14), compared to control mice (Figures 26C and 27; see Table 4 for statistical details). The only families that did not change statistically significantly at d8 were *Saccharimonadaceae* ($p = 0.06$) and *Streptococcaceae* ($p = 0.096$), which were reduced compared to DSS-treated mice, the latter family being increased by CBD (Figure 26C). Nevertheless, at RP (d14), *Akkermansiaceae* and *Tannerellaceae* were increased in the DSS group compared to the control mice, and this increase was also significant at d14 in all three treatments (Figure 26C). Several families that were not modified by DSS, were instead modified by one or more of the three treatments at either d8 or d14. In particular, *Clostridiaceae_1* (reduced by CBD at d8), *Defluviitaleaceae* (increased by CBD and FO at d8), *Marinifilaceae* (decreased by CBD + FO at d8), *Christensenellaceae* (increased

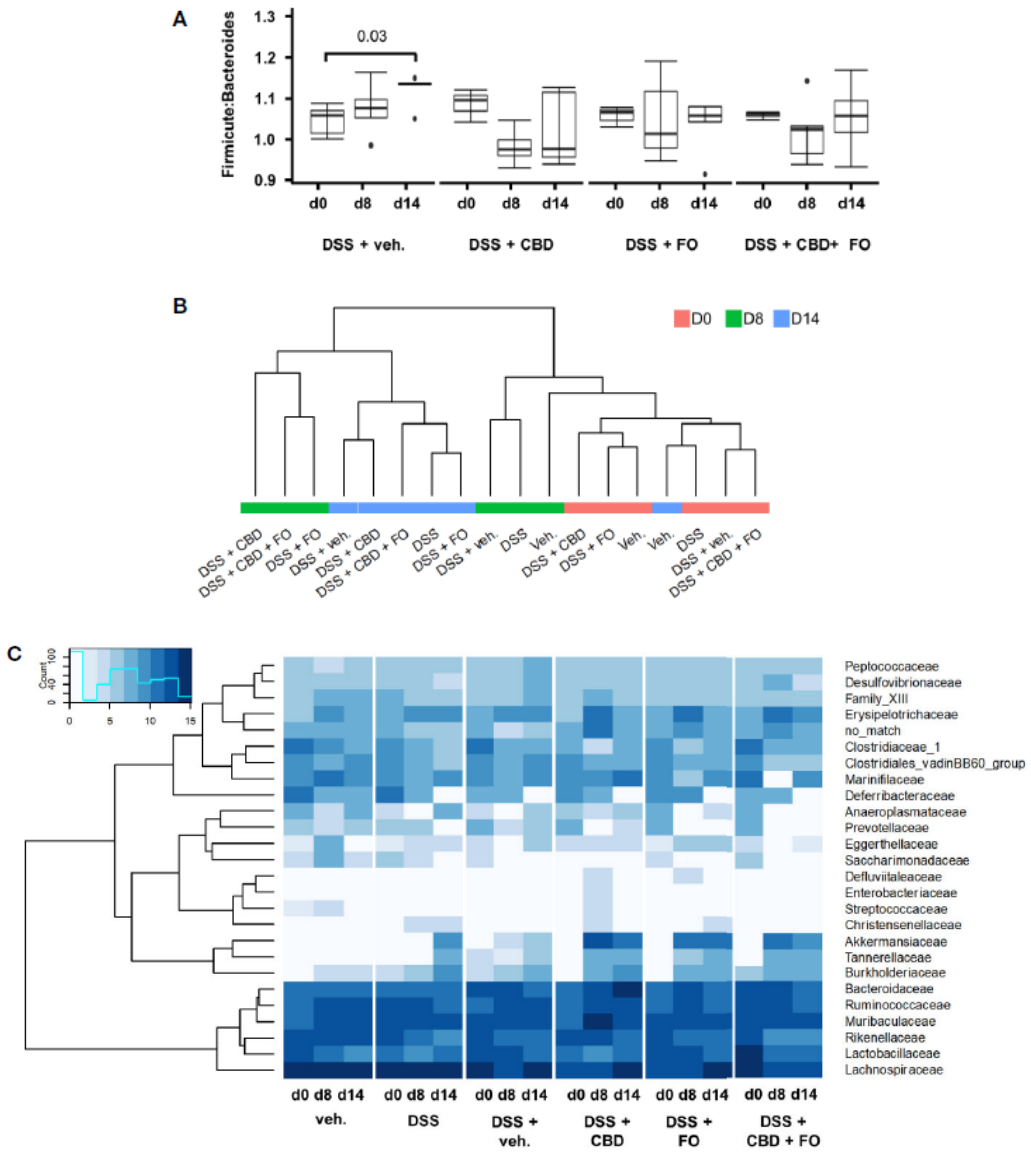

Figure 26. Effect of fish oil (FO, 20 mg/mouse) and cannabidiol (CBD, 1 mg/kg), both alone and in combination, at day 8 and day 14, on microbiota in faecal samples collected from DSS-treated mice belonging to the same treatment groups (10 mice for each experimental group). (A) *Firmicutes:Bacteroidetes ratio*. Wilcoxon p-values for pairwise comparisons are displayed above brackets. (B) Hierarchical clustering of treatment groups using CSS-normalized bacterial family counts. (C) Heat map and hierarchical clustering of family composition using CSS-normalized bacterial counts.

Table 4. Statistical details of bacteria affected by treatments

			DSS *vs* Veh			DSS + CBD *vs* DSS			DSS + FO *vs* DSS			DSS + CBD + FO *vs* DSS		
Family	**F value Group**	**p value Group**	**d0**	**d8**	**d14**	**d0**	**d8**	**d14**	**d0**	**d8**	**d14**	**d0**	**d8**	**d14**
Akkermansiaceae	45.39	4.544e-20	n.s.	n.s.	0.001293	n.s.	1.101e-05	0.01417	n.s.	8.642e-06	0.000765	n.s.	2.566e-05	0.04992
Christensellaceae	3.283	0.01043	n.s.	n.s.	n.s.	n.s.	n.s.	n.s.	n.s.	n.s.	0.02877	n.s.	n.s.	n.s.
Clostridiaceae_1	6.618	4.761e-05	n.s.	n.s.	n.s.	n.s.	0.01093	n.s.	n.s.	n.s.	n.s.	n.s.	n.s.	n.s.
Defulviitalaceae	4.679	0.001023	n.s.	n.s.	n.s.	n.s.	0.01047	n.s.	n.s.	0.06072	n.s.	n.s.	n.s.	n.s.
Desulfovibrionaceae	0.394	n.s.	n.s.	n.s.	n.s.	n.s.	n.s.	n.s.	n.s.	n.s.	n.s.	n.s.	n.s.	0.0417
Marinifilaceae	4.478	0.0014	n.s.	n.s.	n.s.	n.s.	n.s.	n.s.	n.s.	n.s.	n.s.	n.s.	0.0377	n.s.
Saccharimonadaceae	3.897	0.003723	n.s.	0.05972	n.s.	n.s.	n.s.	n.s.	n.s.	n.s.	n.s.	n.s.	n.s.	n.s.
Streptococcaceae	2.278	0.05676	n.s.	0.09645	n.s.	n.s.	0.03859	n.s.	n.s.	n.s.	n.s.	n.s.	n.s.	n.s.
Tannerellaceae	12.58	1.378e-08	n.s.	n.s.	0.09159	n.s.	n.s.	n.s.	n.s.	n.s.	n.s.	n.s.	n.s.	n.s.

			DSS *vs* Veh			DSS + CBD *vs* DSS			DSS + FO *vs* DSS			DSS + CBD + FO *vs* DSS		
Genus	**F value Group**	**p value Group**	**d0**	**d8**	**d14**	**d0**	**d8**	**d14**	**d0**	**d8**	**d14**	**d0**	**d8**	**d14**
Acetitomaculum	6.072	0.00011	n.s.	n.s.	0.000304	n.s.	n.s.	n.s.	n.s.	n.s.	n.s.	n.s.	n.s.	n.s.
Akkermansia	41.19	5.128e-19	n.s.	0.09548	0.02074	n.s.	0.000318	0.01455	n.s.	0.000185	0.000184	n.s.	0.000146	0.002601
Anaerotruncus	7.608	1.079e-05	n.s.	n.s.	n.s.	n.s.	0.000532	n.s.	n.s.	n.s.	n.s.	n.s.	n.s.	n.s.
C. Arthromitus	6.271	8.106e-05	n.s.	n.s.	n.s.	n.s.	0.006139	n.s.	n.s.	n.s.	n.s.	n.s.	n.s.	n.s.
Christensellaceae_R-7	2.325	0.05248	n.s.	n.s.	n.s.	n.s.	n.s.	n.s.	n.s.	n.s.	0.04501	n.s.	n.s.	n.s.
Defulviitalaceae_UG011	4.736	0.000931	n.s.	n.s.	n.s.	n.s.	0.007143	n.s.	n.s.	0.04884	n.s.	n.s.	n.s.	n.s.
Lachnospiraceae_UG004	6.152	9.759e-05	n.s.	n.s.	0.09047	n.s.	n.s.	n.s.	n.s.	n.s.	n.s.	n.s.	n.s.	n.s.
Odoribacter	3.526	0.006935	n.s.	n.s.	n.s.	n.s.	n.s.	n.s.	n.s.	n.s.	n.s.	n.s.	0.02916	n.s.
Ruminococcaceae_UG005	3.148	0.0131	n.s.	n.s.	n.s.	n.s.	n.s.	0.06618	n.s.	n.s.	n.s.	n.s.	n.s.	n.s.
Ruminococcus_1	1.087	n.s.	n.s.	n.s.	n.s.	0.0242	n.s.	n.s.	n.s.	n.s.	n.s.	n.s.	n.s.	n.s.
Tyzzerella_3	14.94	8.637e-10	n.s.	n.s.	n.s.	n.s.	n.s.	n.s.	n.s.	n.s.	0.03499	n.s.	n.s.	0.0472

			DSS *vs* Veh			DSS + CBD *vs* DSS			DSS + FO *vs* DSS			DSS + CBD + FO *vs* DSS		
Species	**F value Group**	**p value Group**	**d0**	**d8**	**d14**	**d0**	**d8**	**d14**	**d0**	**d8**	**d14**	**d0**	**d8**	**d14**
A. muciniphila	36.27	1.119e-17	n.s.	n.s.	0.0004612	n.s.	9.346e-05	n.s.	n.s.	0.0004743	0.01297	n.s.	0.0006649	n.s.
P. goldsteinii	10.91	1.12e-07	n.s.	n.s.	0.04791	n.s.	n.s.	n.s.	n.s.	n.s.	n.s.	n.s.	n.s.	n.s.

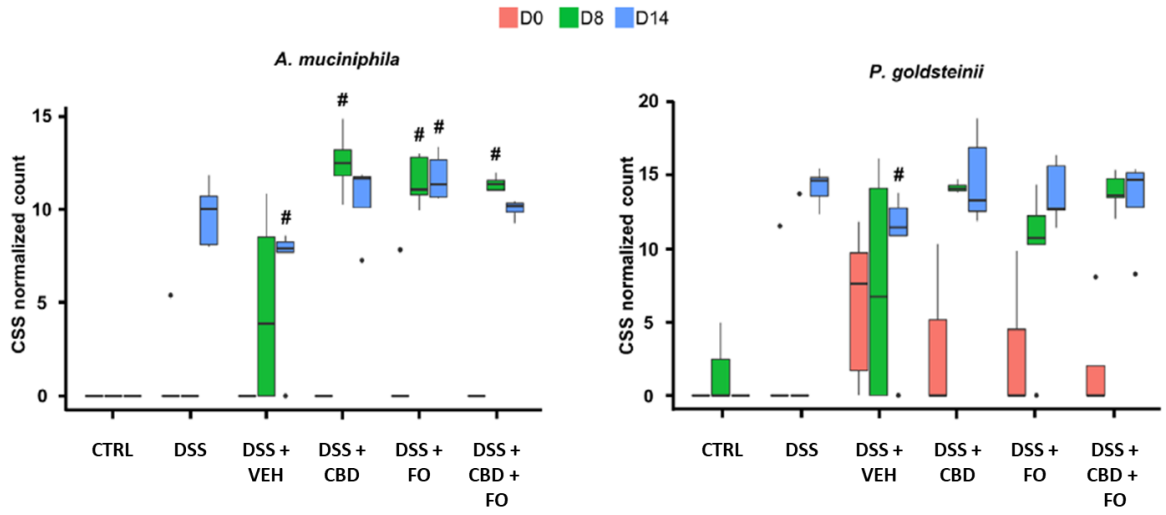

Figure 27 Effect of fish oil (FO, 20 mg/mouse) and cannabidiol (CBD, 1 mg/kg), both alone and in combination, both at day 8 and day 14, on the relative abundance of *Akkermansia muciniphila* and *Parabacteroides goldsteinii* in faecal samples collected from DSS-treated mice belonging to the same treatment groups. Only the species for which statistically significant differences were observed between DSS-Veh and Veh at day 14 are shown. Data are plotted as boxplot with median, Q1-Q3 range and whiskers extended to 1.5 interquartile ranges (10 mice for each experimental group). Data were statistically analyzed using one-way ANOVA followed by the Tuckey's multiple comparisons test. #$p<0.05$ *vs* relevant control of the same day.

in a statistically significant manner by FO at d14 but not at d8) and *Desulfovibrionaceae* (decreased by CBD + FO at d14). A decrease, that did not reach statistical significance ($p = 0.1$), was also observed in *Ruminococcaceae* in the presence of CBD + FO at d14 with (Table 26C).

At the genus level (Table 4B), the only taxa for which a numerical increase, which did not reach statistical significance, was observed at d8 following DSS was *Akkermansia* ($p = 0.09$). This increase was further increased in a statistically significant manner by all treatment groups at d8. *Akkermansia* was increased by DSS on d14, and as on d8, all treatments resulted in even greater increases. The genus *Acetitomaculum*, on the other hand, was significantly decreased only at d14, and none of the treatments could reverse this effect (Table 4B). However, there were several genera that were not affected by DSS but differed significantly from the DSS-treated mice after the treatments (Table 4B): *Anaerotruncus* and *Candidatus_Arthromitus* were both decreased by CBD at d8, while, at the same time point, *Odoribacter* was decreased by CBD + FO, and *Defluviitaleaceae*-UCG011 was increased by CBD and FO. On the other hand, at d14, *Christensenellaceae*_R7- group was increased by FO, *Ruminococcaceae*-UCG-005 was decreased by CBD, and *Tyzzerella*_3 was decreased by FO and CBD + FO (Table 4B).

Finally, although the method used does not usually allow species identification, we were able to identify *Akkermansia muciniphila* and *Parabacteroides goldsteinii*, which were increased by DSS at d14, and, in the presence of all treatments, also at d8 (Figure 27, Table 4C).

2.6 Combined administration of CBD with an active dose of FO abolishes colon inflammation induced by DSS

Fish oil administration, at 75 mg/mouse starting one day after the beginning of the phlogogen agent (Figure 28), reduced the increase in inflammatory parameters induced by DSS administration, such as colon weight/colon length *ratio* and DAI score (Figures 29A and 29B), but not in a statistically significant manner, and had no effect on body weight loss (Figure 29C) in DSS-treated mice. However, it significantly reduced MPO activity (Figure 29D) as observed in the previous experiment. CBD, given by oral gavage at the dose range of 0.3–30 mg/ kg (Figure 28) did not affect DSS-induced intestinal inflammation, but when administered in FO-treated mice reduced DAI score (0.3, 3, and 10 mg/mouse only), colon weight/colon length *ratio* (all CBD doses tested), body weight loss (3 and 10 mg/mouse only) and MPO activity (all CBD doses tested) (Figures 29A–29D).

2.7 Combined administration of CBD with an inactive dose of FO reduces DNBS-induced inflammation

Mice treated with DNBS (Figure 30) showed a significant increase in inflammatory parameters like colon weight/colon length *ratio* (Figure 31A), MPO activity (Figure 31B), IL-1β levels (Figure 31C), and intestinal permeability (Figure 31D). The treatment with fish oil by oral gavage (75 mg/mouse, o.s.), did not significantly reduce inflammatory parameters increased by DNBS administration. In the same way, the treatment with CBD (0.3-30 mg/kg, o.s.) did not attenuate colitis severity as shown by its lack of effect on the increase of colon weight/colon length *ratio* (Figure 32A) induced by DNBS; moreover, CBD 10 mg/kg did not affect either MPO activity (Figure 32B), IL-1β levels (Figure 32C), or the intestinal permeability (Figure 32D) increased by DNBS.

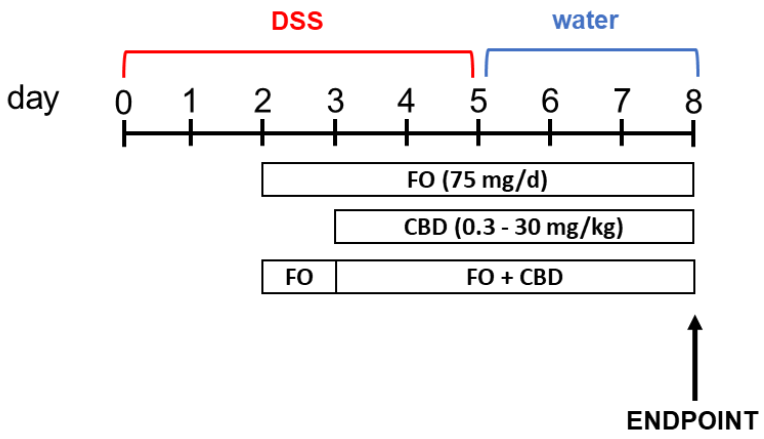

Figure 28. Schematic representation of CBD dose response in association with an effective dose of FO in DSS-induced ulcerative colitis. DSS, dissolved in drinking water at 4% w/v, was given for five consecutive days and then replaced with normal drinking water. Mice were killed on the peak of inflammation, i.e., eight days after the beginning of DSS administration (on day 8).

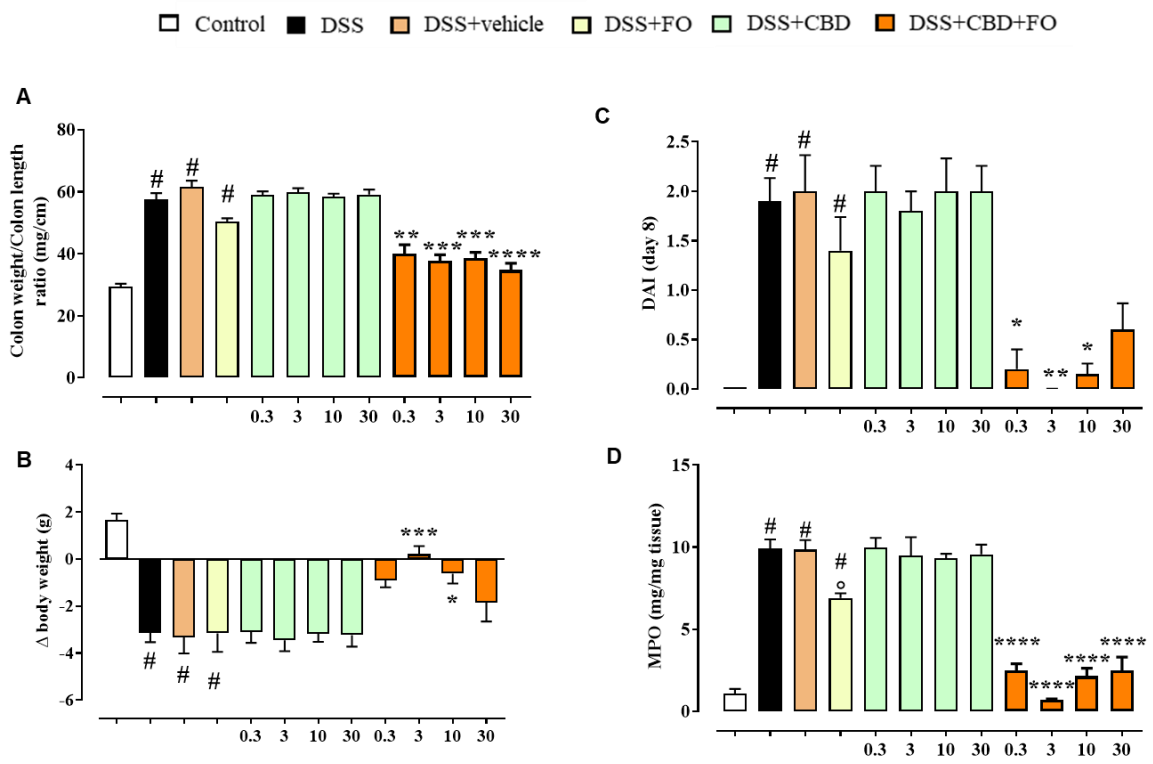

Figure 29. Effect of fish oil (FO, 75 mg/mouse) and cannabidiol (CBD, 0.3–30 mg/kg), both alone and in combination, in DSS-induced inflammation on colon weight/colon length *ratio* (A), disease activity index (DAI) score (B), body weight (C), and MPO activity (D) in DSS-treated mice (weighting 28–30 g). DSS (4% w/v) was given for five consecutive days and then replaced with normal drinking water; FO was administered once a day by oral gavage starting the day after the beginning of DSS administration; CBD was administered daily starting two days after the beginning of DSS administration. Mice were killed on the peak of inflammation, i.e., seven days after the beginning of DSS administration. Data are expressed as mean ± SEM of 10 mice for each experimental group. Data were statistically analyzed using one-way ANOVA followed by the Tuckey's multiple comparisons test. #p<0.01–0.0001 *vs* control; °p<0.05 *vs* DSS alone; *p<0.05, **p<0.01, ***p<0.001 and ****p<0.0001 *vs* DSS + FO.

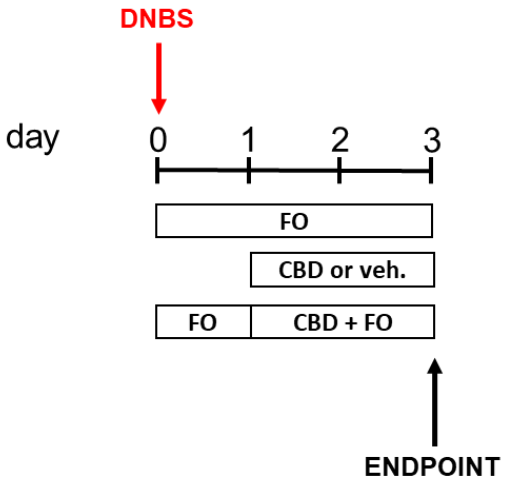

Figure 30. Schematic representation of different combination of CBD (0.3 – 30 mg/kg) and FO (75 mg/mouse) either given alone or in combination tested in the DNBS-induced model of ulcerative colitis. DNBS was injected in mice colon at the dose of 150 mg/kg; mice were killed three days after the DNBS administration.

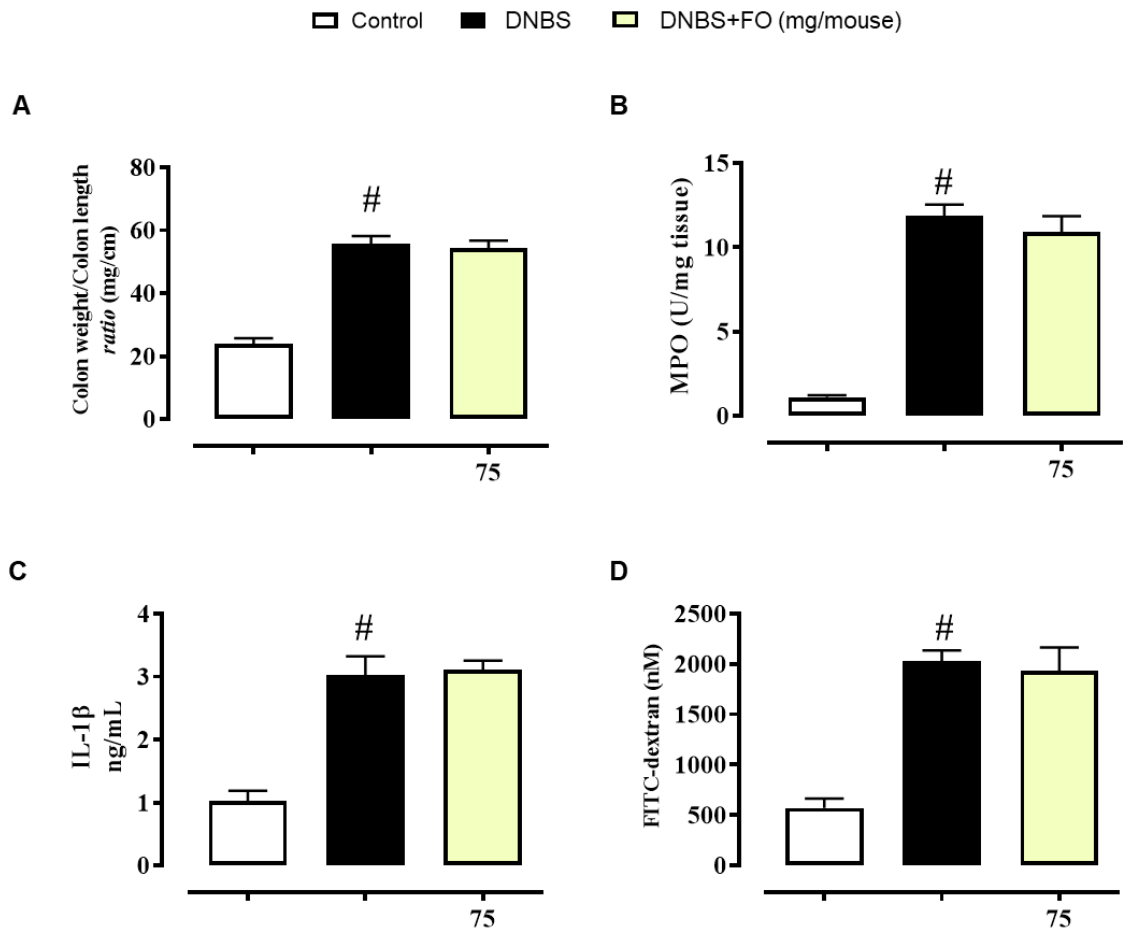

Figure 31. Effect of fish oil (FO, 75 mg/mouse) on A) colon weight/colon length, B) MPO activity, C) IL-1β levels and D) intestinal permeability in a DNBS-induced model of ulcerative colitis. DNBS was injected in mice colon at the dose of 150 mg/kg. FO was administered alone by oral gavage, at the dose of 75 mg/mouse, starting the same day of the DNBS administration; mice were killed three days after DNBS administration. Data are expressed as mean ± SEM of 8-10 mice for each experimental group (colon weight/colon length ratio) or 6 mice for each experimental group (MPO activity, IL-1β levels, and serum FITC-dextran). Data were statistically analyzed using one-way ANOVA followed by the Dunnett's multiple comparisons test. #$p<0.0001$ *vs* control.

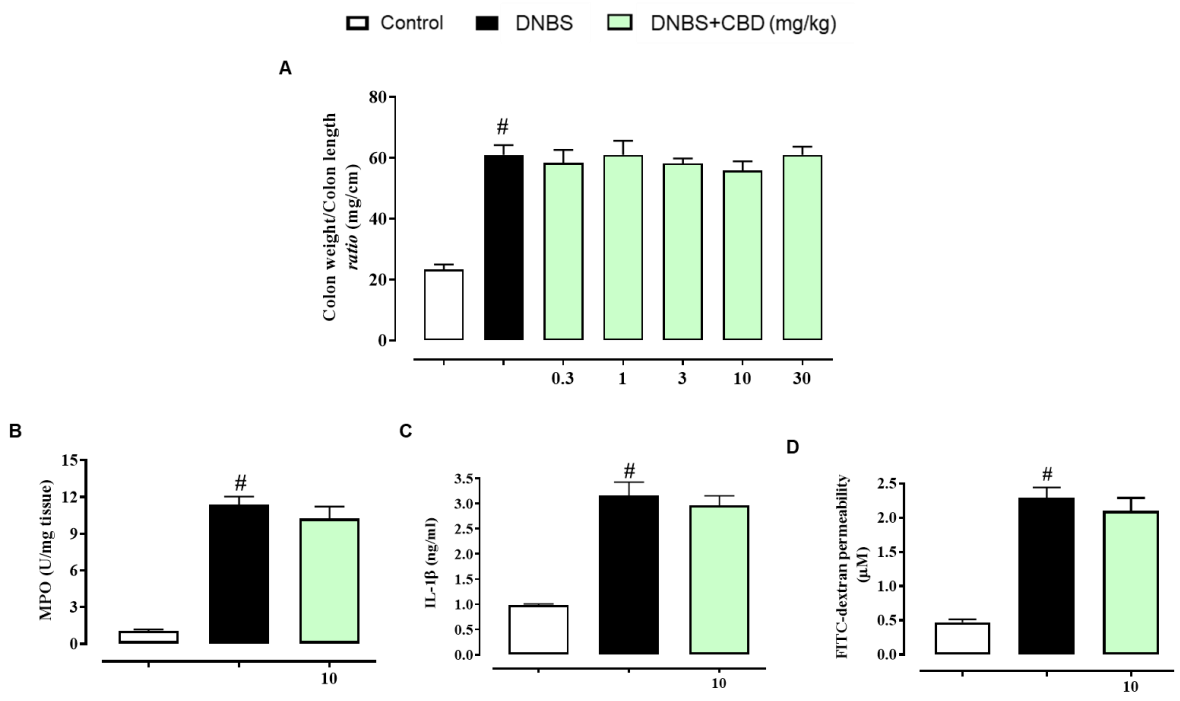

Figure 32. Effect of cannabidiol (CBD, 0.3–30 mg/kg, given by oral gavage) on A) colon weight/colon length *ratio* and of CBD, at the dose of 10 mg/kg, on B) colonic MPO activity, C) colonic IL-1β levels and D) serum FITC-dextran concentration in DNBS-treated mice. DNBS was injected in mice colon at the dose of 150 mg/kg. CBD was administered in a dose range of 0.3-30 mg/kg by oral gavage starting the day after DNBS administration; mice were killed three days after DNBS administration. Data are expressed as mean ± SEM of 8-10 mice for each experimental group (colon weight/colon length ratio) or 6 mice for each experimental group (MPO activity, IL-1β levels, and serum FITC-dextran). Data were statistically analyzed using one-way ANOVA followed by the Dunnett's multiple comparisons test. #p<0.0001 *vs* control

Interestingly, the combination of fish oil (75 mg/mouse, o.s.) with CBD (1–30 mg/kg, o.s.), ameliorated DNBS-induced intestinal inflammation. Specifically, the combination of fish oil and CBD significantly reduced the increase in colon weight/colon length *ratio* caused by DNBS (Figure 33A), in a statistically significant way starting from CBD 1 mg/kg. Nevertheless, fish oil and CBD 1 mg/kg co-administration significantly reduced MPO activity (Figure 33B) and, in a not statistically significant way, IL-1β levels ($p = 0.059$, Figure 33C) and intestinal permeability ($p = 0.102$, Figure 33D). These results reinforce the concept that fish oil potentiates CBD effect even in this model of DNBS-induced ulcerative colitis.

2.8 FO does not affect CBD bioavailability

In order to verify if the potentiating effect of FO on CBD was due to the increase in the oral bioavailability, we quantified CBD levels both in plasma and colon tissues. As shown in Table 5, fish oil (75 mg/mouse, by oral gavage) did not significantly affect the level of CBD (at the 30 mg/kg dose, orally) in the colon or serum (Table 5).

2.9 Combined administration of CBD and FO does not affect endocannabinoidome mediator levels

Finally, to unravel possible alteration of endocannabinoidome mediators' levels we analyzed the lipidomic profile of colons. In particular, we measured the levels of AEA, 2-AG, PEA, OEA, DHEA and 2-DHG (docosahexaenoylethanolamide and 2-docosahexaenoylglycerol, n-3PUFA-derived ethanolamide and acylglycerol). In DNBS treated animals, CBD (30 mg/kg, orally) did not alter any of the endocannabinoids, as well as PEA, and OEA levels, while FO (75 mg/mouse) significantly increased the levels of 2-AG and PEA (compared to control animals) (Figure 34). These significant differences were absent in CBD plus fish oil-treated animals (Figure 34).

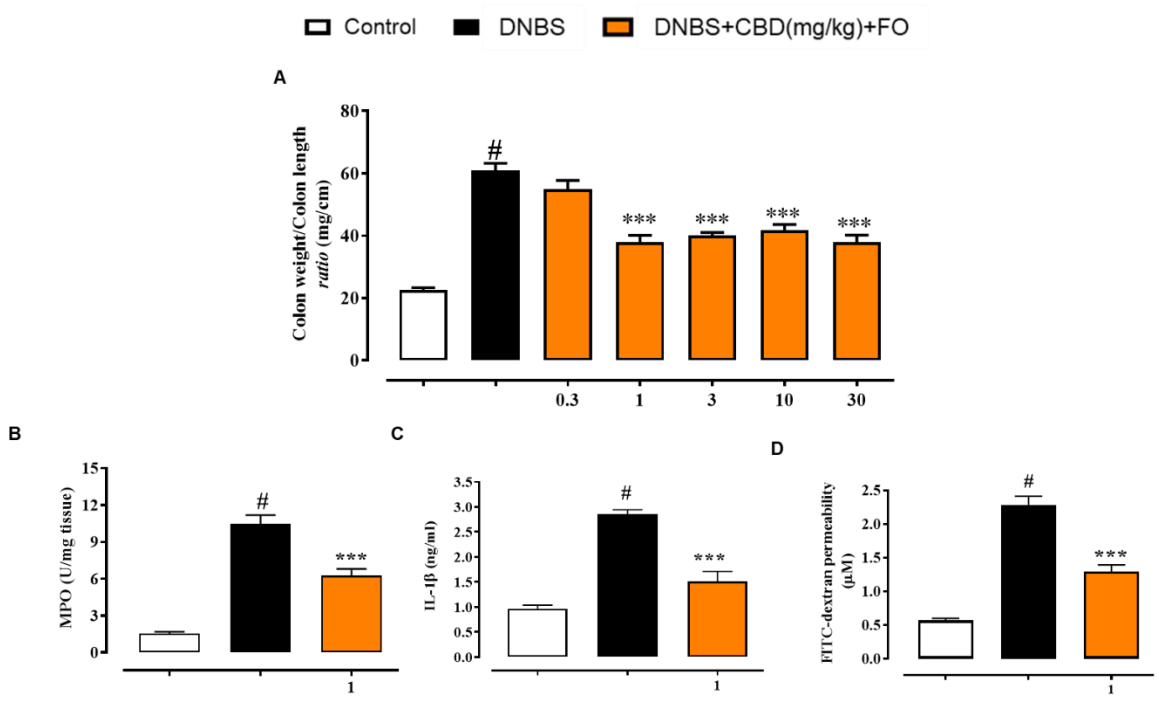

Figure 33. Effect of the combination of fish oil (FO, 75 mg/mouse) with cannabidiol (CBD, 0.3–30 mg/ kg), both given by oral gavage, on A) colon weight/colon length *ratio* and of the combination of fish oil with CBD, at the dose of 1 mg/kg, on B) MPO activity, C) IL-1β levels and D) serum FITC-dextran concentration in DNBS-treated mice. DNBS was injected in mice colon at the dose of 150 mg/kg. FO was administered alone by oral gavage, at the dose of 75 mg/mouse, starting the same day of the DNBS administration, CBD was administered in a dose range of 0.3-30 mg/kg by oral gavage starting the day after DNBS administration; mice were killed three days after DNBS administration. Data are expressed as mean ± SEM of 8-10 mice for each experimental group (colon weight/colon length ratio) or 6 mice for each experimental group (MPO activity, IL-1β levels, and serum FITC-dextran). Data were statistically analyzed using one-way ANOVA followed by the Dunnett's multiple comparisons test. #p<0.0001 *vs* control **p<0.01, ***p<0.001, and ****p<0.0001 *vs* DNBS alone.

Treatment	Colonic CBD levels (ng/mg tissue) (mean ± SEM)	Serum CBD levels (ng/mL) (mean ± SEM)
Control	0 ± 0	0 ± 0
DNBS	0 ± 0	0 ± 0
DNBS+FO	0 ± 0	0 ± 0
DNBS+CBD	3.1 ± 1.7	27.4 ± 10.4
DNBS+CBD+FO	3.3 ± 1.4	47.4 ± 9.4

Table 5. Effect of the combination of fish oil (FO, 75 mg/mouse) with cannabidiol (CBD, 30 mg/kg), both given by oral gavage, on CBD levels in the colon and serum in the DNBS model of colitis. DNBS was injected in mice colon at the dose of 150 mg/kg. FO was administered alone by oral gavage, at the dose of 75 mg/mouse, starting the same day of the DNBS administration, CBD was administered in a dose range of 0.3-30 mg/kg by oral gavage starting the day after DNBS administration; mice were killed three days after DNBS administration. Data are expressed as mean ± SEM of 5 mice for each experimental group. Data were statistically analyzed using one-way ANOVA followed by the Student's *t* test.

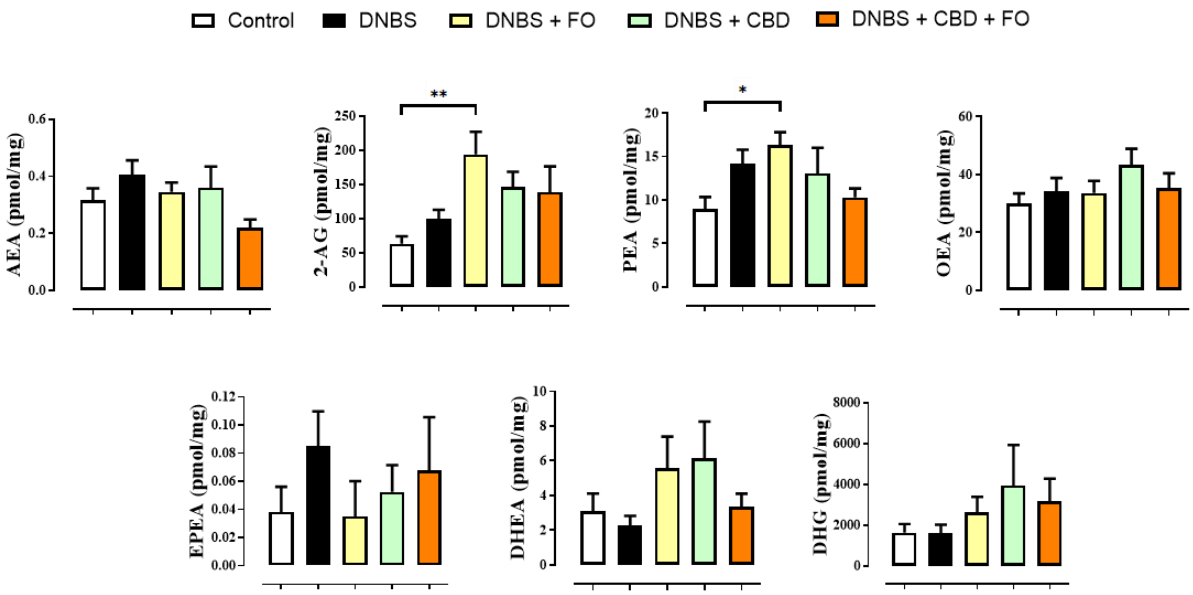

Figure 34. Effect of the combination of fish oil (FO, 75 mg/mouse) with cannabidiol (CBD, 30 mg/kg), both given by oral gavage, on endocannabinoidome mediators' levels in the colon of DNBS-induced colitis in mice. DNBS was injected in mice colon at the dose of 150 mg/kg. FO was administered alone by oral gavage, at the dose of 75 mg/mouse, starting the same day of the DNBS administration, CBD was administered in a dose range of 0.3-30 mg/kg by oral gavage starting the day after DNBS administration; mice were killed three days after DNBS administration. Data are expressed as mean ± SEM of 8-10 mice for each experimental group. Data were statistically analyzed using one-way ANOVA followed by the Dunnett's multiple comparisons test. *$p<0.05$ and **$p<0.01$ *vs* DNBS alone.

Part III – TRPM8 channel deletion reduces murine colon carcinogenesis and modifies gut microbiota composition

3.1 Trpm8 genetic deletion reduces the development of sporadic colon cancer in mice

To identify a possible influence of Trpm8 deletion in experimental colon tumorigenesis, we used a genetic approach in a sporadic tumor model (induced by AOM, Figure 35). Thirteenth week following AOM administration, Trpm8$^{-/-}$ mice had significantly fewer colon tumors than wild-type mice (Figure 36A). Trpm8$^{-/-}$ mice did not show weight loss following AOM treatment (Figure 36B). None of the control treated mice (i.e., without AOM treatment), either wild-type or Trpm8$^{-/-}$, developed tumors.

3.2 Trpm8 genetic deletion induces changes in gut microbiota composition in healthy mice

The gut microbiota composition at the timepoint zero, i.e., before the AOM treatment, was significantly different between wild type and Trpm8$^{-/-}$ mice, as shown by PCoA analysis. The two groups formed two different clusters, showing a different microbiota composition; this difference was statistically significant (PERMANOVA $p<0.001$) (Figure 37). In particular, *Burkholderiaceae* and *Deferribacteraceae* families were under the detection level in Trpm8$^{-/-}$ mice, while *Helicobacteriaceae* and *Enterobacteriaceae* were detected only in Trpm8$^{-/-}$ mice. Moreover, abundance of *Ruminococcaceae* and *Marinifilaceae* families were higher in wild type mice compared to Trpm8$^{-/-}$ mice, while *Tannerellaceae* and *Saccharimonadaceae* were higher in Trpm8$^{-/-}$ mice compare to wild type mice (Figure 38).

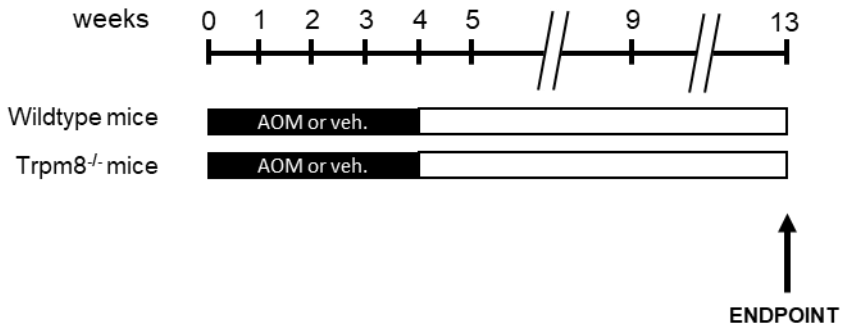

Figure 35. Schematic representation of the AOM-induced model of sporadic colorectal cancer. AOM was administered once a week, at the beginning of the first four weeks at the dose of 10 mg/kg by intraperitoneal injection (cumulative dose injected: 40 mg/kg). Mice were killed at the beginning of the thirteenth week after the first AOM injection. Feces were collected at different timepoints (before AOM administration, week 5, week 9 and week 13) for gut microbiota analysis.

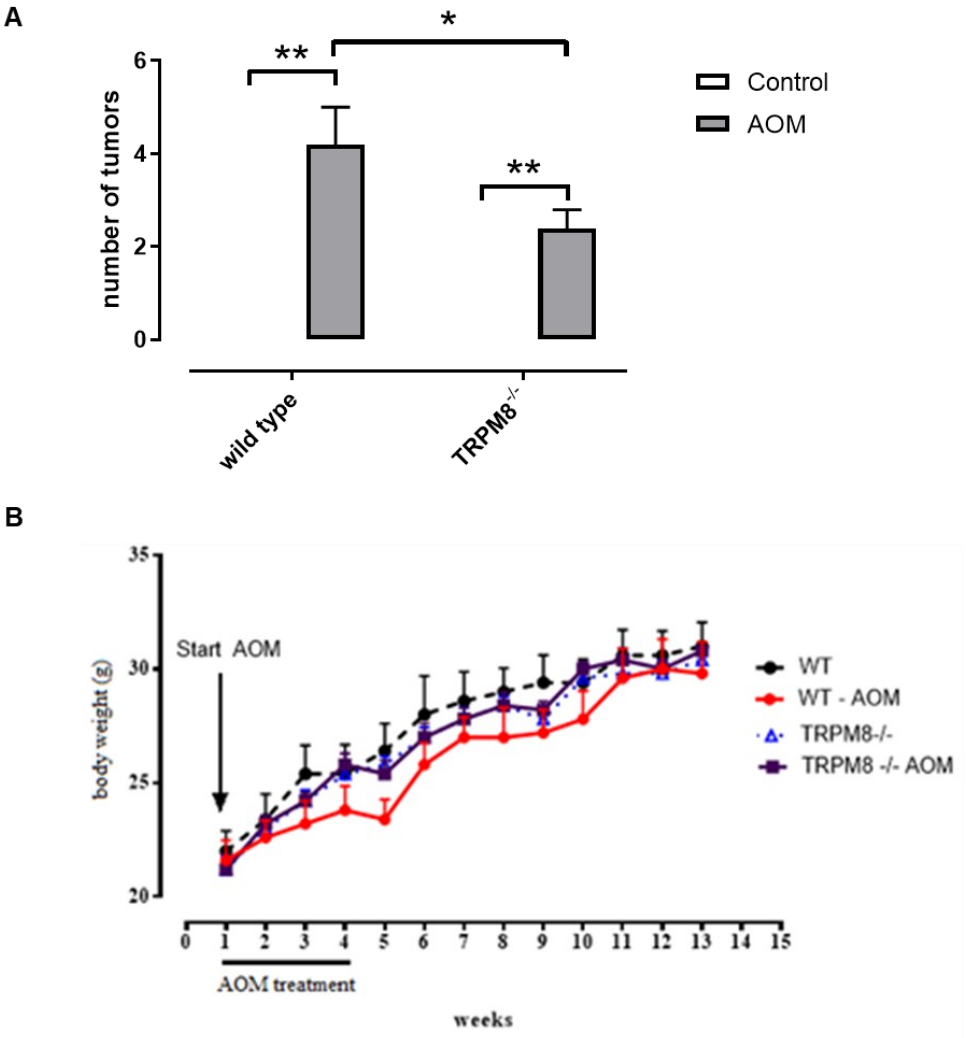

Figure 36. Effect of Trpm8 genetic deletion on A) Number of tumors/mouse counted on Wild Type and Trpm8$^{-/-}$ mice colon, treated with vehicle, or AOM. B) Mice body weight expressed as grams of body weight. AOM was administered once a week for the first four weeks at the dose of 10 mg/kg by intraperitoneal injection (total dose 40 mg/kg/mouse). Mice were killed at the beginning of the thirteenth week after the first AOM injection. Data are expressed as mean ± SEM of 5 mice for each experimental group. Data were statistically analyzed using one-way ANOVA followed by the Dunnett's multiple comparisons test. *$p<0.05$ and **$p<0.01$.

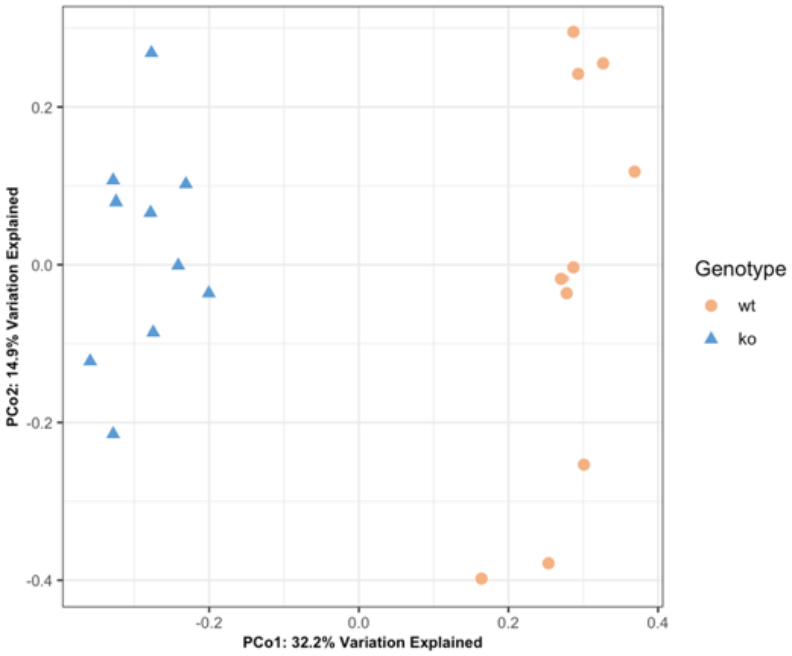

Figure 37. Effect of Trpm8 genetic deletion on gut microbiota composition, performed using Bray-Curtis dissimilarity, an index used to estimate beta-diversity between healthy wildtype and Trpm8$^{-/-}$ mice. Feces were collected before the first administration of AOM. Data were analyzed by using PERMANOVA ($p<0.001$) of 5 mice for each experimental group.

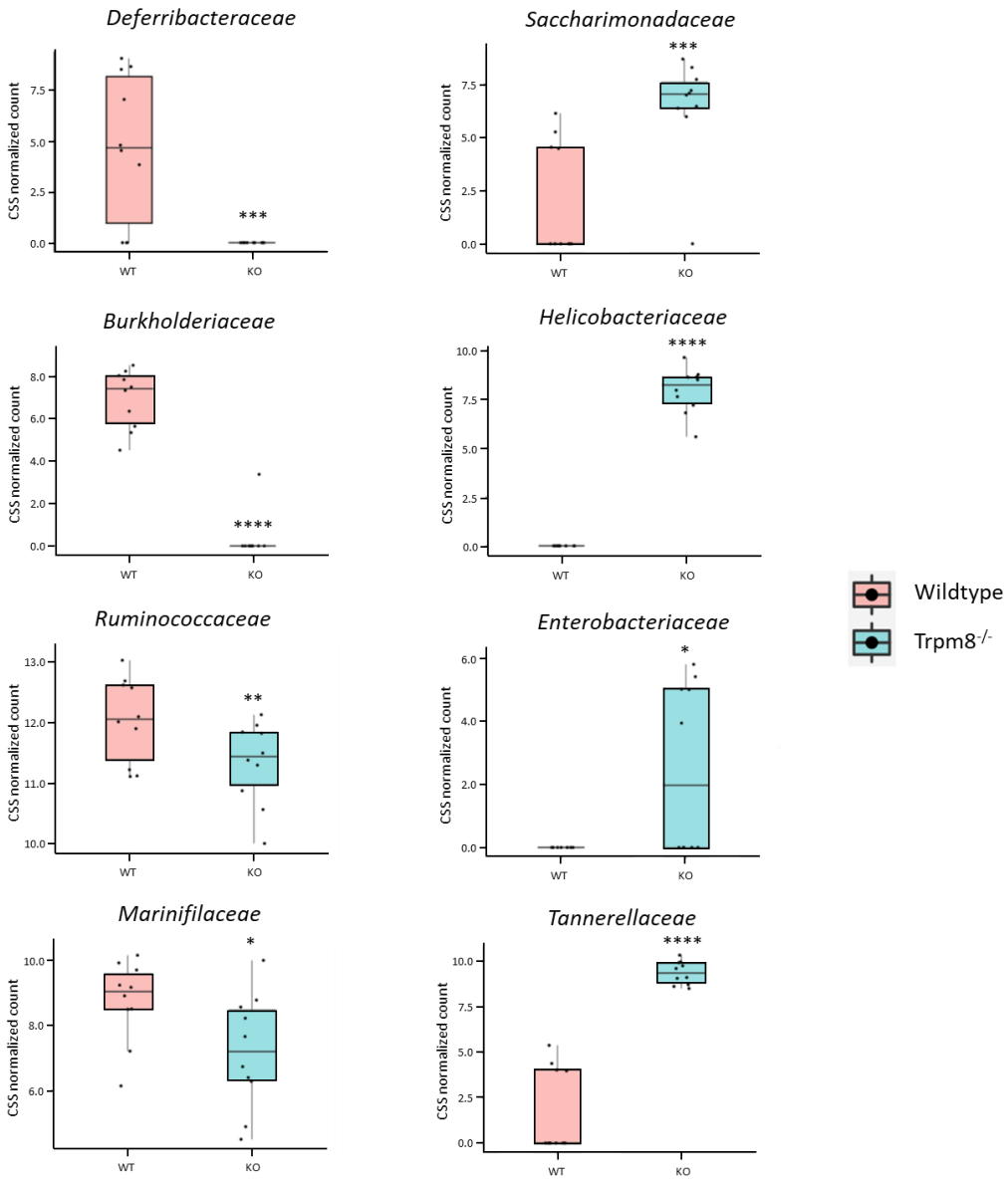

Figure 38. Effect of Trpm8 genetic deletion on relative abundances of bacteria Families altered by Trpm8 genetic deletion in healthy mice. Feces were collected before the first administration of AOM. All the counts were cumulative sum scaled (CSS). Data are plotted as boxplot with median, Q1-Q3 range and whiskers extended to 1.5 interquartile ranges of 5 mice for each experimental group. Data were statistically analyzed using one-way ANOVA followed by Student's t test. *p<0.05, **p<0.01, ***p<0.001 and ****p<0.0001 vs wildtype (WT).

3.3 AOM treatment induces changes in gut microbiota composition in wildtype and Trpm8$^{-/-}$ mice

AOM treatment in both wild type and Trpm8$^{-/-}$ mice induced significant changes in the microbiota composition as shown by PERMANOVA analysis ($p<0.001$). These changes, as shown by the PCoA analysis, were higher at the beginning of the fifth week and then reduced at the ninth and thirteenth week (Figure 39). In AOM-treated wild type mice (Figure 39A) the distance between the timepoint zero and the week 5 is more evident than in Trpm8$^{-/-}$ mice (Figure 39B). Figure 32 shows the relative composition of the gut microbiota at different timepoints in AOM-treated wild type (Figure 40A) and Trpm8$^{-/-}$ mice (Figure 40B). The more abundant families (>1%) in wild type and Trpm8$^{-/-}$ mice were *Akkermansiaceae*, *Bacteroidaceae*, *Clostridiaceae_1*, *Erysipelotrichaceae*, *Lachnospiraceae*, *Lactobacillaceae*, *Muribaculaceae*, *Rikenellaceae*, *Ruminococcaceae* and *Tannerellaceae*, that belong to the two most abundant phyla in the gut microbiota, *Bacteroides* and *Firmicutes*, except for *Akkermansiaceae* (*Verrucomicrobia*) (Figure 40).

AOM treatment induced time- and genotype-dependent changes in gut microbiota composition; in particular, in wild type mice. AOM treatment significantly reduced the relative abundance of *Ruminococcaceae*, *Lachnospiraceae* and *Marinifilaceae* families at the fifth week, and the abundance of *Peptostreptococcaceae* at the thirteenth week (Figure 41); by contrast, *Akkermansiaceae*, *Erysipelotrichaceae* and *Burkholderiaceae* families were significantly increased at the fifth week, *Clostridiaceae_1* at the fifth and ninth week and *Tannerellaceae* at the fifth, ninth and thirteenth week (Figure 42). In Trpm8$^{-/-}$ mice, AOM treatment significantly reduced the relative abundance of *Rikenellaceae* family at the fifth, ninth and thirteenth week, while increased *Erysipelotrichaceae* and *Akkermansiaceae* families at the fifth week and *Burkholderiaceae* at the thirteenth week (Figure 43).

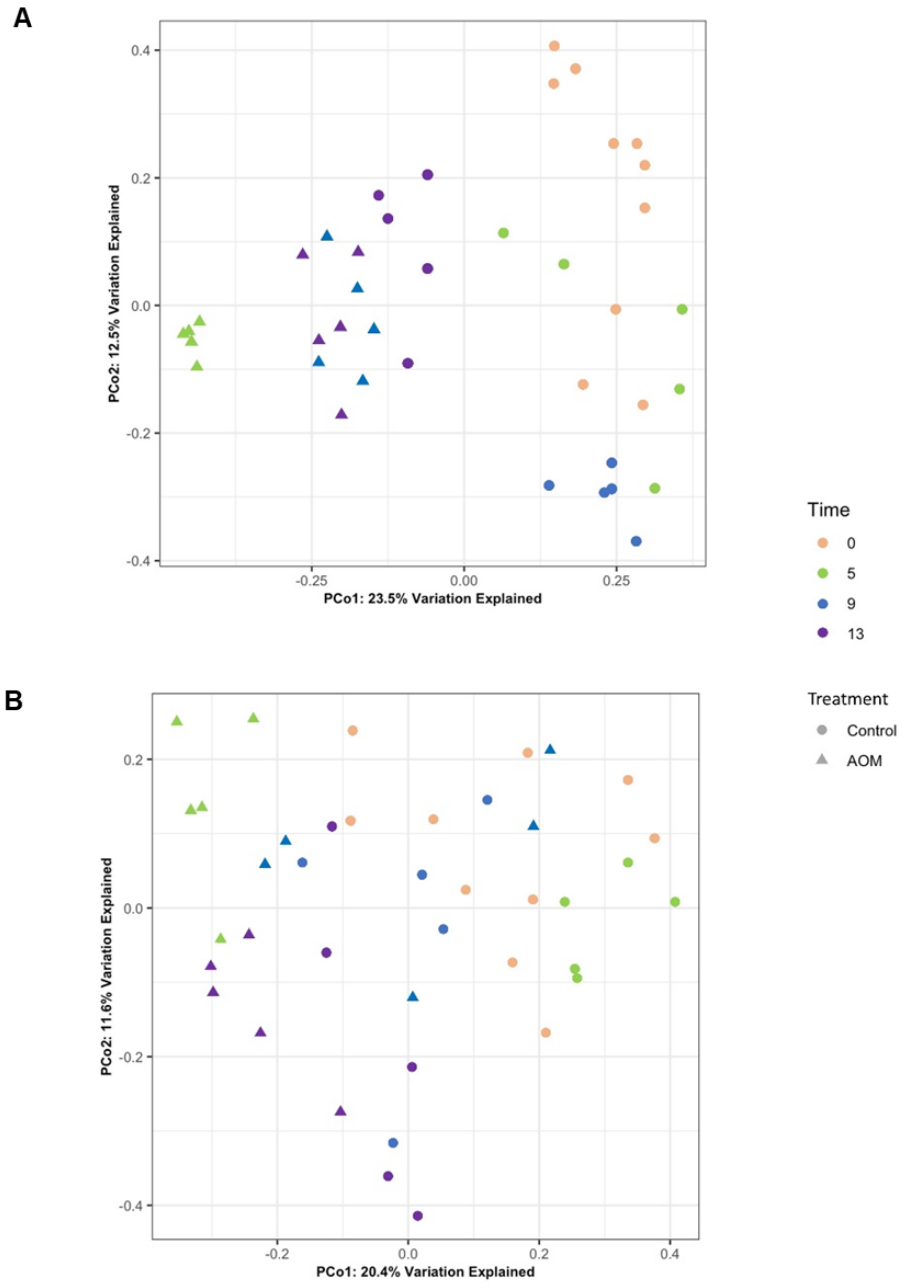

Figure 39. Effect of Trpm8 genetic deletion on gut microbiota composition using Principal coordinate analysis (PCoA) of control and AOM-treated groups in both A) wildtype and B) Trpm8$^{-/-}$ mice at different timepoints (0, 5, 9 and 13 weeks) of 5 mice for each experimental group. AOM was administered once a week for the first four weeks at the dose of 10 mg/kg by intraperitoneal injection (total dose 40 mg/kg/mouse). Mice were killed at the beginning of the thirteenth week after the first AOM injection. Feces were collected before the first administration of AOM and 5, 9 and 13 weeks after. Data were analyzed by using PERMANOVA ($p<0.001$).

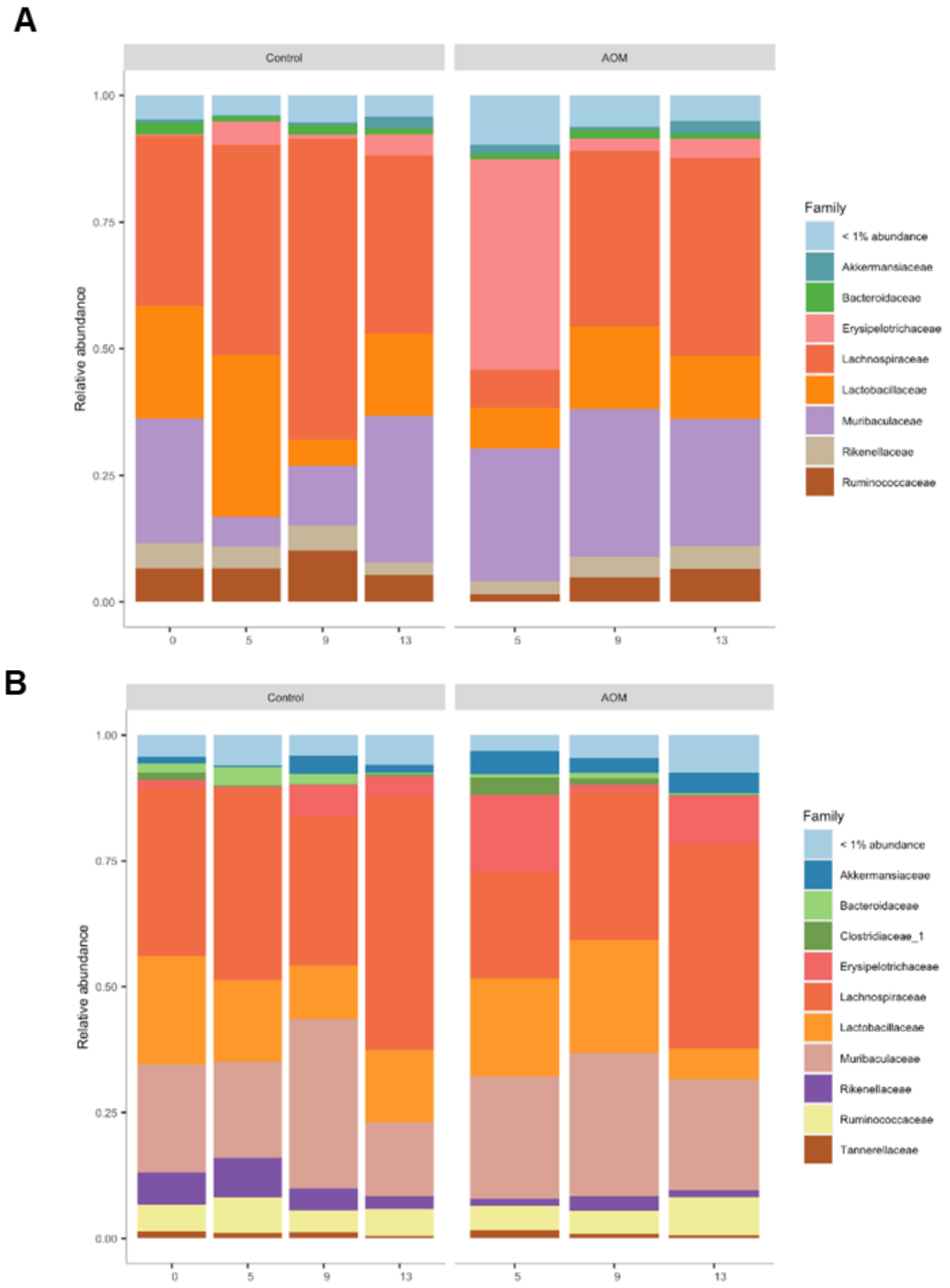

Figure 40. Effect of Trpm8 genetic deletion on gut microbiota composition of control and AOM-treated groups in A) wildtype and B) Trpm8$^{-/-}$ mice expressed as relative abundance of bacteria at Family level at different timepoints (0, 5, 9 and 13 weeks) of 5 mice for each experimental group. AOM was administered once a week for the first four weeks at the dose of 10 mg/kg by intraperitoneal injection (total dose 40 mg/kg/mouse). Mice were killed at the beginning of the thirteenth week after the first AOM injection. Feces were collected before the first administration of AOM and 5, 9 and 13 weeks after.

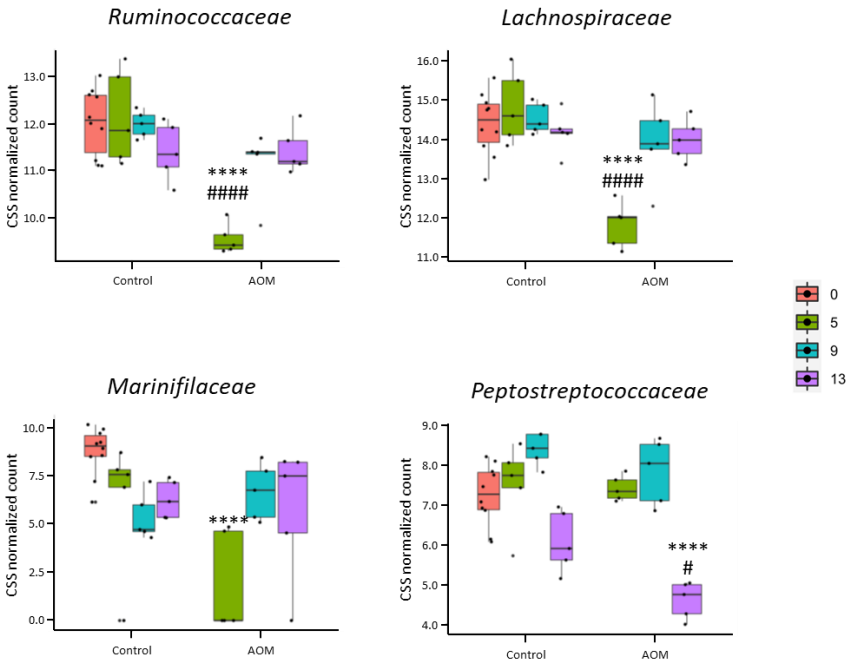

Figure 41. Effect of Trpm8 genetic deletion on the relative abundance of bacteria Families (expressed as cumulative sum scaled) in AOM-treated wildtype mice compared with the control group at different timepoints (0, 5, 9 and 13 weeks): families reduced by AOM treatment. AOM was administered once a week for the first four weeks at the dose of 10 mg/kg by intraperitoneal injection (total dose 40 mg/kg/mouse). Mice were killed at the beginning of the thirteenth week after the first AOM injection. Feces were collected before the first administration of AOM and 5, 9 and 13 weeks after. Data are plotted as boxplot with median, Q1-Q3 range and whiskers extended to 1.5 interquartile ranges. Data were statistically analyzed using two-way ANOVA followed by the Tuckey's multiple comparisons test. ****p<0.0001 *vs* week 0; #p<0.05 *vs* control at the same timepoint).

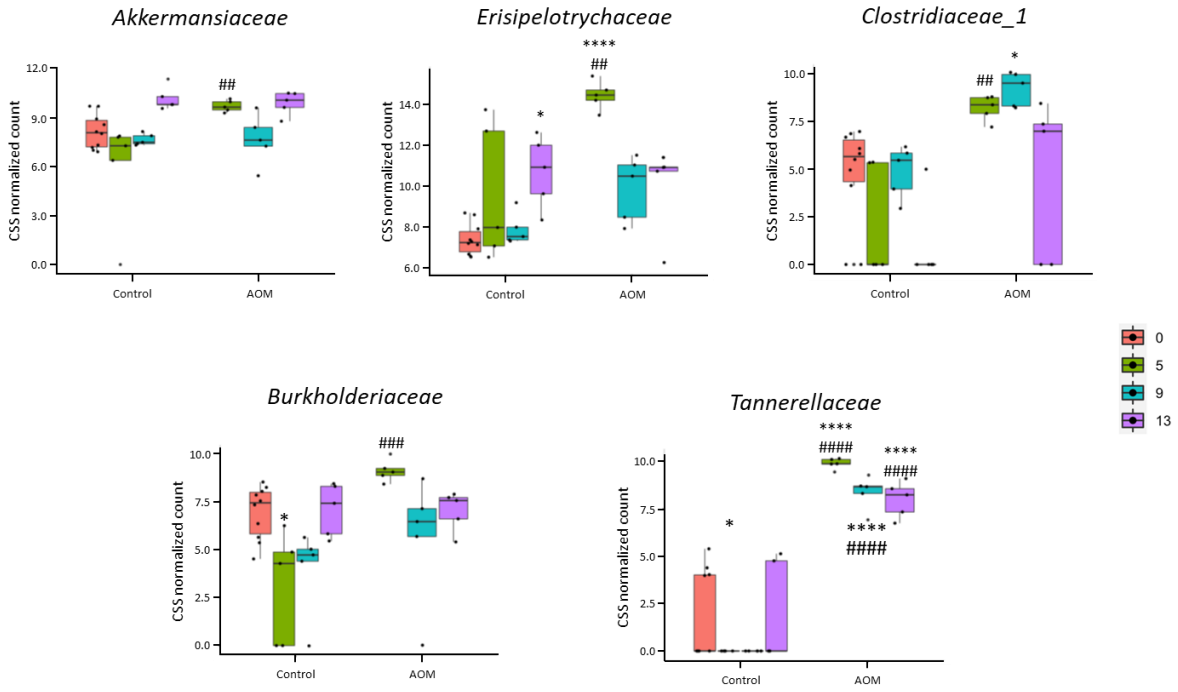

Figure 42. Effect of Trpm8 genetic deletion on the relative abundance of bacteria Families (expressed as cumulative sum scaled) in AOM-treated wildtype mice compared with the control group at different timepoints (0, 5, 9 and 13 weeks): families increased by AOM treatment. AOM was administered once a week for the first four weeks at the dose of 10 mg/kg by intraperitoneal injection (total dose 40 mg/kg/mouse). Mice were killed at the beginning of the thirteenth week after the first AOM injection. Feces were collected before the first administration of AOM and 5, 9 and 13 weeks after. Data are plotted as boxplot with median, Q1-Q3 range and whiskers extended to 1.5 interquartile ranges. Data were statistically analyzed using two-way ANOVA followed by the Tuckey's multiple comparisons test. *p<0.05 and ****p<0.0001 *vs* week 0; ##p<0.01, ###p<0.001 and ####p<0.0001 *vs* control at the same timepoint).

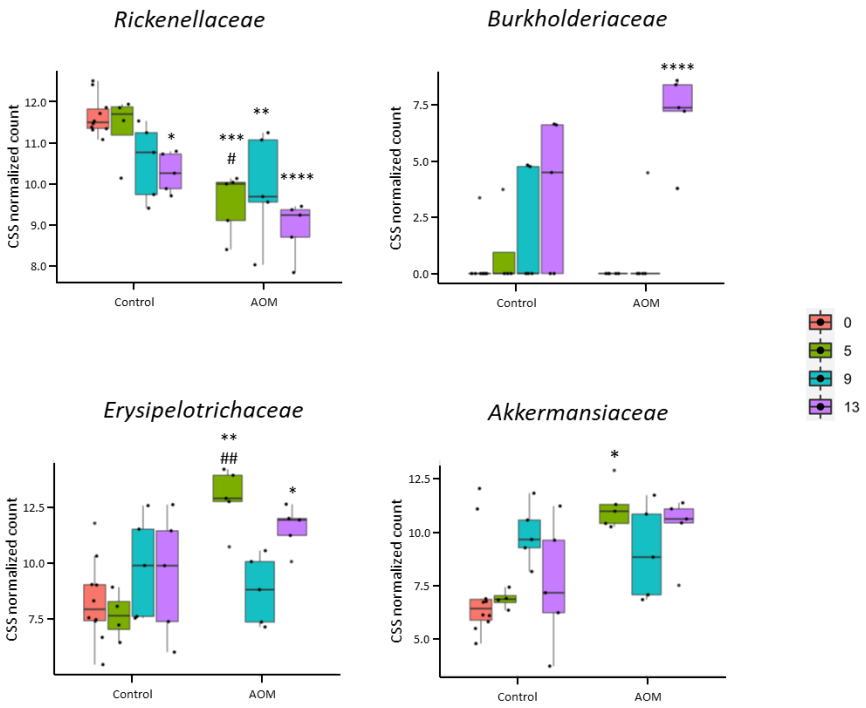

Figure 43. Effect of Trpm8 genetic deletion on the relative abundance of bacteria Families (expressed as cumulative sum scaled) in AOM-treated Trpm8$^{-/-}$ mice compared with the control group at different timepoints (0, 5, 9 and 13 weeks). AOM was administered once a week for the first four weeks at the dose of 10 mg/kg by intraperitoneal injection (total dose 40 mg/kg/mouse). Mice were killed at the beginning of the thirteenth week after the first AOM injection. Feces were collected before the first administration of AOM and 5, 9 and 13 weeks after. Data are plotted as boxplot with median, Q1-Q3 range and whiskers extended to 1.5 interquartile ranges of 5 mice for each experimental group. Data were statistically analyzed using two-way ANOVA followed by the Tuckey's multiple comparisons test. *p<0.05, **p<0.01, ***p<0.001 and ****p<0.0001 *vs* week 0; ##p<0.01 *vs* control at the same timepoint).

3.4 AOM-treated Trpm8$^{-/-}$ mice have a different gut microbiota composition than wild-type mice.

As reported before, AOM treatment induced tumour formation in both wildtype and Trpm8$^{-/-}$ mice, with the latter being less susceptible than the first (Figure 36); moreover, AOM treatment produced changes in gut microbiota composition in both wildtype and Trpm8$^{-/-}$ mice (Figures 31-34). In order to evaluate if the lower susceptibility of Trpm8$^{-/-}$ mice in developing an AOM-induced sporadic colorectal cancer, we compared the gut microbiota of the two AOM-treated groups: PCoA analysis showed a different response of gut microbiota in AOM-treated Trpm8$^{-/-}$ mice, compared to AOM-treated wildtype mice, with a higher difference at the fifth week (Figure 44A); using PERMANOVA, this effect was reported to be statistically significant ($p<0.001$). Moreover, the Shannon alpha diversity showed a reduction in the number of bacteria taxa richness at the fifth week in wildtype mice, while at the same timepoints the Trpm8$^{-/-}$ mice responded differently, indicating that there is a predominance of few bacteria families in the gut microbiota of wildtype mice (Figure 44B). This was confirmed by the relative composition of gut microbiota at family level (Figure 45), that shows a sudden predominance of *Erysipelotrichaceae* in wildtype mice at the fifth week that on the other hand was not so evident in Trpm8$^{-/-}$ mice.

Looking at individual families (Figure 46), there is a difference in the variation of the families *Ruminococcaceae*, *Lachnospiraceae* and *Marinifilaceae*, which were significantly decreased at the fifth week in wild type mice but not in Trpm8$^{-/-}$ mice. Moreover, at the fifth week, the *Erysipelotrichaceae* family increase was higher in wild type mice compared to Trpm8$^{-/-}$ mice. The reduction in the relative abundance of *Rikenellaceae* was higher in Trpm8$^{-/-}$ starting from the fifth week, compared to wild type mice.

Lactobacillaceae, which were significantly lower at the timepoint zero in

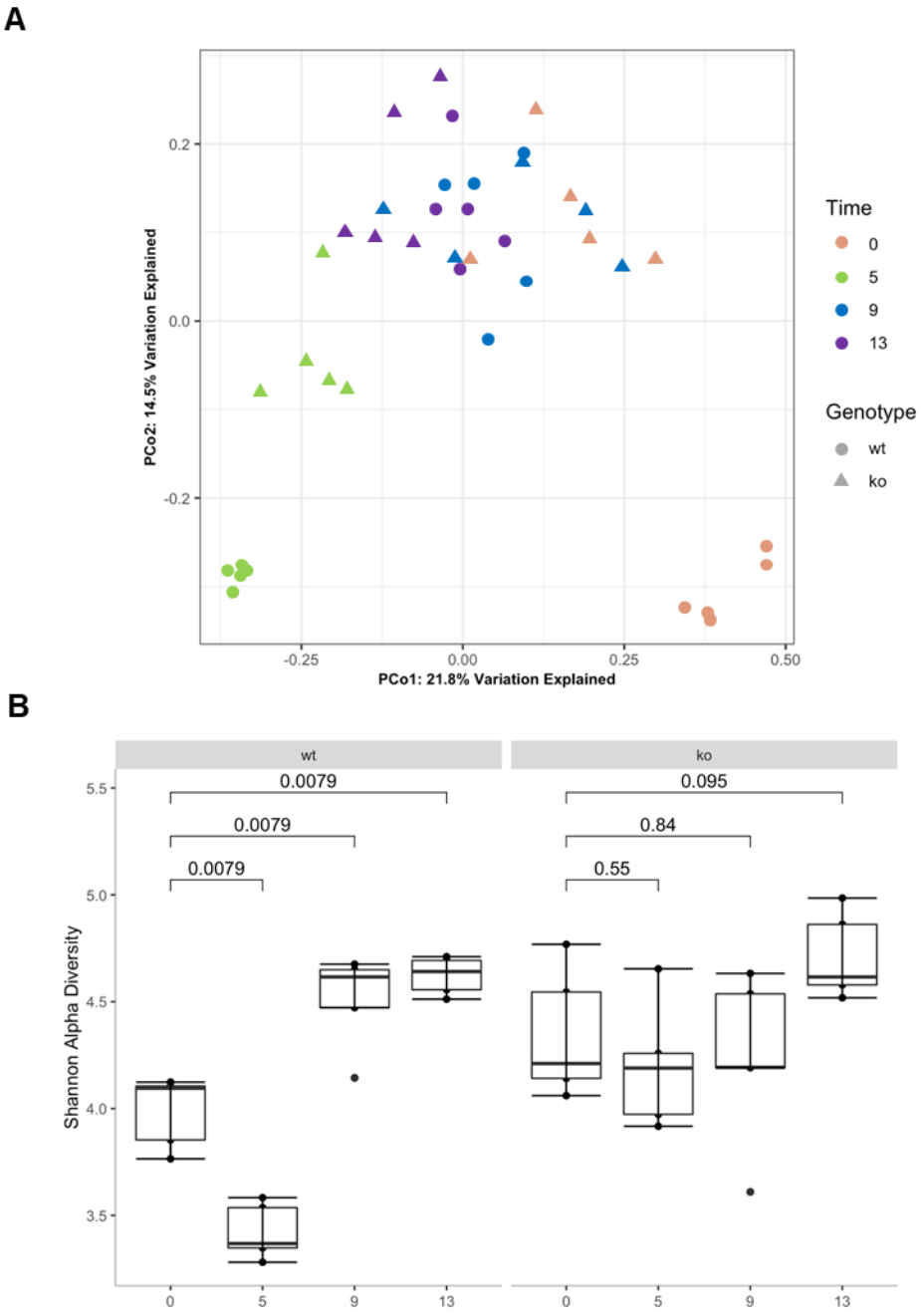

Figure 44. Effect of Trpm8 genetic deletion on gut microbiota composition of AOM-treated wildtype and Trpm8$^{-/-}$ mice. A) Principal coordinate analysis (PCoA) on the gut microbiota composition, performed using Bray-Curtis dissimilarity, an index used to estimate beta-diversity. AOM was administered once a week for the first four weeks at the dose of 10 mg/kg by intraperitoneal injection (total dose 40 mg/kg/mouse). Mice were killed at the beginning of the thirteenth week after the first AOM injection. Feces were collected before the first administration of AOM and 5, 9 and 13 weeks after. Data were analyzed by using PERMANOVA ($p<0.001$). B) Shannon Alpha diversity. Data are plotted as boxplot with median, Q1-Q3 range and whiskers extended to 1.5 interquartile ranges. Data were statistically analyzed using two-way ANOVA followed by the Tuckey's multiple comparisons test of 5 mice for each experimental group.

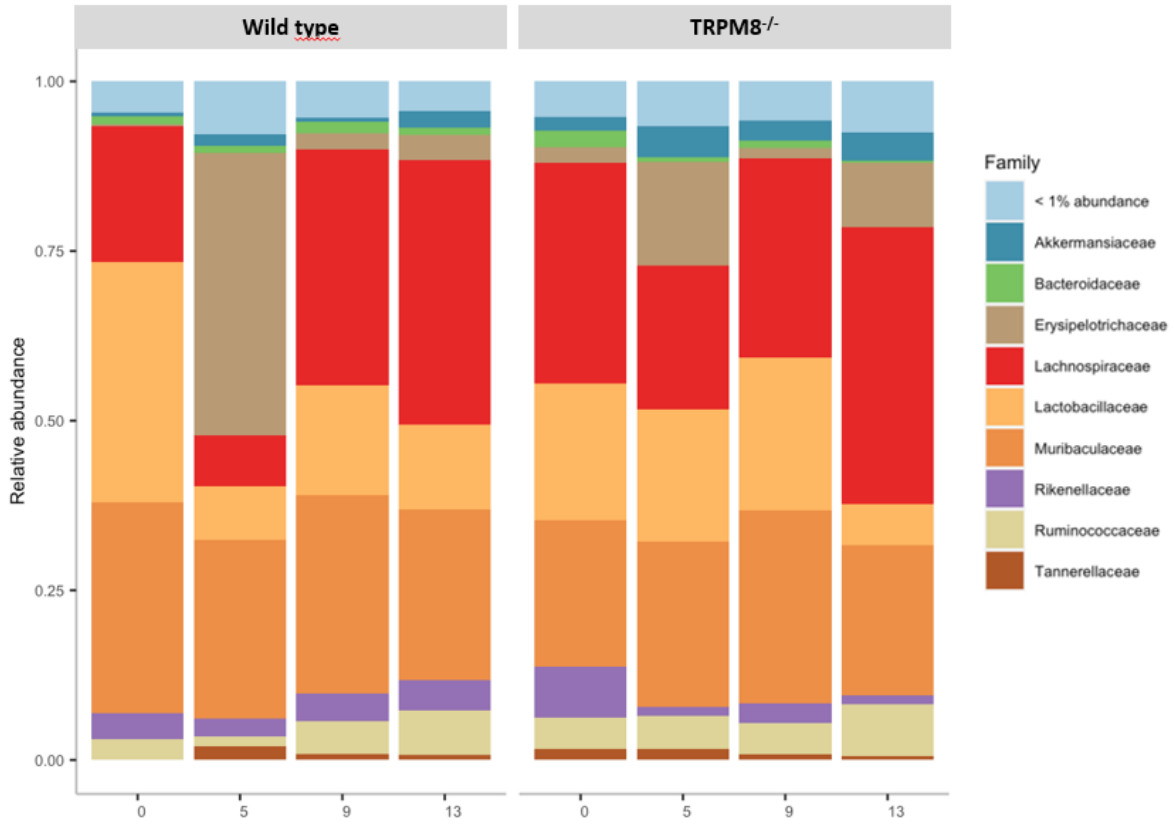

Figure 45. Effect of Trpm8 genetic deletion on gut microbiota composition of AOM-treated wildtype and Trpm8$^{-/-}$ mice expressed as relative abundance of bacteria at Family level at different timepoints (0, 5, 9 and 13 weeks) of 5 mice for each experimental group. AOM was administered once a week for the first four weeks at the dose of 10 mg/kg by intraperitoneal injection (total dose 40 mg/kg/mouse). Mice were killed at the beginning of the thirteenth week after the first AOM injection. Feces were collected before the first administration of AOM and 5, 9 and 13 weeks after.

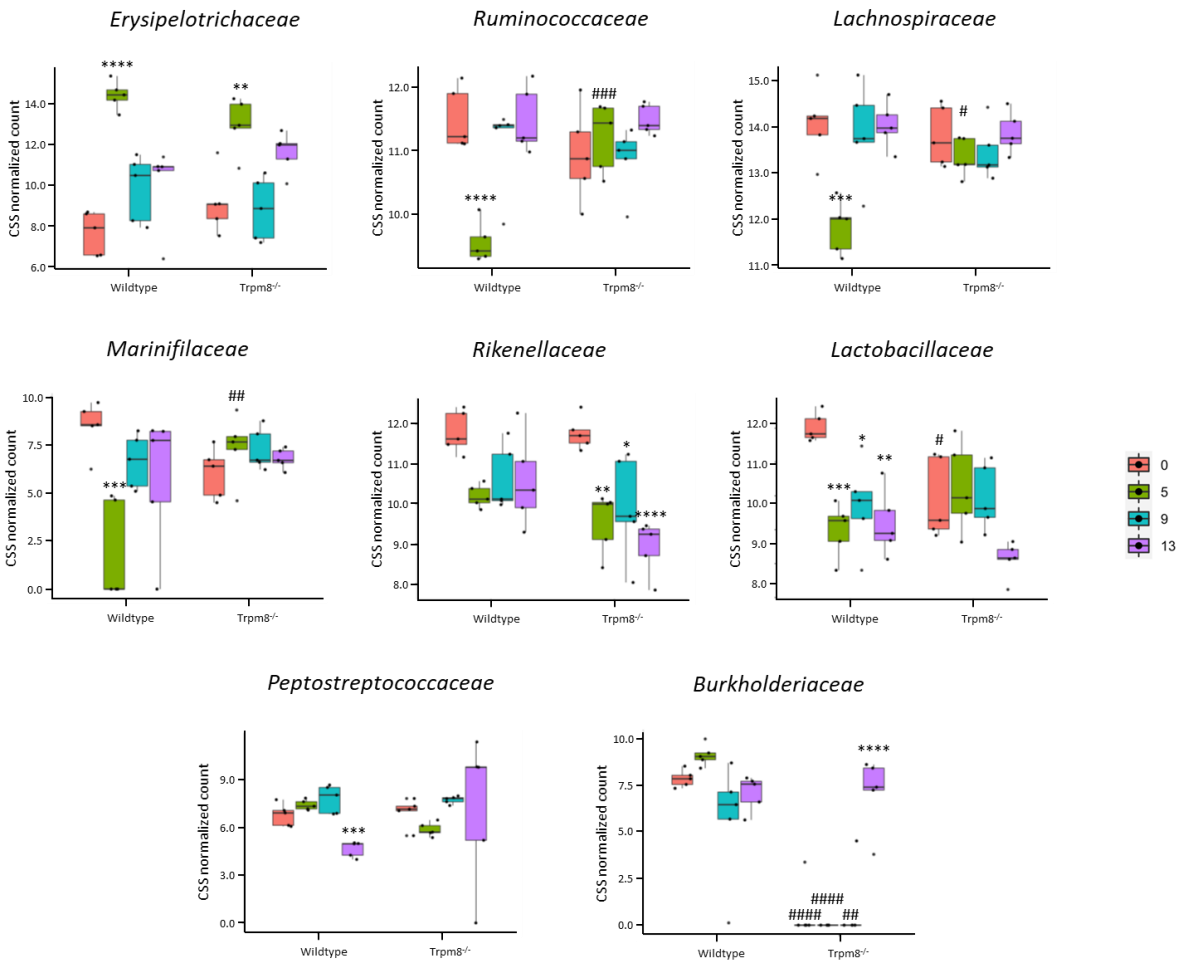

Figure 46. Effect of Trpm8 genetic deletion on the relative abundance of bacteria Families (expressed as cumulative sum scaled) in AOM-treated Trpm8$^{-/-}$ mice compared with AOM-treated wildtype mice at different timepoints (0, 5, 9 and 13 weeks). AOM was administered once a week for the first four weeks at the dose of 10 mg/kg by intraperitoneal injection (total dose 40 mg/kg/mouse). Mice were killed at the beginning of the thirteenth week after the first AOM injection. Feces were collected before the first administration of AOM and 5, 9 and 13 weeks after. Data are plotted as boxplot with median, Q1-Q3 range and whiskers extended to 1.5 interquartile ranges of 5 mice for each experimental group. Data were statistically analyzed using two-way ANOVA followed by the Tuckey's multiple comparisons test. *p<0.05, **p<0.01, ***p<0.001 and ****p<0.0001 *vs* week 0; #p<0.05, ##p<0.01 and ###p<0.001 *vs* wildtype at the same timepoint).

Trpm8$^{-/-}$ mice, were significantly reduced by AOM treatment in wildtype mice starting from the fifth week, effect that was significant in Trpm8$^{-/-}$ mice only at the thirteenth week. The relative abundance of *Peptostreptococcaceae*, on the other hand, was reduced at the thirteenth week by AOM administration but only in wildtype mice.

Finally, the *Burkholderiaceae* family, which was present in each timepoint in wild type mice, was undetectable in Trpm8$^{-/-}$ mice except at the thirteenth week.

Part IV – Gut microbiota impairment modulates endocannabinoidome mediator levels in healthy and inflamed mice

4.1 Gut microbiota impairment does not affect macroscopic inflammatory parameters in DNBS-induced colitis

To understand the role of the eCBome – mBIome axis in the development of experimental colitis, we used different conditions to simulate impairment of the gut microbiota: mice treated with an antibiotic cocktail (ABX) and mice raised under germfree (GF) conditions (Figure 47). The effects of DNBS on ABX and GF mice were compared with those on conventionally-raised (CR) mice.

Intracolonic administration of DNBS elicited remarkable inflammation in the mice regardless of their microbiota (Figure 48). As shown by the colon weight/colon length *ratio*, a macroscopic parameter of colon inflammation, CR, ABX and GF mice treated with DNBS showed a statistically significant increase in this parameter compared to their own control; interestingly, the ratio was significantly smaller in GF mice treated with DNBS than DNBS-treated CR and ABX mice (Figure 48A); when analyzing the DAI score, DNBS-treated CR and ABX mice showed a sudden increase in this parameter on day 1 and 2 and a slight decrease on day 3 (Figure 48B); in contrast, the DAI score in DNBS-treated GF mice was lower in the first days of the protocol and reached the same value as the other two groups on the last day (day 3), suggesting that DNBS colitis develops differently in GF mice. Finally, all DNBS-treated mice, regardless of their microbiota status, showed body weight loss of the same intensity when compared to control mice (Figure 48C).

4.2 Gut microbiota impairment alters the expression of cytokines and MPO activity in healthy and DNBS-treated mice

To take a closer look at the molecular pathways of inflammation, we examined the expression levels of a number of cytokines (IL-1β, IL-6, IL-10 and TNFα)

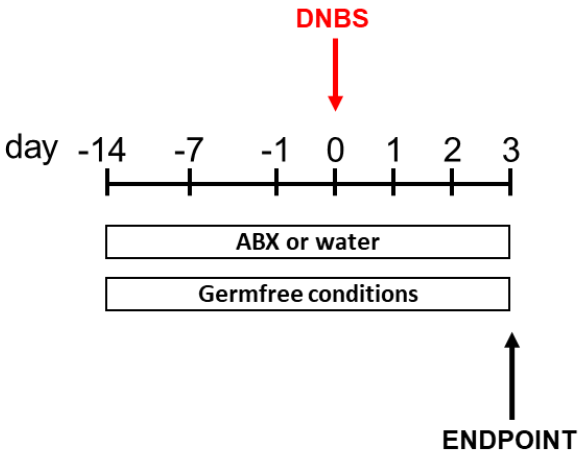

Figure 47. Schematic representation of experimental procedures used to alter gut microbiota composition (antibiotics pre-treatment or germfree conditions) in the DNBS-induced model of ulcerative colitis. Antibiotic cocktail containing ampicillin (1 mg/mL), streptomycin (1 mg/mL) and clindamycin (1 mg/mL) was given to mice for two weeks. DNBS was injected in mice colon at the dose of 120 mg/kg; mice were killed three days after the DNBS administration.

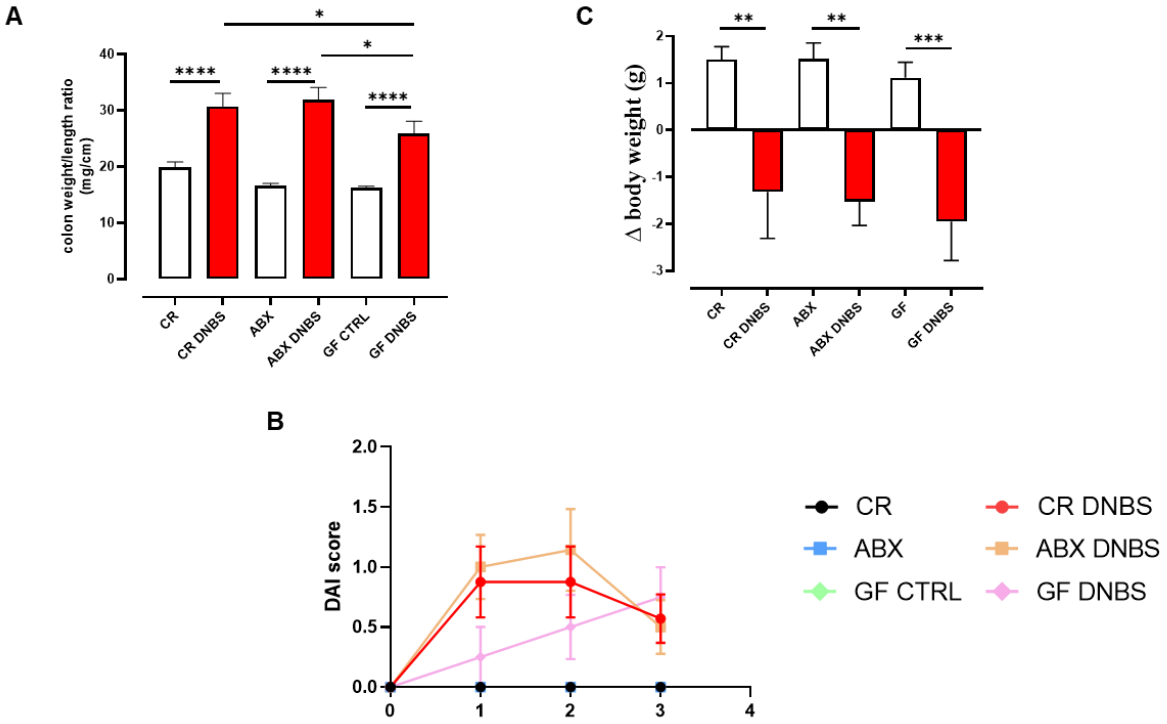

Figure 48. Effect of DNBS administration in conventionally raised (CR), antibiotics- (ABX-) treated and germfree (GF) mice on macroscopic inflammatory parameters. A) colon weight/colon length *ratio*, B) disease activity index (DAI) score and C) body weight loss. DNBS was injected in mice colon at the dose of 120 mg/kg in CR; ABX-treated mice received an antibiotic cocktail (ampicillin, streptomycin and clindamycin 1 mg/mL each) starting 14 days before the DNBS administration and for the whole length of the experiment. Mice were killed three days after the DNBS administration. Data are expressed as mean ± SEM of 8 mice for each experimental group. Data were statistically analyzed using two-way ANOVA followed by the Fisher's LSD test. *p<0.05, **p<0.001, ***p<0.001 and ****p<0.0001.

and MPO activity (a marker of neutrophil infiltration) (Figure 49).

All mice, regardless of microbiota status, showed similar basal levels of IL-1β and IL-6 expression. Treatment with DNBS resulted in an increase in the expression of IL-1β and IL-6 in CR and ABX mice, with the effect being significant only in ABX mice (p value for CR vs CR DNBS was 0.0526). No changes in IL-1β and IL-6 expression were observed in GF mice (Figures 49A and B). CR mice have basal TNFα expression levels that are significantly higher than ABX and GF mice. DNBS treatment resulted in a significant increase in TNFα expression levels in CR and ABX mice, but not in GF mice (Figure 49C). Germfree mice have lower basal levels of IL-10 than CR and ABX mice; in all mice, IL-10 levels were unaffected by DNBS administration (Figure 49D). Finally, basal MPO activity was significantly higher in GF mice than in CR and ABX mice. DNBS administration resulted in a significant increase in MPO activity in CR, but not in ABX and GF mice. All these data suggest that mice treated with antibiotics and raised under germfree conditions show a different evolution of DNBS-induced colitis (Figure 49E).

4.3 Conventionally raised and germfree mice show different levels of endocannabinoidome mediators under healthy and inflammatory conditions

To understand whether this different response in colon inflammation correlates with a different response in the amount of endocannabinoidome mediators, we analyzed the levels of lipid mediators in colonic tissue (Figures 50 and 51).

Regarding the NAEs levels, no differences were found in AEA and PEA basal levels between all groups (Figure 50). In contrast, GF mice showed significantly higher basal levels of OEA, LEA and DHEA than CR and ABX mice; basal levels of 13-HODE-EA were significantly higher in GF mice than in CR mice (Figure 50).

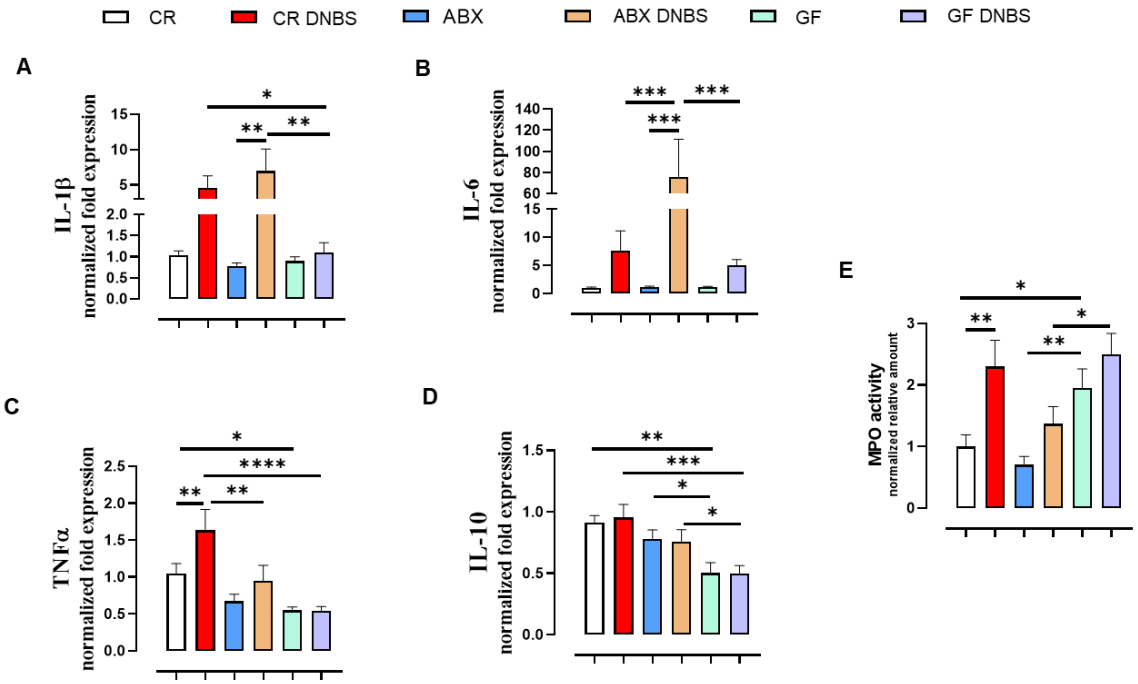

Figure 49. Effect of DNBS administration in conventionally raised (CR), antibiotics- (ABX-) treated and germfree (GF) mice on microscopic inflammatory parameters. A-D) expression levels of cytokines involved in inflammation, E) MPO activity (expressed as normalized relative amount). DNBS was injected in mice colon at the dose of 120 mg/kg in CR; ABX-treated mice received an antibiotic cocktail (ampicillin, streptomycin and clindamycin 1 mg/mL each) starting 14 days before the DNBS administration and for the whole length of the experiment. Mice were killed three days after the DNBS administration. Data are expressed as mean ± SEM of 8 mice for each experimental group. Data were statistically analyzed using two-way ANOVA followed by the Fisher's LSD test. *p<0.05, **p<0.01 and ***p<0.001.

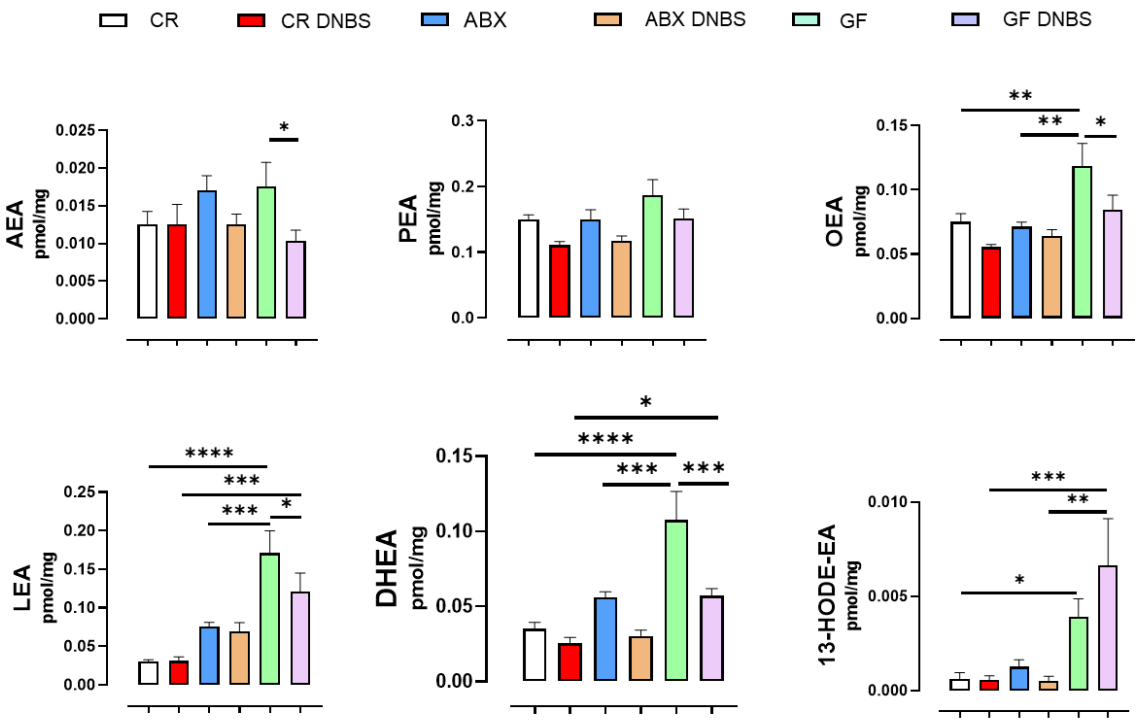

Figure 50. Effect of DNBS administration in conventionally raised (CR), antibiotics- (ABX-) treated and germfree (GF) mice on acylethanolamines (NAEs) levels in colonic tissues. DNBS was injected in mice colon at the dose of 120 mg/kg in CR; ABX-treated mice received an antibiotic cocktail (ampicillin, streptomycin and clindamycin 1 mg/mL each) starting 14 days before the DNBS administration and for the whole length of the experiment. Mice were killed three days after the DNBS administration. Data are expressed as mean ± SEM of 8 mice for each experimental group. Data were statistically analyzed using two-way ANOVA followed by the Fisher's LSD test. *p<0.05, **p<0.01, ***p<0.001 and ****p<0.0001.

DNBS treatment had no significant effect on NAE levels in CR and ABX mice (Figure 50). In contrast, the levels of AEA, OEA, LEA and DHEA were significantly reduced by DNBS administration in GF mice (Figure 50). In inflamed tissues, the levels of LEA and DHEA were significantly higher in GF mice than in CR, while 13-HODE-EA was significantly higher in GF mice than in CR and ABX mice (Figure 50).

Regarding acylglycerols levels, basal 2-AG levels were significantly higher in GF mice than in ABX mice (no difference was observed with CR mice) (Figure 51). In contrast, lower basal 2-LG levels were observed in GF and ABX mice than in CR mice (Figure 51). In all groups, DNBS administration had no significant effect on MAG levels (Figure 51). In inflamed tissues, levels of 2-LG were significantly lower in ABX mice compared to CR, while levels of 13-HODE-G were significantly higher in GF mice than in ABX mice (Figure 51).

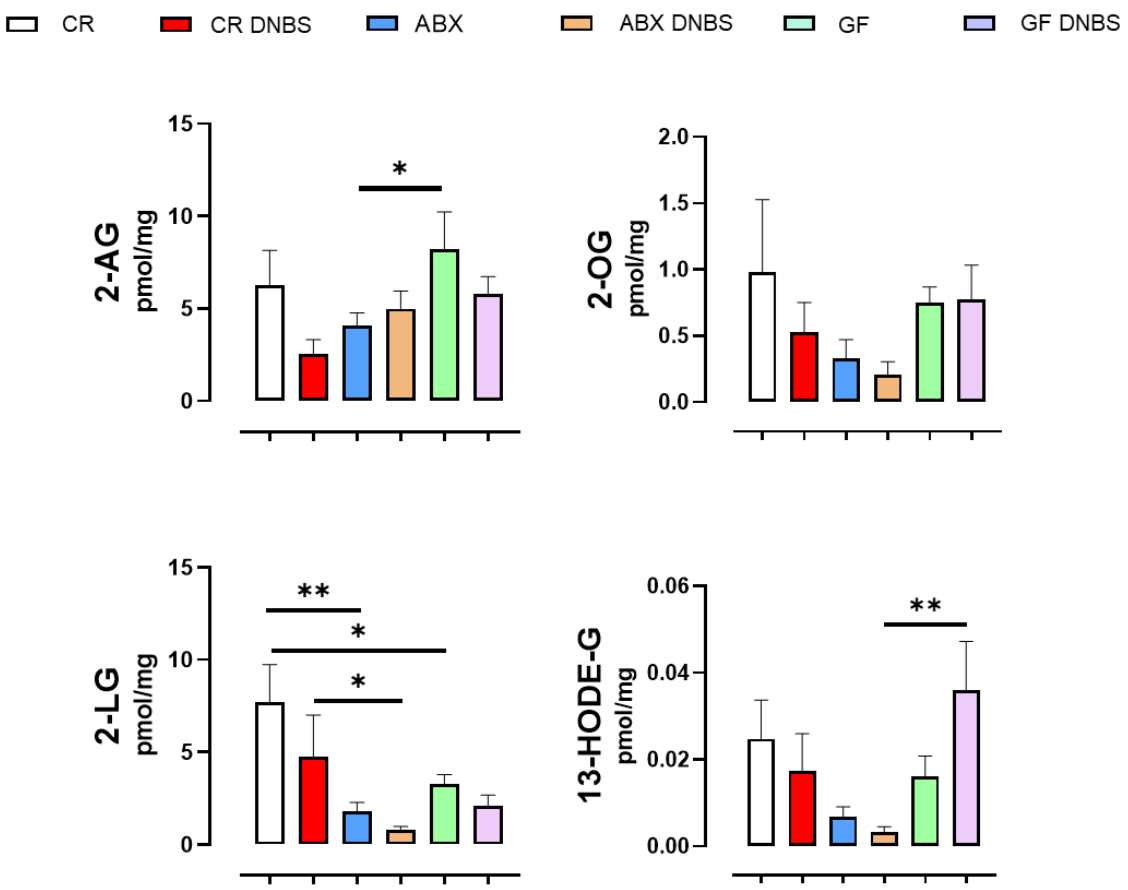

Figure 51. Effect of DNBS administration in conventionally raised (CR), antibiotics- (ABX-) treated and germfree (GF) mice on 2-monoacylglycerols (MAGs) levels in colonic tissues. DNBS was injected in mice colon at the dose of 120 mg/kg in CR; ABX-treated mice received an antibiotic cocktail (ampicillin, streptomycin and clindamycin 1 mg/mL each) starting 14 days before the DNBS administration and for the whole length of the experiment. Mice were killed three days after the DNBS administration. Data are expressed as mean ± SEM of 8 mice for each experimental group. Data were statistically analyzed two-way ANOVA followed by the Fisher's LSD test. *p<0.05, **p<0.01 and ***p<0.001.

DISCUSSION

As previously reported, IBD and CRC are health problems that affect millions of people worldwide and for which there are no effective treatments. A plethora of recent studies have highlighted the involvement of gut dysbiosis in the development of these pathologies (Pittayanon et al., 2020; Sultan et al., 2021). Dysbiosis of the gut microbiota (altered composition of the gut microbiota) has been demonstrated in patients with IBD and CRC (Lucas et al., 2017; Tilg et al., 2018; Pittayanon et al., 2020; Sultan et al., 2021). The gut microbiota has also been shown to mediate the effects of pharmacological, nutraceutical and dietary interventions that have a positive impact on gut diseases (Wu et al., 2019a; Fernandez et al., 2020; Gu et al., 2020).

The endocannabinoidome has been described as an "expanded endocannabinoid system" and contains approximately 100 lipid mediators, 20 enzymes, and 20 receptors (Di Marzo, 2020). This complex system is the target responsible for the pharmacological effects of phytocannabinoids, active molecules found in the plant *Cannabis sativa* (Di Marzo, 2020). In addition, a close link between the eCBome and the microbiome (mBIome) has recently been established, known as the eCBome-mBIome axis (Shen et al., 2021), which appears to play a role in several physiological and physio-pathological functions, including energy intake and processing (Sihag and Di Marzo, 2022). Moreover, the gut microbiota has been reported to influence, strongly and directly, eCBome signalling in the small intestine and exploits eCBome signaling to exert some of its physio-pathological functions (Manca et al., 2020).

In this thesis we have demonstrated that the existing link between eCBome and the gut microbiota (eCBome-mBIome axis) impacts on the development of ulcerative colitis and colorectal cancer.

Part I – Cannabidivarin (CBDV) counteracts chemically-induced ulcerative colitis and microbiota dysbiosis in mice via TRPA1 activation

Although *Cannabis* use is a common practice in patients with IBD in USA to relieve their symptoms (Izzo et al., 2015), our study is the first to show that CBDV, the propyl analogue of one of the most studied phytocannabinoids cannabidiol (Morales et al., 2017), exerts anti-inflammatory effects in an ulcerative colitis mouse model Recently, CBDV has been investigated for its potential use in the treatment of epilepsy. A double-blind, randomized, placebo-controlled phase 2 trial showed that CBDV was well tolerated in patients with inadequately controlled focal seizures (NCT02369471). In addition, a phase 2 clinical trial is currently in the recruitment phase to determine whether CBDV has the necessary efficacy and safety to be used to treat autism spectrum disorders in children (NCT03202303).

In this study, using two different models of chemically-induced ulcerative colitis and an *in vitro* model using colonic biopsies from paediatric ulcerative colitis patients, we have shown that CBDV exerts an anti-inflammatory effect on the gut attenuating colon inflammatory parameters in all these models and this effect involves the TRPA1 channel.

In the DNBS-induced ulcerative colitis model, we showed that CBDV administered orally or intraperitoneally attenuated inflammation by: a) reducing the colon weight/ colon length *ratio* in inflamed colonic tissue, a macroscopic parameter of colon inflammation ; b) partially restoring the change in intestinal permeability induced by DNBS administration; c) counteracting leucocyte infiltration into colonic tissue through a reduction of MPO activity and MCP-1 expression (Krawisz et al., 1984; Grimm et al., 1996); d) decreasing the histological damage of colonic epithelium and e) reducing levels of pro-inflammatory cytokines. Administration of CBDV in the dose ranges evaluated (0.3-30 mg/kg) did not show a full dose-response effect, with the stronger effect

occurring at 3 mg/kg dose after oral administration. Interestingly, the oral dose of 3 mg/kg CBDV oral was about 70-fold lower than the dose that reduced the severity of seizure in rodents (Hill et al., 2012). The lack of a full dose-response curve is not uncommon for phytochemicals such as other phytocannabinoids (Jamontt et al., 2010)); the lack of a dose-response curve is likely due to the multi-target action of these compounds (Morales et al., 2017). Surprisingly, CBDV was more active after oral gavage administration than after intraperitoneal injection. Although it was not proven in this work, this result seems to suggest that a more active metabolite of CBDV is produced after oral gavage, but not after intraperitoneal administration.

The anti-inflammatory effect of CBDV has also been confirmed by a second model of ulcerative colitis, namely DSS-induced colitis. Unlike DNBS, which acts as a haptenizing agent, DSS exerts its inflammatory effect by disrupting the mucosal barrier of the colonic epithelium, allowing bacteria to enter the mucosal layer, thereby activating the innate immune response (Kiesler et al., 2015). The fact that CBDV given by oral gavage at a 3 mg/kg dose reduced inflammatory parameters (colon weight/colon length *ratio*, MPO, reduction of pro-inflammatory cytokines and splenomegaly) even in the DSS-induced ulcerative colitis model highlights the fact that CBDV has anti-inflammatory properties.

Although the exact role of the gut microbiota in the pathogenesis of IBD has not fully elucidated, changes in the composition of the gut microbiota have been reported to be positively correlated with the development of IBD and dysbiosis plays a crucial role in these diseases (Pittayanon et al., 2020; Sultan et al., 2021).

Here, we showed that DNBS administration leads to a shift in bacterial communities in the gut and that CBDV administration was able to partially modify this DNBS-induced imbalance, particularly by reducing the presence of *Proteobacteria*, a strain known to be associated with colonic inflammation

(Nishida et al., 2018). CBDV increased the relative abundance of an u.g. of *Bacteroidales* reported to contain members that play a role in gut homeostasis by recruiting IL-6 producing lymphocytes and promoting gut barrier function (Kuhn et al., 2018). We did not detect an increase in IL-6 in the inflamed mice treated with CBDV, suggesting that the protective increase in some u.g. of *Bacteroidales* can act through other mechanisms. This hypothesis is also supported by the findings that some species present in the u.g. of *Bacteroidales* play an opposite role in colonic inflammation (Dziarski et al., 2016). We also observed that DNBS decreased the relative abundance of members of *Clostridium* cluster XIVa and IV, which are known for their role in intestinal homeostasis; administration of CBVD had a positive effect on the level of *Clostridium aldense*, which was decreased by DNBS administration. These results show that CBDV caused a partial reversal of DNBS-induced dysbiosis, although a causal effect of CBDV administration cannot be assumed.

To understand the mechanism of action of CBDV we have investigated the possible involvement of TRPA1, one of the CBDV targets (De Petrocellis et al., 2011); in particular, CBDV is able to activate and then desensitize this receptor (De Petrocellis et al., 2011). TRPA1 is a calcium-permeable channel of the TRP family that has been reported to be involved in IBD via the release of substance P (Engel et al., 2011; Bertin et al., 2014). Other TRPA1 agonists have been reported to ameliorate experimental colitis via receptor desensitization (Kistner et al., 2016), and pharmacological blockade or ablation has been reported to ameliorates experimental colitis (Engel et al., 2011; Pereira et al., 2013; Vermeulen et al., 2013).

In our experiments, DNBS administration caused a significant increase in TRPA1, whereas CBDV administration in DNBS-treated mice completely counteracted this effect; moreover, two other members of TRP channel family, TRPV1 and TRPV2, known to be target of CBDV and involved in colitis (De Petrocellis et al., 2011; Bertin et al., 2014; Issa et al., 2014), were not modified

in their expression by CBDV administration, suggesting a possible involvement of TRPA1 in CBDV mechanism of action.

This hypothesis was supported by the use of a selective TRPA1 antagonist HC030031 (Berrout et al., 2017). Interestingly, co-administration of CBDV and HC030031 in DNBS-treated mice reduced the anti-inflammatory effect of CBVD as measured by MPO activity. At the dose used in this work (30 mg/kg), HC030031 had no anti-inflammatory effect per se (data not shown). On the other hand, a higher dose of HC030031 (300 mg/kg) is reported to be protective against experimental colitis (Engel et al., 2011). These results suggest that the effect of CBDV on DNBS-induced colitis in mice depends on the presence of TRPA1 and probably acts by desensitising this channel, which is overexpressed in DNBS-treated mice.

IBD is at increasing incidence in the adult population as well as in paediatric patients (Malaty et al., 2010), who exhibit a more aggressive form of the disease and a more rapid course compared to adults (Levine, 2009). We have shown that TRPA1 is overexpressed in biopsies from UC paediatric patients compared to control tissues, a condition that has also been observed in mouse tissues. This suggests that our results could be generalised to UC paediatric patients, which would have a potential therapeutic benefit.

Finally, using an *in vitro* system for culturing colonic biopsies (Petito et al., 2016), we showed that incubation with CBDV in UC paediatric patient biopsies lowered IL-1β levels compared to untreated biopsies, suggesting a possible therapeutic effect of CBDV in paediatric patients as well.

In conclusion we have shown that the phytocannabinoid CBDV attenuates intestinal inflammation in mice via a mechanism likely involving TRPA1. This effect was also associated with changes in the composition of the gut microbiota, which may contribute to the beneficial effect of CBDV in IBD. The effect of CBDV was also seen in biopsies from paediatric patients. This suggests a possible

clinical application of CBDV, as it is already therapeutically effective at very low doses after oral administration and can attenuate inflammation.

Part II – Combined administration of cannabidiol (CBD) and fish oil (FO) counteracts chemically-induced ulcerative colitis and microbiota dysbiosis in mice

It has already been discussed that the use of *Cannabis* in IBD patients for symptom relief is widespread, but the clinical studies are still unclear and controversial (Kienzl et al., 2020). On the contrary, several preclinical studies, including the study I conducted in the first year of my PhD, have shown that phytocannabinoids exert anti-inflammatory effects in models of IBD (Borrelli et al., 2009; Romano et al., 2013; Pagano et al., 2016; Pagano et al., 2019).
Fish oil (FO) is a natural source of numerous n-3-polyunsaturated fatty acids (PUFAs) that have been suggested as a potential complementary treatment for IBD, although clinical data are still controversial (Marton et al., 2019).

In this study, we have shown that inactive doses of FO and CBD in combination exert an anti-inflammatory effect in the DSS- and DNBS-induced ulcerative colitis models.

First, we showed that oral administration of FO has a moderate anti-inflammatory effect reducing several inflammatory parameters that are increased by DSS administration (colon weight/colon length *ratio*, DAI score and MPO activity), with a maximum effect between 50 and 75 mg/mouse doses.
In contrast, oral administration of CBD in a dose range of 0.3-10 mg/kg did not improve the increase in DSS-induced inflammatory parameters (colon weight/colon length *ratio*, body weight loss, DAI score and MPO activity).
Subsequently, we demonstrated that oral concomitant administration of an inactive dose of FO (20 mg/mouse) with inactive doses of CBD (0.3-10 mg/kg) resulted in a reduction in the inflammatory parameters increased by DSS administration, with the maximum response achieved with CBD at the 1 mg/kg dose; in particular, this combination reduced the colon weight/colon length *ratio*, MPO activity (marker of leukocyte infiltration) and DAI score, but not body

weight loss. Of note, co-administration of an active dose of FO (75 mg/mouse) with CBD (0.3-30 mg/kg) elicited an even greater effect in reducing inflammatory parameters, with the maximum effect achieved at CBD 1 mg/kg dose.

In another experiment, we demonstrated the efficacy of the combination of CBD (1 mg/kg) plus FO (20 mg/mouse) at two different time points of DSS-induced inflammation, namely in the acute phase (day 8, d8) and in the remission phase (day 14, d14) (Emge et al., 2016). Specifically, during the peak of inflammation (d8), the combination of CBD (1 mg/kg) and FO (20 mg/mouse) significantly reduced pro-inflammatory cytokine levels (IL-1β and IL-6) and intestinal permeability increased by DSS administration, and increased levels of IL-10, an anti-inflammatory cytokine, which were reduced by DSS administration. The same effect was present in the remission phase (d14).

Due to bidirectional communication via the gut-brain axis, it has been reported that patients with IBD may experience symptoms of common mental disorders such as anxiety and depression (Barberio et al., 2021; Hu et al., 2021). There is a high prevalence of anxiety and depression symptoms in patients with IBD, with up to one third of patients affected by anxiety symptoms and one quarter affected by depression symptoms (Barberio et al., 2021; Hu et al., 2021). The prevalence was also increased in patients with active disease: half of these patients met criteria for anxiety symptoms and a third met criteria for depressive symptoms. It has also been shown that these mental disorders can lead to a high risk of relapse and poor treatment adherence in patients with IBD (Barberio et al., 2021; Hu et al., 2021). For this reason, in this work we also investigated whether the combination of CBD and FO can reduce behavioral disturbances in DSS-treated mice. Consistent with the literature (Emge et al., 2016), the DSS-treated mice in our experiments showed signs of anxiety and decreased recognition memory. In our experiments, the combined administration of CDB plus FO did

not improve DSS-induced behavioral impairment in mice at d8, i.e., when the behavior impairment is maximal (Emge et al., 2016).

DSS administration affected only a few phyla, families, genera and species on d8 in this study, suggesting that the gut microbiota does not play an important role in DSS-induced colitis under these experimental conditions on d8. However, at d14, during the recovery phase, several taxa were altered, suggesting that bacteria may play a role in the recovery phase rather than at the peak of inflammation.

In our experimental design the combination of CBD (1 mg/kg) plus FO (20 mg/mouse) in DSS-treated mice resulted in similar changes in several taxa as in healthy mice (without DSS), suggesting that the anti-inflammatory effect of the combination CBD plus FO could be dependent on its effect on gut microbiota composition. In other words, some of these changes may have enhanced the effect of CBD plus FO and some may have counteracted it.

Among these changes, the *Firmicutes:Bacteroidetes ratio* was increased by DSS only during the recovery phase (d14); this parameter has been reported to be increased in experimental models of IBD as well as in human IBD patients (Manichanh et al., 2012; Santoru et al., 2017). CBD or FO alone, as well as co-administration of CBD plus FO, counteracted this increase, suggesting that the anti-inflammatory effect may have been enhanced by this effect, but was not dependent on it (as the drugs have no effect on inflammation when administered alone).

Interestingly, the combination of CBD+FO (1 mg/kg + 20 mg/mouse) reduced the relative abundance of a small number of bacterial families (*Marinifilaceae* at d8 and *Desulfovibrionaceae* and *Ruminococcaceae* at d14) and one genus (*Odoribacter* at d8) in DSS-treated mice, all of which have been previously shown by others to be modified either in patients with IBD or their preclinical models (Morgan et al., 2012; Berry and Reinisch, 2013; Yang and Yang, 2018; Zhai et al., 2019a; Zhai et al., 2019b).

The *Desulfovibrionaceae* family has been reported to be increased in IBD patients (Berry and Reinisch, 2013), while *Ruminococcaceae* are increased in UC patients but decreased in patients with CD (Morgan et al., 2012; Alam et al., 2020). They have been shown to play a role in IBD in preclinical studies. For example, the increase in *Desulfovibrionaceae* in DSS-treated mice was counterbalanced by treatment with the prebiotic *Bifidobacterium breve* (Yang and Yang, 2018). On the other hand, others reported that both *Desulfovibrionaceae* and *Ruminococcaceae* in DSS-treated mice were reduced by gentamicin administration, resulting in an improvement in DAI score and inflammation (Zhai et al., 2019b). The data reported in this paper are counterintuitive given our results. On the other hand, *Marinifilaceae* were increased in inflamed mice, consistent with the significant decrease in this family by CBD plus FO at d8, which was associated with a decrease in inflammation (Zhai et al., 2019b). Moreover, the relative abundances of *Marinifilaceae* and *Ruminococcaceae* were reduced in rats fed high levels of monounsaturated fatty acids concomitant with a prevention of DSS-induced inflammation (Fernandez et al., 2020).

The genus *Odoribacter* has been described as a producer of SCFAs (short-chain fatty acids), which are thought to have anti-inflammatory effects (Morrison and Preston, 2016; Adak and Khan, 2019); this genus is also found reduced in CD and UC patients (Morgan et al., 2012). However it is reported to be increased by DSS (Wei et al., 2019) and in azoxymethane and DSS-induced colitis associated with colorectal cancer (Song et al., 2018). Here, we showed that although the relative abundance of this genus was not affected by DSS, it was reduced by treatment with CBD plus FO, which could either contribute to or inhibit its anti-inflammatory effect.

The species *Akkermansia muciniphila* is thought to have a protective role in inflammation and has been reported to be elevated in mouse models of IBD, mediating the effects of various treatments (Bian et al., 2019; Li et al., 2019; Zhai et al., 2019a; Zhang et al., 2019). However, in other models, *A. muciniphila* has

been shown to increase intestinal inflammation (Seregin et al., 2017), so the exact role of this bacterium in DSS-induced colitis is still unclear. In our model, *A. muciniphila* was increased by DSS administration only at d14, suggesting that this effect could potentially represent an adaptive and protective mechanism interfering with the resolution of inflammation. Importantly, this effect also became statistically significant with a combination of per se ineffective doses of FO and CBD and with the single treatments, at d8. This bacterial species may therefore be partly involved in the beneficial effects of the FO+CBD combination on DSS-induced inflammation.

We also detected *Parabacteroides goldsteinii*, which has been attributed a protective role in intestinal inflammation and obesity (Chang et al., 2019; Wu et al., 2019b). *P. goldsteinii* was increased in DSS-treated mice during the recovery phase (d14), which again may be an adaptive protective mechanism. Accordingly, this increase was already observed at d8 after simultaneous treatment with the anti-inflammatory combination of FO and CBD (but also in the single treatments).

Finally, we confirmed the efficacy of non-active doses of CBD+FO in a second model of ulcerative colitis namely DNBS-induced colitis. In this model, the dose of FO, previously active in the DSS model, i.e., 75 mg/mouse, was ineffective and did not cause a reduction in monitored inflammatory parameters (colon weight/colon length *ratio*, intestinal permeability, IL-1β levels and MPO activity); similarly, oral administration of CBD in the dose range of 0.3-30 mg/kg was completely ineffective, which is consistent with findings in the literature (Schicho and Storr, 2012; Pagano et al., 2016). Administration of FO (75 mg/mouse) in conjunction with ineffective doses of CBD resulted in a significant reduction in inflammatory parameters (colon weight/colon length *ratio* and MPO activity) at a dose of 1 mg/kg, confirming the synergistic effect of CBD and FO also in this model of UC. Furthermore, plasma and colonic levels of CBD in mice pretreated with FO showed no increase in CBD concentration compared to mice

receiving CBD alone, refuting the hypothesis that FO might increase the oral bioavailability of CBD.

It is known that the effects of non-euphoric phytocannabinoids such as CBD are due to their interaction with the endocannabinoid system (Di Marzo, 2020). CBD can, indeed, increase endocannabinoid levels by inactivating FAAH, one of the NAEs metabolising enzymes. However, the plasmatic concentration required to inhibit this enzyme and thus increase NAEs is very high and difficult to achieve in humans (De Petrocellis et al., 2011).

Nevertheless, it has recently been suggested that the n-3 PUFAs present in FO owe part of their beneficial effects to the interaction with the endocannabinoid system (Batetta et al., 2009; de Bus et al., 2019). In light of these data, we investigated whether alteration of endocannabinoidome mediators by co-administration of CBD+FO could explain their synergistic effects. Unfortunately, neither CBD alone (30 mg/kg) nor the combination CBD plus FO (30 mg/kg+75 mg/mouse) altered the levels of endocannabinoidome mediators. Surprisingly, administration of FO (75 mg/mouse) altered the levels of endocannabinoidome mediators in colonic tissue increasing 2-AG and PEA levels, both known for their anti-inflammatory effects in experimental colitis (Borrelli et al., 2009), but FO did not alter the levels of NAEs or MAGs derived from n-3 PUFAs. Unfortunately, these results do not provide information on the possible involvement of lipid mediators in the potentiating effect of FO on CBD.

In conclusion, we have shown that oral CBD, when co-administered with inactive or minimally active doses of FO in the DSS mouse model of colitis, exerts an anti-inflammatory effect even at relatively low doses; both FO and CBD, alone or in combination, can also affect the gut microbiota in mice, an effect that seems to explain, at least in part, their anti-inflammatory activity; finally, the possible involvement of endocannabinoidome mediators in the mechanism of this synergy is still unclear.

Part III – TRPM8 channel deletion reduces murine colon carcinogenesis and modifies gut microbiota composition

Colorectal cancer (CRC) is the most common malignancy of the gastrointestinal tract worldwide (Malvezzi et al., 2018; Siegel et al., 2021). The gut microbiota has been shown to play a crucial role in the development of CRC (Lucas et al., 2017). Several hypotheses have been put forward in the scientific community to understand the role of the gut microbiota in the initiation and development of colorectal cancer. In particular, two hypotheses are most widely accepted: the presence of bacteria capable of causing DNA damage by releasing toxins into intestinal epithelial cells (alfa-bug hypothesis), and the transition from a microbial community containing pro-inflammatory bacteria (driver bacteria) to one containing taxa capable of promoting tumor growth (passenger bacteria) (Cheng et al., 2020).

TRPM8, a member of the thermo-TRP channels family, is the main receptor involved in cold sensation (Clapham, 2003). It can be activated by cold (8–28 °C) and is enhanced by compounds that provide a cooling sensation, such as menthol and icilin (Clapham, 2003). TRPM8 was first discovered in the prostate, but is also widely expressed in sensory neurons (Clapham, 2003). Its role in carcinogenesis is being studied primarily in prostate cancer, where androgen-dependent overexpression of TRPM8 appears to be required for cancer cell survival (Zhang and Barritt, 2004), and TRPM8 has been proposed as a prognostic marker for prostate cancer (Zhang and Barritt, 2006). Abnormal expression of TRPM8 has also been found in many other cancers such as pancreatic cancer (Yee et al., 2012), gastric cancer (Xu et al., 2021a), breast cancer (Chodon et al., 2010) and melanoma (Kijpornyongpan et al., 2014). In preclinical *in vitro* studies, it has been shown that either activation (by increasing cytosolic Ca^{2+} levels) or antagonization/desensitization (by decreasing cytosolic

Ca^{2+} levels) of TRPM8 can affect *in vitro* cell growth and/or survival of cancer cells (Li et al., 2009; Okamoto et al., 2012; Yee, 2015).
In addition, the *C. sativa* constituent cannabigerol, which unselectively binds and antagonizes TRPM8 (De Petrocellis et al., 2011), has previously been shown to reduce Caco-2 cell viability *in vitro* and tumor number in mice in an experimental model of sporadic colorectal cancer (Borrelli et al., 2014). Finally, a recent study has shown that abnormal TRPM8 expression is present in CRC patients with liver metastases (Liu et al., 2021).

In this study, using an experimental colorectal cancer model and a genetic approach, we have demonstrated i) a role of TRPM8 in the development of colorectal cancer and ii) a possible involvement of the gut microbiota in its effect; in particular, TRPM8 appears to influence the development of colorectal cancer, at least in part, through an effect on the composition of the gut microbiota.

We demonstrated that genetic deletion of Trpm8 reduces the susceptibility of mice to develop sporadic colorectal cancer: indeed, knockout mice developed a lower number of tumors compared to wild-type; furthermore, $Trpm8^{-/-}$ mice treated with AOM did not lose weight after AOM administration compared to wild-type mice treated with AOM. This result is consistent with our previous experiment in which the TRPM8 antagonist cannabigerol reduced the number of tumors in the same experimental model (Borrelli et al., 2009).

The genetic deletion of Trpm8 also affected the gut microbiota. First, we showed that the relative abundance of some families differed significantly between wild-type and $Trpm8^{-/-}$ mice even in healthy mice (under basal conditions); among them, the family *Burkholderiaceae*, which has been shown to correlate positively with the development of colorectal cancer (Oresta et al., 2020), was below the detection level in the knockout mice. The *Deferribacteraceae* and *Marinifilaceae* families have been reported to be over-represented in DSS-induced colitis (Zhang et al., 2017; Xu et al., 2021b) and *Deferribacteraceae* is also elevated in mice fed a high-fat diet enriched with n-

6PUFAS, a diet reported to exacerbate ulcerative colitis, one of the best-known risk factors for CRC (Selmin et al., 2021); notably, *Marinifilaceae* is detected at lower abundance in Trpm8$^{-/-}$ mice than in wild-type mice, while *Deferribacteraceae* remained completely undetected. All these data suggest that genetic deletion of Trpm8 reduces the presence of bacterial families positively involved in the development of colorectal cancer.

In our experimental model of colorectal carcinoma, administration of AOM resulted in changes in gut microbiota composition in both genotypes, but the microbiota of Trpm8$^{-/-}$ mice responded differently to AOM administration than that of wild-type mice. Specifically, we observed a reduction in the *Ruminococcaceae* and *Lachnospiraceae* families, previously reported to be reduced in experimental carcinogenesis (Wang et al., 2020; Yu et al., 2020), in wild-type mice but not in knockout mice at week five. These two families have been shown to be protective against CRC by producing short-chain fatty acids (SCFAs) such as propionic acid and/or butyric acid, key metabolites that regulate gut homeostasis (Vital et al., 2017; Choi et al., 2021); therefore, resistance to alterations in these families in Trpm8$^{-/-}$ mice, but not in wild type, may be involved in the reduced susceptibility of knockout mice to develop AOM-induced tumors. Of note, *Ruminococcaceae* was significantly lower in healthy Trpm8$^{-/-}$ mice than in wild-type, whereas no differences were observed in *Lachnospiraceae* between wild-type and Trpm8$^{-/-}$ mice.

We also observed a reduction in *Peptostreptococcaceae* in wild types but not in Trpm8$^{-/-}$ mice (week 13). *Peptostreptococcaceae* is significantly lower in patients with ulcerative colitis (one of the main risk factors for the development of CRC) than in healthy subjects (Chen et al., 2014).

Erysipelotrichaceae was significantly increased in both wild-type and knockout mice, with no statistically significant difference between the two genotypes. It is worth noting that this family is positively correlated with tumorigenesis in the colon and that its presence is increased in CRC patients (Yang et al., 2020).

In our study, *Akkermansiaceae* was increased in both wild-type and knockout mice at week five, with no statistically significant difference between the two genotypes. *Akkermansia muciniphila* is largely studied for its role in mucous regulation in intestinal epithelial cells. It is reported that *A. muciniphila* can both degrade the protective intestinal mucous layer, allowing the invasion of other bacteria, and stimulate mucous production. Previous studies have shown that i) this bacterium is increased in mice with prostate cancer (Huang et al., 2021), ii) administration of *A. muciniphila* exacerbates the development of colorectal cancer in mice (Wang et al., 2022), and iii) there is a high increase in the abundance of *Akkermansia* in CRC patients stools (Weir et al., 2013).

Burkholderiaceae levels were undetectable in knockout mice, except at week 13, while their abundance was constant in wild type. This family is associated with an increased risk of colorectal (Yang et al., 2019), laryngeal (Wang et al., 2019) and bladder cancers (Oresta et al., 2020). These data suggest involvement of this family in the protective effect of Trpm8$^{-/-}$ mice.

Finally, the relative abundance of *Lactobacillaceae* showed a sudden reduction (observed as early as week five) in wild-type mice, but a delayed reduction in Trpm8$^{-/-}$ mice, which was not apparent until week thirteen; *Lactobacillaceae* is one of the best-known families of probiotics that play an important role in maintaining gut homeostasis (Youssef et al., 2018); reduction in their abundance is reported in CRC, while their administration has a protective effect on the development of CRC (Zou et al., 2018); thus, delayed reduction in Trpm8$^{-/-}$ mice may exert a protective role against AOM-induced CRC here.

Given these data, we can conclude that mice with a genetic deletion of Trpm8 i) develop a lower number of tumors in the AOM model of colorectal cancer, ii) have a different gut microbiota composition than wild-type mice, and iii) show different changes in gut microbiota composition in response to AOM treatment than wild-type mice. The different bacterial community between wild-type and knockout mice, as well as the different changes in the composition of

the gut microbiota in response to AOM treatment, may be, at least partly, responsible for the reduced susceptibility of knockout mice to the development of AOM-induced sporadic colorectal cancer. These findings support the existence of a relationship between the endocannabinoidome and the gut microbiota which may have an impact on the development of colorectal cancer.

Part IV – Gut microbiota impairment modulates endocannabinoidome mediator levels in healthy and inflamed mice

Our previous studies seem to show that the relationship between the eCBome and the gut microbiota influences the development of IBD. To confirm this hypothesis, we decided to investigate whether the absence of gut microbiota (known to influence the development of IBD) triggers changes in the eCBome in healthy and DSS-induced ulcerative colitis mice.

In this study, using two methods to affect the mice gut microbiota (antibiotic cocktail and germfree status), we showed that the absence of gut microbiota reduces inflammation in the DNBS-induced model of ulcerative colitis, which is likely the result of altered eCBome signalling. Indeed, germfree mice have elevated levels of eCBome mediators, which are known to have an anti-inflammatory effect.

In the DNBS-induced model, all groups treated with the phlogogen developed intestinal inflammation, as shown by the macroscopic parameters of colon inflammation, i.e., colon weight/ colon length ratio, body weight loss and DAI score. Germfree mice treated with DNBS showed lower levels of inflammation compared to mice from the CR and ABX groups, as the colon weight/colon length ratio was significantly lower and the increase in DAI score was slower during the three days of observation. Looking at microscopic parameters of inflammation, DNBS treatment did not increase expression levels of pro-inflammatory cytokines in germfree mice. Although not always in a significant manner, increases in IL-1β, IL-6 and TNFα were observed after DNBS treatment in CR and ABX mice. Similarly, MPO activity increased in DNBS-treated CR mice, but not in ABX and GF mice. Of note, basal levels of MPO activity were higher in germfree mice than in CR and ABX mice. Basal expression levels of the major anti-inflammatory cytokine IL-10 were significantly lower in germfree mice compared to CR and ABX mice; DNBS

administration did not alter IL-10 levels in all groups. Our results are partially consistent with the results of another paper in which inflammation was induced in ABX-treated and germfree mice with the phlogogen DSS (Hernandez-Chirlaque et al., 2016). The results of Hernández-Chirlaque et al. showed that germfree mice developed minimal colonic inflammation, while ABX-treated mice developed milder inflammation compared to CR mice. More specifically, DSS-treated germfree mice did not differ from CR mice in terms of weight loss and showed no increase in IL-1β levels and MPO activity (comparable to our results). However, the authors found similar basal MPO activity in germfree and CR (our results showed higher MPO activity in germfree mice). Surprisingly, Hernández-Chirlaque et al. reported that DSS-treated germfree mice had increased levels of TNFα (in contrast to our results) and lower levels of IL-10 (comparable to our results) compared to CR.

Analysis of the levels of eCBome mediators in the colon of mice revealed that eCBome lipid mediators had different levels depending on the status of the gut microbiota and responded differently to colon inflammation in germfree mice than in CR and ABX-treated mice. At the basal level, i.e., in non-inflamed mice, germfree mice had significantly higher levels of NAEs such as oleoylethanolamide (OEA), linoleoylethanolamide (LEA), docosahexaenoylethanolamide (DHEA) and 13-hydroxyoctadecadienoicethanolamide (13-HODE-EA) compared to CR and ABX-treated healthy mice; an increasing trend was also seen in AEA levels, but not statistically significant. OEA has been reported to exert anti-inflammatory effects in experimental colitis (Lama et al., 2020; Otagiri et al., 2020), while LEA is able to inhibit NF-kB signalling and thus exert anti-inflammatory effects (Ishida et al., 2013). DHEA, synthesised by NAPE-PLD from the n-3 PUFA DHA, has been reported to have a strong anti-inflammatory effect, even stronger than AEA (de Bus et al., 2019). Thus, the higher levels of anti-inflammatory mediators in germfree mice could at least partially explain the lower production

of pro-inflammatory cytokines, and this effect could be explained as a compensatory effect of the endocannabinoidome due to the absence of the gut microbiota.

Regarding MAGs, 13-HODE-EA and 13-HODE-G are produced in human neutrophils and eosinophils by the metabolization of LEA by 15-lipooxygenase (15-LOX), but their biological activity is still unclear (Archambault et al., 2021; Tinto et al., 2021). Interestingly, DNBS-treated germfree mice had higher concentrations of LEA and 2-LG metabolites, i.e., 13-HODE-EA and 13-HODE-G respectively, and this increase is paired with the reduction of LEA and LG in DNBS-treated mice compared to healthy germfree mice, suggesting that high concentrations of 15-LOX metabolites (13-HODE) are produced in the inflammatory process as consequence of a higher concentration of the precursors under healthy conditions. In addition, further analyses are needed to unravel the metabolic pathways underlying these differences, especially the altered levels of the newly identified 13-HODE derivatives.

In summary, we have shown that mice raised in germfree conditions develop a lower degree of inflammation in the experimental model of DNBS-induced ulcerative colitis, whereas mice with a depletion of the gut microbiota achieved by ABX treatment do not show this effect. The lack of gut microbiota and the resulting differential development of the gut immune system in germfree mice is followed by a compensatory effect on mediators of the endocannabinoidome, which may explain the lower susceptibility of the germfree mice to develop ulcerative colitis. In a nutshell, we demonstrate that the relationship between the gut microbiota and the endocannabinoidome affects the development of colon inflammation.

GENERAL CONCLUSIONS

IBD and CRC are health problems affecting millions of people worldwide which lack of effective treatments. Links have been established between the onset/progression of these pathologies and gut dysbiosis; indeed, gut microbiota plays a crucial role in intestinal homeostasis. Moreover, a recently described expanded endocannabinoid system, known as "endocannabinoidome", is considered to have pivotal roles in immune response and a close connection with the gut microbiota, known as eCBome-mBIome axis.

The evidence reported in this PhD thesis highlights that the functional interaction between endocannabinoidome and gut microbiota impacts on the development of inflammatory bowel disease and colorectal cancer. Briefly, through the manipulation of the eCBome and gut microbiota, using receptor ligands, enzymatic inhibitors, receptor genetic deletion and gut microbiota depletion we showed that:

- Cannabidivarin exerts anti-inflammatory activity in preclinical models of ulcerative colitis, acting via TRPA1 channel, with concomitant changes in gut microbiota composition.
- A combination of inactive doses of fish oil and cannabidiol exerts an anti-inflammatory effect in in preclinical models of ulcerative colitis, with changes in gut microbiota that seem to explain, at least in part, this effect.
- Genetic deletion of Trpm8 is associated to changes in gut microbiota composition that, at least in part, may be responsible for the low susceptibility in colon carcinogenesis.
- The absence of gut microbiota in germfree mice has an effect on the endocannabinoidome signalling in the colon that seems to be responsible for the reduced inflammation in the preclinical model of ulcerative colitis

In conclusion, this PhD thesis contributes to elucidate the physiopathological role of the eCBome-mBIome axis in IBD and CRC and thus may offer novel future pharmacological opportunities for the prevention and cure of these diseases.

REFERENCES

Adak A, Khan MR. An insight into gut microbiota and its functionalities. Cell Mol Life Sci. 2019;76(3):473-493.

Ahn JY, Lee JS, Min HY, Lee HY. Acquired resistance to 5-fluorouracil via HSP90/Src-mediated increase in thymidylate synthase expression in colon cancer. Oncotarget. 2015;6(32):32622-33.

AIOM, AIRTUM. I numeri del cancro in Italia - 2021. 2021;

Alam MT, Amos GCA, Murphy ARJ, Murch S, Wellington EMH, Arasaradnam RP. Microbial imbalance in inflammatory bowel disease patients at different taxonomic levels. Gut Pathog. 2020;12:1.

Alhouayek M, Lambert DM, Delzenne NM, Cani PD, Muccioli GG. Increasing endogenous 2-arachidonoylglycerol levels counteracts colitis and related systemic inflammation. FASEB J. 2011;25(8):2711-21.

Alhouayek M, Bottemanne P, Subramanian KV, Lambert DM, Makriyannis A, Cani PD, Muccioli GG. N-Acylethanolamine-hydrolyzing acid amidase inhibition increases colon N-palmitoylethanolamine levels and counteracts murine colitis. FASEB J. 2015;29(2):650-61.

Allard G, Ryan FJ, Jeffery IB, Claesson MJ. SPINGO: a rapid species-classifier for microbial amplicon sequences. BMC Bioinformatics. 2015;16:324.

Ambrose T, Simmons A. Cannabis, Cannabinoids, and the Endocannabinoid System-Is there Therapeutic Potential for Inflammatory Bowel Disease? J Crohns Colitis. 2019;13(4):525-535.

An D, Peigneur S, Hendrickx LA, Tytgat J. Targeting Cannabinoid Receptors: Current Status and Prospects of Natural Products. Int J Mol Sci. 2020;21(14)

Ananthakrishnan AN. Epidemiology and risk factors for IBD. Nat Rev Gastroenterol Hepatol. 2015;12(4):205-17.

Ananthakrishnan AN, Kaplan GG, Ng SC. Changing Global Epidemiology of Inflammatory Bowel Diseases: Sustaining Health Care Delivery Into the 21st Century. Clin Gastroenterol Hepatol. 2020;18(6):1252-1260.

Archambault AS, Tinto F, Dumais E, Rakotoarivelo V, Kostrzewa M, Plante PL, Martin C, Simard M, Silvestri C, Pouliot R, Laviolette M, Boulet LP, Vitale RM, Ligresti A, Di Marzo V, Flamand N. Biosynthesis of the Novel Endogenous 15-Lipoxygenase Metabolites N-13-Hydroxy-octodecadienoyl-ethanolamine and 13-Hydroxy-octodecadienoyl-glycerol by Human Neutrophils and Eosinophils. Cells. 2021;10(9)

Atreya R, Neurath MF. IBD pathogenesis in 2014: Molecular pathways controlling barrier function in IBD. Nat Rev Gastroenterol Hepatol. 2015;12(2):67-8.

Aviello G, Romano B, Borrelli F, Capasso R, Gallo L, Piscitelli F, Di Marzo V, Izzo AA. Chemopreventive effect of the non-psychotropic phytocannabinoid cannabidiol on experimental colon cancer. J Mol Med (Berl). 2012;90(8):925-34.

Backhed F, Ley RE, Sonnenburg JL, Peterson DA, Gordon JI. Host-bacterial mutualism in the human intestine. Science. 2005;307(5717):1915-20.

Barberio B, Zamani M, Black CJ, Savarino EV, Ford AC. Prevalence of symptoms of anxiety and depression in patients with inflammatory bowel disease: a systematic review and meta-analysis. Lancet Gastroenterol Hepatol. 2021;6(5):359-370.

Batetta B, Griinari M, Carta G, Murru E, Ligresti A, Cordeddu L, Giordano E, Sanna F, Bisogno T, Uda S, Collu M, Bruheim I, Di Marzo V, Banni S. Endocannabinoids may mediate the ability of (n-3) fatty acids to reduce ectopic fat and inflammatory mediators in obese Zucker rats. J Nutr. 2009;139(8):1495-501.

Bernstein CN, Blanchard JF, Kliewer E, Wajda A. Cancer risk in patients with inflammatory bowel disease: a population-based study. Cancer. 2001;91(4):854-62.

Berrout J, Kyriakopoulou E, Moparthi L, Hogea AS, Berrout L, Ivan C, Lorger M, Boyle J, Peers C, Muench S, Gomez JE, Hu X, Hurst C, Hall T, Umamaheswaran S, Wesley L, Gagea M, Shires M, Manfield I, Knowles MA, Davies S, Suhling K, Gonzalez YT, Carragher N, Macleod K, Abbott NJ, Calin GA, Gamper N, Zygmunt PM, Timsah Z. TRPA1-FGFR2 binding event is a regulatory oncogenic driver modulated by miRNA-142-3p. Nat Commun. 2017;8(1):947.

Berry D, Reinisch W. Intestinal microbiota: a source of novel biomarkers in inflammatory bowel diseases? Best Pract Res Clin Gastroenterol. 2013;27(1):47-58.

Bertin S, Aoki-Nonaka Y, de Jong PR, Nohara LL, Xu H, Stanwood SR, Srikanth S, Lee J, To K, Abramson L, Yu T, Han T, Touma R, Li X, Gonzalez-Navajas JM, Herdman S, Corr M, Fu G, Dong H, Gwack Y, Franco A, Jefferies WA, Raz E. The ion channel TRPV1 regulates the activation and proinflammatory properties of CD4(+) T cells. Nat Immunol. 2014;15(11):1055-1063.

Biagi E, Franceschi C, Rampelli S, Severgnini M, Ostan R, Turroni S, Consolandi C, Quercia S, Scurti M, Monti D, Capri M, Brigidi P, Candela M. Gut Microbiota and Extreme Longevity. Curr Biol. 2016;26(11):1480-5.

Bian X, Wu W, Yang L, Lv L, Wang Q, Li Y, Ye J, Fang D, Wu J, Jiang X, Shi D, Li L. Administration of Akkermansia muciniphila Ameliorates Dextran Sulfate Sodium-Induced Ulcerative Colitis in Mice. Front Microbiol. 2019;10:2259.

Bligh EG, Dyer WJ. A rapid method of total lipid extraction and purification. Can J Biochem Physiol. 1959;37(8):911-7.

Borrelli F, Aviello G, Romano B, Orlando P, Capasso R, Maiello F, Guadagno F, Petrosino S, Capasso F, Di Marzo V, Izzo AA. Cannabidiol, a safe and non-psychotropic ingredient of the marijuana plant Cannabis sativa, is protective in a murine model of colitis. J Mol Med (Berl). 2009;87(11):1111-21.

Borrelli F, Fasolino I, Romano B, Capasso R, Maiello F, Coppola D, Orlando P, Battista G, Pagano E, Di Marzo V, Izzo AA. Beneficial effect of the non-psychotropic plant cannabinoid cannabigerol on experimental inflammatory bowel disease. Biochem Pharmacol. 2013;85(9):1306-16.

Borrelli F, Pagano E, Romano B, Panzera S, Maiello F, Coppola D, De Petrocellis L, Buono L, Orlando P, Izzo AA. Colon carcinogenesis is inhibited by the TRPM8 antagonist cannabigerol, a Cannabis-derived non-psychotropic cannabinoid. Carcinogenesis. 2014;35(12):2787-97.

Borrelli F, Romano B, Petrosino S, Pagano E, Capasso R, Coppola D, Battista G, Orlando P, Di Marzo V, Izzo AA. Palmitoylethanolamide, a naturally occurring lipid, is an orally effective intestinal anti-inflammatory agent. Br J Pharmacol. 2015;172(1):142-58.

Brenner H, Kloor M, Pox CP. Colorectal cancer. Lancet. 2014;383(9927):1490-1502.

Callahan BJ, McMurdie PJ, Rosen MJ, Han AW, Johnson AJ, Holmes SP. DADA2: High-resolution sample inference from Illumina amplicon data. Nat Methods. 2016;13(7):581-3.

Caporaso JG, Kuczynski J, Stombaugh J, Bittinger K, Bushman FD, Costello EK, Fierer N, Pena AG, Goodrich JK, Gordon JI, Huttley GA, Kelley ST, Knights D, Koenig JE, Ley RE, Lozupone CA, McDonald D, Muegge BD, Pirrung M, Reeder J, Sevinsky JR, Turnbaugh PJ, Walters WA, Widmann J, Yatsunenko T, Zaneveld J, Knight R. QIIME allows analysis of high-throughput community sequencing data. Nat Methods. 2010;7(5):335-6.

Carioli G, Malvezzi M, Bertuccio P, Boffetta P, Levi F, La Vecchia C, Negri E. European cancer mortality predictions for the year 2021 with focus on pancreatic and female lung cancer. Ann Oncol. 2021;32(4):478-487.

Chang CJ, Lin TL, Tsai YL, Wu TR, Lai WF, Lu CC, Lai HC. Next generation probiotics in disease amelioration. J Food Drug Anal. 2019;27(3):615-622.

Chassaing B, Aitken JD, Malleshappa M, Vijay-Kumar M. Dextran sulfate sodium (DSS)-induced colitis in mice. Curr Protoc Immunol. 2014;104:15 25 1-15 25 14.

Chen L, Wang W, Zhou R, Ng SC, Li J, Huang M, Zhou F, Wang X, Shen B, M AK, Wu K, Xia B. Characteristics of fecal and mucosa-associated microbiota in

Chinese patients with inflammatory bowel disease. Medicine (Baltimore). 2014;93(8):e51.

Cheng Y, Ling Z, Li L. The Intestinal Microbiota and Colorectal Cancer. Front Immunol. 2020;11:615056.

Chodon D, Guilbert A, Dhennin-Duthille I, Gautier M, Telliez MS, Sevestre H, Ouadid-Ahidouch H. Estrogen regulation of TRPM8 expression in breast cancer cells. BMC Cancer. 2010;10:212.

Choi SI, Son JH, Kim N, Kim YS, Nam RH, Park JH, Song CH, Yu JE, Lee DH, Yoon K, Min H, Kim YR, Seok YJ. Changes in Cecal Microbiota and Short-chain Fatty Acid During Lifespan of the Rat. J Neurogastroenterol Motil. 2021;27(1):134-146.

Clapham DE. TRP channels as cellular sensors. Nature. 2003;426(6966):517-24.

Cseko K, Beckers B, Keszthelyi D, Helyes Z. Role of TRPV1 and TRPA1 Ion Channels in Inflammatory Bowel Diseases: Potential Therapeutic Targets? Pharmaceuticals (Basel). 2019;12(2)

Daris B, Tancer Verboten M, Knez Z, Ferk P. Cannabinoids in cancer treatment: Therapeutic potential and legislation. Bosn J Basic Med Sci. 2019;19(1):14-23.

de Bus I, Witkamp R, Zuilhof H, Albada B, Balvers M. The role of n-3 PUFA-derived fatty acid derivatives and their oxygenated metabolites in the modulation of inflammation. Prostaglandins Other Lipid Mediat. 2019;144:106351.

De Filippis D, Esposito G, Cirillo C, Cipriano M, De Winter BY, Scuderi C, Sarnelli G, Cuomo R, Steardo L, De Man JG, Iuvone T. Cannabidiol reduces intestinal inflammation through the control of neuroimmune axis. PLoS One. 2011;6(12):e28159.

De Petrocellis L, Di Marzo V. Non-CB1, non-CB2 receptors for endocannabinoids, plant cannabinoids, and synthetic cannabimimetics: focus on G-protein-coupled receptors and transient receptor potential channels. J Neuroimmune Pharmacol. 2010;5(1):103-21.

De Petrocellis L, Ligresti A, Moriello AS, Allara M, Bisogno T, Petrosino S, Stott CG, Di Marzo V. Effects of cannabinoids and cannabinoid-enriched Cannabis extracts on TRP channels and endocannabinoid metabolic enzymes. Br J Pharmacol. 2011;163(7):1479-94.

De Petrocellis L, Orlando P, Moriello AS, Aviello G, Stott C, Izzo AA, Di Marzo V. Cannabinoid actions at TRPV channels: effects on TRPV3 and TRPV4 and their potential relevance to gastrointestinal inflammation. Acta Physiol (Oxf). 2012;204(2):255-66.

DeSantis TZ, Hugenholtz P, Larsen N, Rojas M, Brodie EL, Keller K, Huber T, Dalevi D, Hu P, Andersen GL. Greengenes, a chimera-checked 16S rRNA gene

database and workbench compatible with ARB. Appl Environ Microbiol. 2006;72(7):5069-72.

Devane WA, Hanus L, Breuer A, Pertwee RG, Stevenson LA, Griffin G, Gibson D, Mandelbaum A, Etinger A, Mechoulam R. Isolation and structure of a brain constituent that binds to the cannabinoid receptor. Science. 1992;258(5090):1946-9.

Di Marzo V, Fontana A, Cadas H, Schinelli S, Cimino G, Schwartz JC, Piomelli D. Formation and inactivation of endogenous cannabinoid anandamide in central neurons. Nature. 1994;372(6507):686-91.

Di Marzo V, De Petrocellis L. Why do cannabinoid receptors have more than one endogenous ligand? Philos Trans R Soc Lond B Biol Sci. 2012;367(1607):3216-28.

Di Marzo V, Piscitelli F. The Endocannabinoid System and its Modulation by Phytocannabinoids. Neurotherapeutics. 2015;12(4):692-8.

Di Marzo V, Silvestri C. Lifestyle and Metabolic Syndrome: Contribution of the Endocannabinoidome. Nutrients. 2019;11(8)

Di Marzo V. The endocannabinoidome as a substrate for noneuphoric phytocannabinoid action and gut microbiome dysfunction in neuropsychiatric disorders. Dialogues Clin Neurosci. 2020;22(3):259-269.

Donohoe DR, Garge N, Zhang X, Sun W, O'Connell TM, Bunger MK, Bultman SJ. The microbiome and butyrate regulate energy metabolism and autophagy in the mammalian colon. Cell Metab. 2011;13(5):517-26.

Duncan SH, Belenguer A, Holtrop G, Johnstone AM, Flint HJ, Lobley GE. Reduced dietary intake of carbohydrates by obese subjects results in decreased concentrations of butyrate and butyrate-producing bacteria in feces. Appl Environ Microbiol. 2007;73(4):1073-8.

Duo L, Wu T, Ke Z, Hu L, Wang C, Teng G, Zhang W, Wang W, Ge Q, Yang Y, Dai Y. Gain of Function of Ion Channel TRPV1 Exacerbates Experimental Colitis by Promoting Dendritic Cell Activation. Mol Ther Nucleic Acids. 2020;22:924-936.

Dziarski R, Park SY, Kashyap DR, Dowd SE, Gupta D. Pglyrp-Regulated Gut Microflora Prevotella falsenii, Parabacteroides distasonis and Bacteroides eggerthii Enhance and Alistipes finegoldii Attenuates Colitis in Mice. PLoS One. 2016;11(1):e0146162.

Eckburg PB, Bik EM, Bernstein CN, Purdom E, Dethlefsen L, Sargent M, Gill SR, Nelson KE, Relman DA. Diversity of the human intestinal microbial flora. Science. 2005;308(5728):1635-8.

El Aidy S, van den Bogert B, Kleerebezem M. The small intestine microbiota, nutritional modulation and relevance for health. Curr Opin Biotechnol. 2015;32:14-20.

Elsohly MA, Slade D. Chemical constituents of marijuana: the complex mixture of natural cannabinoids. Life Sci. 2005;78(5):539-48.

ElSohly MA, Radwan MM, Gul W, Chandra S, Galal A. Phytochemistry of Cannabis sativa L. Prog Chem Org Nat Prod. 2017;103:1-36.

Emge JR, Huynh K, Miller EN, Kaur M, Reardon C, Barrett KE, Gareau MG. Modulation of the microbiota-gut-brain axis by probiotics in a murine model of inflammatory bowel disease. Am J Physiol Gastrointest Liver Physiol. 2016;310(11):G989-98.

Engel MA, Leffler A, Niedermirtl F, Babes A, Zimmermann K, Filipovic MR, Izydorczyk I, Eberhardt M, Kichko TI, Mueller-Tribbensee SM, Khalil M, Siklosi N, Nau C, Ivanovic-Burmazovic I, Neuhuber WL, Becker C, Neurath MF, Reeh PW. TRPA1 and substance P mediate colitis in mice. Gastroenterology. 2011;141(4):1346-58.

Esposito G, Filippis DD, Cirillo C, Iuvone T, Capoccia E, Scuderi C, Steardo A, Cuomo R, Steardo L. Cannabidiol in inflammatory bowel diseases: a brief overview. Phytother Res. 2013;27(5):633-6.

Esposito G, Capoccia E, Turco F, Palumbo I, Lu J, Steardo A, Cuomo R, Sarnelli G, Steardo L. Palmitoylethanolamide improves colon inflammation through an enteric glia/toll like receptor 4-dependent PPAR-alpha activation. Gut. 2014;63(8):1300-12.

Esposito G, Pesce M, Seguella L, Lu J, Corpetti C, Del Re A, De Palma FDE, Esposito G, Sanseverino W, Sarnelli G. Engineered Lactobacillus paracasei Producing Palmitoylethanolamide (PEA) Prevents Colitis in Mice. Int J Mol Sci. 2021;22(6)

Faul F, Erdfelder E, Lang AG, Buchner A. G*Power 3: a flexible statistical power analysis program for the social, behavioral, and biomedical sciences. Behav Res Methods. 2007;39(2):175-91.

Fernandez J, de la Fuente VG, Garcia MTF, Sanchez JG, Redondo BI, Villar CJ, Lombo F. A diet based on cured acorn-fed ham with oleic acid content promotes anti-inflammatory gut microbiota and prevents ulcerative colitis in an animal model. Lipids Health Dis. 2020;19(1):28.

Flynn S, Eisenstein S. Inflammatory Bowel Disease Presentation and Diagnosis. Surgical Clinics of North America. 2019;99(6):1051-1062.

Gao R, Gao Z, Huang L, Qin H. Gut microbiota and colorectal cancer. Eur J Clin Microbiol Infect Dis. 2017;36(5):757-769.

Geboes K, Riddell R, Ost A, Jensfelt B, Persson T, Lofberg R. A reproducible grading scale for histological assessment of inflammation in ulcerative colitis. Gut. 2000;47(3):404-9.

Gensollen T, Iyer SS, Kasper DL, Blumberg RS. How colonization by microbiota in early life shapes the immune system. Science. 2016;352(6285):539-44.

Gerard CM, Mollereau C, Vassart G, Parmentier M. Molecular cloning of a human cannabinoid receptor which is also expressed in testis. Biochem J. 1991;279 (Pt 1):129-34.

Gevers D, Kugathasan S, Denson LA, Vazquez-Baeza Y, Van Treuren W, Ren B, Schwager E, Knights D, Song SJ, Yassour M, Morgan XC, Kostic AD, Luo C, Gonzalez A, McDonald D, Haberman Y, Walters T, Baker S, Rosh J, Stephens M, Heyman M, Markowitz J, Baldassano R, Griffiths A, Sylvester F, Mack D, Kim S, Crandall W, Hyams J, Huttenhower C, Knight R, Xavier RJ. The treatment-naive microbiome in new-onset Crohn's disease. Cell Host Microbe. 2014;15(3):382-392.

Grill M, Hogenauer C, Blesl A, Haybaeck J, Golob-Schwarzl N, Ferreiros N, Thomas D, Gurke R, Trotzmuller M, Kofeler HC, Galle B, Schicho R. Members of the endocannabinoid system are distinctly regulated in inflammatory bowel disease and colorectal cancer. Sci Rep. 2019;9(1):2358.

Grimm MC, Elsbury SK, Pavli P, Doe WF. Enhanced expression and production of monocyte chemoattractant protein-1 in inflammatory bowel disease mucosa. J Leukoc Biol. 1996;59(6):804-12.

Grivennikov SI, Cominelli F. Colitis-Associated and Sporadic Colon Cancers: Different Diseases, Different Mutations? Gastroenterology. 2016;150(4):808-10.

Gu Z, Zhu Y, Jiang S, Xia G, Li C, Zhang X, Zhang J, Shen X. Tilapia head glycolipids reduce inflammation by regulating the gut microbiota in dextran sulphate sodium-induced colitis mice. Food Funct. 2020;

Guida F, Boccella S, Iannotta M, De Gregorio D, Giordano C, Belardo C, Romano R, Palazzo E, Scafuro MA, Serra N, de Novellis V, Rossi F, Maione S, Luongo L. Palmitoylethanolamide Reduces Neuropsychiatric Behaviors by Restoring Cortical Electrophysiological Activity in a Mouse Model of Mild Traumatic Brain Injury. Front Pharmacol. 2017;8:95.

Guida F, Turco F, Iannotta M, De Gregorio D, Palumbo I, Sarnelli G, Furiano A, Napolitano F, Boccella S, Luongo L, Mazzitelli M, Usiello A, De Filippis F, Iannotti FA, Piscitelli F, Ercolini D, de Novellis V, Di Marzo V, Cuomo R, Maione S. Antibiotic-induced microbiota perturbation causes gut endocannabinoidome changes, hippocampal neuroglial reorganization and depression in mice. Brain Behav Immun. 2018;67:230-245.

Gulck T, Moller BL. Phytocannabinoids: Origins and Biosynthesis. Trends Plant Sci. 2020;25(10):985-1004.

Gulyas AI, Cravatt BF, Bracey MH, Dinh TP, Piomelli D, Boscia F, Freund TF. Segregation of two endocannabinoid-hydrolyzing enzymes into pre- and postsynaptic compartments in the rat hippocampus, cerebellum and amygdala. Eur J Neurosci. 2004;20(2):441-58.

Gustavsson B, Carlsson G, Machover D, Petrelli N, Roth A, Schmoll HJ, Tveit KM, Gibson F. A review of the evolution of systemic chemotherapy in the management of colorectal cancer. Clin Colorectal Cancer. 2015;14(1):1-10.

Haspula D, Clark MA. Cannabinoid Receptors: An Update on Cell Signaling, Pathophysiological Roles and Therapeutic Opportunities in Neurological, Cardiovascular, and Inflammatory Diseases. Int J Mol Sci. 2020;21(20)

Herkenham M, Lynn AB, Johnson MR, Melvin LS, de Costa BR, Rice KC. Characterization and localization of cannabinoid receptors in rat brain: a quantitative in vitro autoradiographic study. J Neurosci. 1991;11(2):563-83.

Hill AJ, Mercier MS, Hill TD, Glyn SE, Jones NA, Yamasaki Y, Futamura T, Duncan M, Stott CG, Stephens GJ, Williams CM, Whalley BJ. Cannabidivarin is anticonvulsant in mouse and rat. Br J Pharmacol. 2012;167(8):1629-42.

Howlett AC, Fleming RM. Cannabinoid inhibition of adenylate cyclase. Pharmacology of the response in neuroblastoma cell membranes. Mol Pharmacol. 1984;26(3):532-8.

Howlett AC, Barth F, Bonner TI, Cabral G, Casellas P, Devane WA, Felder CC, Herkenham M, Mackie K, Martin BR, Mechoulam R, Pertwee RG. International Union of Pharmacology. XXVII. Classification of cannabinoid receptors. Pharmacol Rev. 2002;54(2):161-202.

Hu S, Chen Y, Chen Y, Wang C. Depression and Anxiety Disorders in Patients With Inflammatory Bowel Disease. Front Psychiatry. 2021;12:714057.

Hua T, Li X, Wu L, Iliopoulos-Tsoutsouvas C, Wang Y, Wu M, Shen L, Brust CA, Nikas SP, Song F, Song X, Yuan S, Sun Q, Wu Y, Jiang S, Grim TW, Benchama O, Stahl EL, Zvonok N, Zhao S, Bohn LM, Makriyannis A, Liu ZJ. Activation and Signaling Mechanism Revealed by Cannabinoid Receptor-Gi Complex Structures. Cell. 2020;180(4):655-665 e18.

Huang PY, Yang YC, Wang CI, Hsiao PW, Chiang HI, Chen TW. Increase in Akkermansiaceae in Gut Microbiota of Prostate Cancer-Bearing Mice. Int J Mol Sci. 2021;22(17)

Ishida T, Nishiumi S, Tanahashi T, Yamasaki A, Yamazaki A, Akashi T, Miki I, Kondo Y, Inoue J, Kawauchi S, Azuma T, Yoshida M, Mizuno S. Linoleoyl ethanolamide reduces lipopolysaccharide-induced inflammation in macrophages

and ameliorates 2,4-dinitrofluorobenzene-induced contact dermatitis in mice. Eur J Pharmacol. 2013;699(1-3):6-13.

Issa CM, Hambly BD, Wang Y, Maleki S, Wang W, Fei J, Bao S. TRPV2 in the development of experimental colitis. Scand J Immunol. 2014;80(5):307-12.

Izzo AA, Borrelli F, Capasso R, Di Marzo V, Mechoulam R. Non-psychotropic plant cannabinoids: new therapeutic opportunities from an ancient herb. Trends Pharmacol Sci. 2009;30(10):515-27.

Izzo AA, Sharkey KA. Cannabinoids and the gut: new developments and emerging concepts. Pharmacol Ther. 2010;126(1):21-38.

Izzo AA, Muccioli GG, Ruggieri MR, Schicho R. Endocannabinoids and the Digestive Tract and Bladder in Health and Disease. Handb Exp Pharmacol. 2015;231:423-47.

Jamontt JM, Molleman A, Pertwee RG, Parsons ME. The effects of Delta-tetrahydrocannabinol and cannabidiol alone and in combination on damage, inflammation and in vitro motility disturbances in rat colitis. Br J Pharmacol. 2010;160(3):712-23.

Jeong DY, Kim S, Son MJ, Son CY, Kim JY, Kronbichler A, Lee KH, Shin JI. Induction and maintenance treatment of inflammatory bowel disease: A comprehensive review. Autoimmun Rev. 2019a;18(5):439-454.

Jeong S, Kim BG, Kim DY, Kim BR, Kim JL, Park SH, Na YJ, Jo MJ, Yun HK, Jeong YA, Kim HJ, Lee SI, Kim HD, Kim DH, Oh SC, Lee DH. Cannabidiol Overcomes Oxaliplatin Resistance by Enhancing NOS3- and SOD2-Induced Autophagy in Human Colorectal Cancer Cells. Cancers (Basel). 2019b;11(6)

Jeong S, Yun HK, Jeong YA, Jo MJ, Kang SH, Kim JL, Kim DY, Park SH, Kim BR, Na YJ, Lee SI, Kim HD, Kim DH, Oh SC, Lee DH. Cannabidiol-induced apoptosis is mediated by activation of Noxa in human colorectal cancer cells. Cancer Lett. 2019c;447:12-23.

Jin J. JAMA patient page. Inflammatory bowel disease. JAMA. 2014;311(19):2034.

Johnson M, Devane W, Howlett A, Melvin L, Milne G. Structural studies leading to the discovery of a cannabinoid binding site. NIDA Res Monogr. 1988;90:129-35.

Kafil TS, Nguyen TM, MacDonald JK, Chande N. Cannabis for the treatment of Crohn's disease. Cochrane Database Syst Rev. 2018a;11:CD012853.

Kafil TS, Nguyen TM, MacDonald JK, Chande N. Cannabis for the treatment of ulcerative colitis. Cochrane Database Syst Rev. 2018b;11:CD012954.

Kaplan GG, Ng SC. Understanding and Preventing the Global Increase of Inflammatory Bowel Disease. Gastroenterology. 2017;152(2):313-321 e2.

Kargl J, Haybaeck J, Stancic A, Andersen L, Marsche G, Heinemann A, Schicho R. O-1602, an atypical cannabinoid, inhibits tumor growth in colitis-associated colon cancer through multiple mechanisms. J Mol Med (Berl). 2013;91(4):449-58.

Kargl J, Andersen L, Hasenohrl C, Feuersinger D, Stancic A, Fauland A, Magnes C, El-Heliebi A, Lax S, Uranitsch S, Haybaeck J, Heinemann A, Schicho R. GPR55 promotes migration and adhesion of colon cancer cells indicating a role in metastasis. Br J Pharmacol. 2016;173(1):142-54.

Kienzl M, Storr M, Schicho R. Cannabinoids and Opioids in the Treatment of Inflammatory Bowel Diseases. Clin Transl Gastroenterol. 2020;11(1):e00120.

Kiesler P, Fuss IJ, Strober W. Experimental Models of Inflammatory Bowel Diseases. Cell Mol Gastroenterol Hepatol. 2015;1(2):154-170.

Kijpornyongpan T, Sereemaspun A, Chanchao C. Dose-dependent cytotoxic effects of menthol on human malignant melanoma A-375 cells: correlation with TRPM8 transcript expression. Asian Pac J Cancer Prev. 2014;15(4):1551-6.

Kilkenny C, Browne W, Cuthill IC, Emerson M, Altman DG, Group NCRRGW. Animal research: reporting in vivo experiments: the ARRIVE guidelines. Br J Pharmacol. 2010;160(7):1577-9.

Kirstein MM, Lange A, Prenzler A, Manns MP, Kubicka S, Vogel A. Targeted therapies in metastatic colorectal cancer: a systematic review and assessment of currently available data. Oncologist. 2014;19(11):1156-68.

Kis B, Ifrim FC, Buda V, Avram S, Pavel IZ, Antal D, Paunescu V, Dehelean CA, Ardelean F, Diaconeasa Z, Soica C, Danciu C. Cannabidiol-from Plant to Human Body: A Promising Bioactive Molecule with Multi-Target Effects in Cancer. Int J Mol Sci. 2019;20(23)

Kistner K, Siklosi N, Babes A, Khalil M, Selescu T, Zimmermann K, Wirtz S, Becker C, Neurath MF, Reeh PW, Engel MA. Systemic desensitization through TRPA1 channels by capsazepine and mustard oil - a novel strategy against inflammation and pain. Sci Rep. 2016;6:28621.

Kostic AD, Xavier RJ, Gevers D. The microbiome in inflammatory bowel disease: current status and the future ahead. Gastroenterology. 2014;146(6):1489-99.

Koveitypour Z, Panahi F, Vakilian M, Peymani M, Seyed Forootan F, Nasr Esfahani MH, Ghaedi K. Signaling pathways involved in colorectal cancer progression. Cell Biosci. 2019;9:97.

Krawisz JE, Sharon P, Stenson WF. Quantitative assay for acute intestinal inflammation based on myeloperoxidase activity. Assessment of inflammation in rat and hamster models. Gastroenterology. 1984;87(6):1344-50.

Kuhn KA, Schulz HM, Regner EH, Severs EL, Hendrickson JD, Mehta G, Whitney AK, Ir D, Ohri N, Robertson CE, Frank DN, Campbell EL, Colgan SP. Bacteroidales recruit IL-6-producing intraepithelial lymphocytes in the colon to promote barrier integrity. Mucosal Immunol. 2018;11(2):357-368.

Kun J, Szitter I, Kemeny A, Perkecz A, Kereskai L, Pohoczky K, Vincze A, Godi S, Szabo I, Szolcsanyi J, Pinter E, Helyes Z. Upregulation of the transient receptor potential ankyrin 1 ion channel in the inflamed human and mouse colon and its protective roles. PLoS One. 2014;9(9):e108164.

Lama A, Provensi G, Amoriello R, Pirozzi C, Rani B, Mollica MP, Raso GM, Ballerini C, Meli R, Passani MB. The anti-inflammatory and immune-modulatory effects of OEA limit DSS-induced colitis in mice. Biomed Pharmacother. 2020;129:110368.

Lao VV, Grady WM. Epigenetics and colorectal cancer. Nat Rev Gastroenterol Hepatol. 2011;8(12):686-700.

Lazzerini M, Villanacci V, Pellegrin MC, Martelossi S, Magazzu G, Pellegrino S, Lucanto MC, Barabino A, Calvi A, Arrigo S, Lionetti P, Fontana M, Zuin G, Maggiore G, Bramuzzo M, Maschio M, Salemme M, Manenti S, Lorenzi L, Decorti G, Montico M, Ventura A. Endoscopic and Histologic Healing in Children With Inflammatory Bowel Diseases Treated With Thalidomide. Clin Gastroenterol Hepatol. 2017;15(9):1382-1389 e1.

Lee Y, Jo J, Chung HY, Pothoulakis C, Im E. Endocannabinoids in the gastrointestinal tract. Am J Physiol Gastrointest Liver Physiol. 2016;311(4):G655-G666.

Lees CW, Barrett JC, Parkes M, Satsangi J. New IBD genetics: common pathways with other diseases. Gut. 2011;60(12):1739-53.

Levine A. Pediatric inflammatory bowel disease: is it different? Dig Dis. 2009;27(3):212-4.

Li Q, Wang X, Yang Z, Wang B, Li S. Menthol induces cell death via the TRPM8 channel in the human bladder cancer cell line T24. Oncology. 2009;77(6):335-41.

Li S, Fu C, Zhao Y, He J. Intervention with alpha-Ketoglutarate Ameliorates Colitis-Related Colorectal Carcinoma via Modulation of the Gut Microbiome. Biomed Res Int. 2019;2019:8020785.

Liu JJ, Li LZ, Xu P. Upregulation of TRPM8 can promote the colon cancer liver metastasis through mediating Akt/GSK-3 signal pathway. Biotechnol Appl Biochem. 2021;

Louis P, Flint HJ. Diversity, metabolism and microbial ecology of butyrate-producing bacteria from the human large intestine. FEMS Microbiol Lett. 2009;294(1):1-8.

Lozupone CA, Stombaugh JI, Gordon JI, Jansson JK, Knight R. Diversity, stability and resilience of the human gut microbiota. Nature. 2012;489(7415):220-30.

Lucas C, Barnich N, Nguyen HTT. Microbiota, Inflammation and Colorectal Cancer. Int J Mol Sci. 2017;18(6)

Lynch HT, de la Chapelle A. Hereditary colorectal cancer. N Engl J Med. 2003;348(10):919-32.

Mackie K. Cannabinoid receptors: where they are and what they do. J Neuroendocrinol. 2008;20 Suppl 1:10-4.

Mak WY, Zhao M, Ng SC, Burisch J. The epidemiology of inflammatory bowel disease: East meets west. J Gastroenterol Hepatol. 2020;35(3):380-389.

Malaty HM, Fan X, Opekun AR, Thibodeaux C, Ferry GD. Rising incidence of inflammatory bowel disease among children: a 12-year study. J Pediatr Gastroenterol Nutr. 2010;50(1):27-31.

Malvezzi M, Carioli G, Bertuccio P, Boffetta P, Levi F, La Vecchia C, Negri E. European cancer mortality predictions for the year 2018 with focus on colorectal cancer. Ann Oncol. 2018;29(4):1016-1022.

Manca C, Boubertakh B, Leblanc N, Deschenes T, Lacroix S, Martin C, Houde A, Veilleux A, Flamand N, Muccioli GG, Raymond F, Cani PD, Di Marzo V, Silvestri C. Germ-free mice exhibit profound gut microbiota-dependent alterations of intestinal endocannabinoidome signaling. J Lipid Res. 2020;61(1):70-85.

Manichanh C, Borruel N, Casellas F, Guarner F. The gut microbiota in IBD. Nat Rev Gastroenterol Hepatol. 2012;9(10):599-608.

Mariat D, Firmesse O, Levenez F, Guimaraes V, Sokol H, Dore J, Corthier G, Furet JP. The Firmicutes/Bacteroidetes ratio of the human microbiota changes with age. BMC Microbiol. 2009;9:123.

Marley AR, Nan H. Epidemiology of colorectal cancer. Int J Mol Epidemiol Genet. 2016;7(3):105-114.

Martinez V, Iriondo De-Hond A, Borrelli F, Capasso R, Del Castillo MD, Abalo R. Cannabidiol and Other Non-Psychoactive Cannabinoids for Prevention and Treatment of Gastrointestinal Disorders: Useful Nutraceuticals? Int J Mol Sci. 2020;21(9)

Marton LT, Goulart RA, Carvalho ACA, Barbalho SM. Omega Fatty Acids and Inflammatory Bowel Diseases: An Overview. Int J Mol Sci. 2019;20(19)

Matsuda LA, Lolait SJ, Brownstein MJ, Young AC, Bonner TI. Structure of a cannabinoid receptor and functional expression of the cloned cDNA. Nature. 1990;346(6284):561-4.

McGrath JC, Lilley E. Implementing guidelines on reporting research using animals (ARRIVE etc.): new requirements for publication in BJP. Br J Pharmacol. 2015;172(13):3189-93.

Mechoulam R, Ben-Shabat S, Hanus L, Ligumsky M, Kaminski NE, Schatz AR, Gopher A, Almog S, Martin BR, Compton DR, et al. Identification of an endogenous 2-monoglyceride, present in canine gut, that binds to cannabinoid receptors. Biochem Pharmacol. 1995;50(1):83-90.

Mechoulam R. Looking back at Cannabis research. Curr Pharm Des. 2000;6(13):1313-22.

Mody K, Baldeo C, Bekaii-Saab T. Antiangiogenic Therapy in Colorectal Cancer. Cancer J. 2018;24(4):165-170.

Morales P, Hurst DP, Reggio PH. Molecular Targets of the Phytocannabinoids: A Complex Picture. Prog Chem Org Nat Prod. 2017;103:103-131.

Morampudi V, Bhinder G, Wu X, Dai C, Sham HP, Vallance BA, Jacobson K. DNBS/TNBS colitis models: providing insights into inflammatory bowel disease and effects of dietary fat. J Vis Exp. 2014;(84):e51297.

Morgan XC, Tickle TL, Sokol H, Gevers D, Devaney KL, Ward DV, Reyes JA, Shah SA, LeLeiko N, Snapper SB, Bousvaros A, Korzenik J, Sands BE, Xavier RJ, Huttenhower C. Dysfunction of the intestinal microbiome in inflammatory bowel disease and treatment. Genome Biol. 2012;13(9):R79.

Morrison DJ, Preston T. Formation of short chain fatty acids by the gut microbiota and their impact on human metabolism. Gut Microbes. 2016;7(3):189-200.

Munro S, Thomas KL, Abu-Shaar M. Molecular characterization of a peripheral receptor for cannabinoids. Nature. 1993;365(6441):61-5.

Naftali T, Bar-Lev Schleider L, Almog S, Meiri D, Konikoff FM. Oral CBD-rich Cannabis Induces Clinical but Not Endoscopic Response in Patients with Crohn's Disease, a Randomised Controlled Trial. J Crohns Colitis. 2021;15(11):1799-1806.

Nardone G, Compare D. The human gastric microbiota: Is it time to rethink the pathogenesis of stomach diseases? United European Gastroenterol J. 2015;3(3):255-60.

Nishida A, Inoue R, Inatomi O, Bamba S, Naito Y, Andoh A. Gut microbiota in the pathogenesis of inflammatory bowel disease. Clin J Gastroenterol. 2018;11(1):1-10.

Nishiyama Y, Kataoka T, Yamato K, Taguchi T, Yamaoka K. Suppression of dextran sulfate sodium-induced colitis in mice by radon inhalation. Mediators Inflamm. 2012;2012:239617.

Okamoto Y, Ohkubo T, Ikebe T, Yamazaki J. Blockade of TRPM8 activity reduces the invasion potential of oral squamous carcinoma cell lines. Int J Oncol. 2012;40(5):1431-40.

Oresta B, Braga D, Lazzeri M, Frego N, Saita A, Faccani C, Fasulo V, Colombo P, Guazzoni G, Hurle R, Rescigno M. The Microbiome of Catheter Collected Urine in Males with Bladder Cancer According to Disease Stage. J Urol. 2020:101097JU0000000000001336.

Otagiri S, Ohnishi S, Ohara M, Fu Q, Yamamoto K, Yamamoto K, Katsurada T, Sakamoto N. Oleoylethanolamide Ameliorates Dextran Sulfate Sodium-Induced Colitis in Rats. Front Pharmacol. 2020;11:1277.

Pacheco AR, Barile D, Underwood MA, Mills DA. The impact of the milk glycobiome on the neonate gut microbiota. Annu Rev Anim Biosci. 2015;3:419-45.

Pagano E, Capasso R, Piscitelli F, Romano B, Parisi OA, Finizio S, Lauritano A, Marzo VD, Izzo AA, Borrelli F. An Orally Active Cannabis Extract with High Content in Cannabidiol attenuates Chemically-induced Intestinal Inflammation and Hypermotility in the Mouse. Front Pharmacol. 2016;7:341.

Pagano E, Borrelli F, Orlando P, Romano B, Monti M, Morbidelli L, Aviello G, Imperatore R, Capasso R, Piscitelli F, Buono L, Di Marzo V, Izzo AA. Pharmacological inhibition of MAGL attenuates experimental colon carcinogenesis. Pharmacol Res. 2017;119:227-236.

Pagano E, Romano B, Iannotti FA, Parisi OA, D'Armiento M, Pignatiello S, Coretti L, Lucafo M, Venneri T, Stocco G, Lembo F, Orlando P, Capasso R, Di Marzo V, Izzo AA, Borrelli F. The non-euphoric phytocannabinoid cannabidivarin counteracts intestinal inflammation in mice and cytokine expression in biopsies from UC pediatric patients. Pharmacol Res. 2019;149:104464.

Pagano E, Venneri T, Lucariello G, Cicia D, Brancaleone V, Nani MF, Cacciola NA, Capasso R, Izzo AA, Borrelli F, Romano B. Palmitoylethanolamide Reduces Colon Cancer Cell Proliferation and Migration, Influences Tumor Cell Cycle and Exerts In Vivo Chemopreventive Effects. Cancers (Basel). 2021;13(8)

Paulson JN, Stine OC, Bravo HC, Pop M. Differential abundance analysis for microbial marker-gene surveys. Nat Methods. 2013;10(12):1200-2.

Pereira LM, Lima-Junior RC, Bem AX, Teixeira CG, Grassi LS, Medeiros RP, Marques-Neto RD, Callado RB, Aragao KS, Wong DV, Vale ML, Brito GA, Ribeiro RA. Blockade of TRPA1 with HC-030031 attenuates visceral nociception by a mechanism independent of inflammatory resident cells, nitric oxide and the opioid system. Eur J Pain. 2013;17(2):223-33.

Pertwee RG. Cannabinoid pharmacology: the first 66 years. Br J Pharmacol. 2006;147 Suppl 1:S163-71.

Pertwee RG. Endocannabinoids and Their Pharmacological Actions. Handb Exp Pharmacol. 2015;231:1-37.

Petito V, Lopetuso LR, Arena V, Stigliano E, Boninsegna A, Bibbo S, Poscia A, Alfieri S, Rosa F, Amato A, Cammarota G, Papa A, Sgambato A, Gasbarrini A, Scaldaferri F. Direct effect of infliximab on intestinal mucosa sustains mucosal healing: exploring new mechanisms of action. Dig Liver Dis. 2016;48(4):391-8.

Piovani D, Danese S, Peyrin-Biroulet L, Nikolopoulos GK, Lytras T, Bonovas S. Environmental Risk Factors for Inflammatory Bowel Diseases: An Umbrella Review of Meta-analyses. Gastroenterology. 2019;157(3):647-659 e4.

Piscitelli F, Pagano E, Lauritano A, Izzo AA, Di Marzo V. Development of a Rapid LC-MS/MS Method for the Quantification of Cannabidiol, Cannabidivarin, Delta(9)-Tetrahydrocannabivarin, and Cannabigerol in Mouse Peripheral Tissues. Anal Chem. 2017;89(8):4749-4755.

Pithadia AB, Jain S. Treatment of inflammatory bowel disease (IBD). Pharmacol Rep. 2011;63(3):629-42.

Pittayanon R, Lau JT, Leontiadis GI, Tse F, Yuan Y, Surette M, Moayyedi P. Differences in Gut Microbiota in Patients With vs Without Inflammatory Bowel Diseases: A Systematic Review. Gastroenterology. 2020;158(4):930-946 e1.

Qin J, Li R, Raes J, Arumugam M, Burgdorf KS, Manichanh C, Nielsen T, Pons N, Levenez F, Yamada T, Mende DR, Li J, Xu J, Li S, Li D, Cao J, Wang B, Liang H, Zheng H, Xie Y, Tap J, Lepage P, Bertalan M, Batto JM, Hansen T, Le Paslier D, Linneberg A, Nielsen HB, Pelletier E, Renault P, Sicheritz-Ponten T, Turner K, Zhu H, Yu C, Li S, Jian M, Zhou Y, Li Y, Zhang X, Li S, Qin N, Yang H, Wang J, Brunak S, Dore J, Guarner F, Kristiansen K, Pedersen O, Parkhill J, Weissenbach J, Meta HITC, Bork P, Ehrlich SD, Wang J. A human gut microbial gene catalogue established by metagenomic sequencing. Nature. 2010;464(7285):59-65.

Rausch P, Ruhlemann M, Hermes BM, Doms S, Dagan T, Dierking K, Domin H, Fraune S, von Frieling J, Hentschel U, Heinsen FA, Hoppner M, Jahn MT, Jaspers C, Kissoyan KAB, Langfeldt D, Rehman A, Reusch TBH, Roeder T, Schmitz RA, Schulenburg H, Soluch R, Sommer F, Stukenbrock E, Weiland-Brauer N, Rosenstiel P, Franke A, Bosch T, Baines JF. Comparative analysis of amplicon and metagenomic sequencing methods reveals key features in the evolution of animal metaorganisms. Microbiome. 2019;7(1):133.

Romano B, Borrelli F, Fasolino I, Capasso R, Piscitelli F, Cascio M, Pertwee R, Coppola D, Vassallo L, Orlando P, Di Marzo V, Izzo A. The cannabinoid TRPA1

agonist cannabichromene inhibits nitric oxide production in macrophages and ameliorates murine colitis. Br J Pharmacol. 2013;169(1):213-29.

Romano B, Borrelli F, Pagano E, Cascio MG, Pertwee RG, Izzo AA. Inhibition of colon carcinogenesis by a standardized Cannabis sativa extract with high content of cannabidiol. Phytomedicine. 2014;21(5):631-9.

Romano B, Pagano E, Iannotti FA, Piscitelli F, Brancaleone V, Lucariello G, Nani MF, Fiorino F, Sparaco R, Vanacore G, Di Tella F, Cicia D, Lionetti R, Makriyannis A, Malamas M, De Luca M, Aprea G, D'Armiento M, Capasso R, Sbarro B, Venneri T, Di Marzo V, Borrelli F, Izzo AA. N-Acylethanolamine acid amidase (NAAA) is dysregulated in colorectal cancer patients and its inhibition reduces experimental cancer growth. Br J Pharmacol. 2021;

Rouzer CA, Marnett LJ. Endocannabinoid oxygenation by cyclooxygenases, lipoxygenases, and cytochromes P450: cross-talk between the eicosanoid and endocannabinoid signaling pathways. Chem Rev. 2011;111(10):5899-921.

Rustgi AK. The genetics of hereditary colon cancer. Genes Dev. 2007;21(20):2525-38.

Santoru ML, Piras C, Murgia A, Palmas V, Camboni T, Liggi S, Ibba I, Lai MA, Orru S, Blois S, Loizedda AL, Griffin JL, Usai P, Caboni P, Atzori L, Manzin A. Cross sectional evaluation of the gut-microbiome metabolome axis in an Italian cohort of IBD patients. Sci Rep. 2017;7(1):9523.

Schicho R, Storr M. Topical and systemic cannabidiol improves trinitrobenzene sulfonic acid colitis in mice. Pharmacology. 2012;89(3-4):149-55.

Schmieder R, Edwards R. Quality control and preprocessing of metagenomic datasets. Bioinformatics. 2011;27(6):863-4.

Sears CL, Pardoll DM. Perspective: alpha-bugs, their microbial partners, and the link to colon cancer. J Infect Dis. 2011;203(3):306-11.

Selmin OI, Papoutsis AJ, Hazan S, Smith C, Greenfield N, Donovan MG, Wren SN, Doetschman TC, Snider JM, Snider AJ, Chow SH, Romagnolo DF. n-6 High Fat Diet Induces Gut Microbiome Dysbiosis and Colonic Inflammation. Int J Mol Sci. 2021;22(13)

Seregin SS, Golovchenko N, Schaf B, Chen J, Pudlo NA, Mitchell J, Baxter NT, Zhao L, Schloss PD, Martens EC, Eaton KA, Chen GY. NLRP6 Protects Il10(-/-) Mice from Colitis by Limiting Colonization of Akkermansia muciniphila. Cell Rep. 2017;19(4):733-745.

Shamran H, Singh NP, Zumbrun EE, Murphy A, Taub DD, Mishra MK, Price RL, Chatterjee S, Nagarkatti M, Nagarkatti PS, Singh UP. Fatty acid amide hydrolase (FAAH) blockade ameliorates experimental colitis by altering microRNA expression and suppressing inflammation. Brain Behav Immun. 2017;59:10-20.

Shen M, Manca C, Suriano F, Nallabelli N, Pechereau F, Allam-Ndoul B, Iannotti FA, Flamand N, Veilleux A, Cani PD, Silvestri C, Di Marzo V. Three of a Kind: Control of the Expression of Liver-Expressed Antimicrobial Peptide 2 (LEAP2) by the Endocannabinoidome and the Gut Microbiome. Molecules. 2021;27(1)

Siegel RL, Miller KD, Fuchs HE, Jemal A. Cancer Statistics, 2021. CA Cancer J Clin. 2021;71(1):7-33.

Sihag J, Di Marzo V. (Wh)olistic (E)ndocannabinoidome-Microbiome-Axis Modulation through (N)utrition (WHEN) to Curb Obesity and Related Disorders. Lipids Health Dis. 2022;21(1):9.

Song H, Wang W, Shen B, Jia H, Hou Z, Chen P, Sun Y. Pretreatment with probiotic Bifico ameliorates colitis-associated cancer in mice: Transcriptome and gut flora profiling. Cancer Sci. 2018;109(3):666-677.

Song M, Chan AT, Sun J. Influence of the Gut Microbiome, Diet, and Environment on Risk of Colorectal Cancer. Gastroenterology. 2020;158(2):322-340.

Stancic A, Jandl K, Hasenohrl C, Reichmann F, Marsche G, Schuligoi R, Heinemann A, Storr M, Schicho R. The GPR55 antagonist CID16020046 protects against intestinal inflammation. Neurogastroenterol Motil. 2015;27(10):1432-45.

Sugiura T, Kondo S, Sukagawa A, Nakane S, Shinoda A, Itoh K, Yamashita A, Waku K. 2-Arachidonoylglycerol: a possible endogenous cannabinoid receptor ligand in brain. Biochem Biophys Res Commun. 1995;215(1):89-97.

Sultan S, El-Mowafy M, Elgaml A, Ahmed TAE, Hassan H, Mottawea W. Metabolic Influences of Gut Microbiota Dysbiosis on Inflammatory Bowel Disease. Front Physiol. 2021;12:715506.

Thanikachalam K, Khan G. Colorectal Cancer and Nutrition. Nutrients. 2019;11(1)

Tilg H, Adolph TE, Gerner RR, Moschen AR. The Intestinal Microbiota in Colorectal Cancer. Cancer Cell. 2018;33(6):954-964.

Tinto F, Archambault AS, Dumais E, Rakotoarivelo V, Kostrzewa M, Martin C, Plante PL, Desjardins Y, Simard M, Pouliot R, De Petrocellis L, Ligresti A, Di Marzo V, Flamand N. Synthesis and molecular targets of N-13-hydroxy-octadienoyl-ethanolamine, a novel endogenous bioactive 15-lipoxygenase-derived metabolite of N-linoleoyl-ethanolamine found in the skin and saliva. Biochim Biophys Acta Mol Cell Biol Lipids. 2021;1866(8):158954.

Tjalsma H, Boleij A, Marchesi JR, Dutilh BE. A bacterial driver-passenger model for colorectal cancer: beyond the usual suspects. Nat Rev Microbiol. 2012;10(8):575-82.

Tsuboi K, Zhao LY, Okamoto Y, Araki N, Ueno M, Sakamoto H, Ueda N. Predominant expression of lysosomal N-acylethanolamine-hydrolyzing acid amidase in macrophages revealed by immunochemical studies. Biochim Biophys Acta. 2007;1771(5):623-32.

Turcotte C, Chouinard F, Lefebvre JS, Flamand N. Regulation of inflammation by cannabinoids, the endocannabinoids 2-arachidonoyl-glycerol and arachidonoyl-ethanolamide, and their metabolites. J Leukoc Biol. 2015;97(6):1049-70.

Tutino V, Caruso MG, De Nunzio V, Lorusso D, Veronese N, Gigante I, Notarnicola M, Giannelli G. Down-Regulation of Cannabinoid Type 1 (CB1) Receptor and its Downstream Signaling Pathways in Metastatic Colorectal Cancer. Cancers (Basel). 2019;11(5)

Ueda N, Tsuboi K, Uyama T. Metabolism of endocannabinoids and related N-acylethanolamines: canonical and alternative pathways. FEBS J. 2013;280(9):1874-94.

Velasco G, Sanchez C, Guzman M. Towards the use of cannabinoids as antitumour agents. Nat Rev Cancer. 2012;12(6):436-44.

Vermeulen W, De Man JG, De Schepper HU, Bult H, Moreels TG, Pelckmans PA, De Winter BY. Role of TRPV1 and TRPA1 in visceral hypersensitivity to colorectal distension during experimental colitis in rats. Eur J Pharmacol. 2013;698(1-3):404-12.

Vital M, Karch A, Pieper DH. Colonic Butyrate-Producing Communities in Humans: an Overview Using Omics Data. mSystems. 2017;2(6)

Wang F, Cai K, Xiao Q, He L, Xie L, Liu Z. Akkermansia muciniphila administration exacerbated the development of colitis-associated colorectal cancer in mice. J Cancer. 2022;13(1):124-133.

Wang L, Yin G, Guo Y, Zhao Y, Zhao M, Lai Y, Sui P, Shi T, Guo W, Huang Z. Variations in Oral Microbiota Composition Are Associated With a Risk of Throat Cancer. Front Cell Infect Microbiol. 2019;9:205.

Wang Q, Wang K, Wu W, Lv L, Bian X, Yang L, Wang Q, Li Y, Ye J, Fang D, Wu J, Jiang X, Xie J, Lu Y, Li L. Administration of Bifidobacterium bifidum CGMCC 15068 modulates gut microbiota and metabolome in azoxymethane (AOM)/dextran sulphate sodium (DSS)-induced colitis-associated colon cancer (CAC) in mice. Appl Microbiol Biotechnol. 2020;104(13):5915-5928.

Wasilewski A, Krajewska U, Owczarek K, Lewandowska U, Fichna J. Fatty acid amide hydrolase (FAAH) inhibitor PF-3845 reduces viability, migration and invasiveness of human colon adenocarcinoma Colo-205 cell line: an in vitro study. Acta Biochim Pol. 2017;64(3):519-525.

Watanabe T, Konishi T, Kishimoto J, Kotake K, Muto T, Sugihara K, Japanese Society for Cancer of the C, Rectum. Ulcerative colitis-associated colorectal cancer shows a poorer survival than sporadic colorectal cancer: a nationwide Japanese study. Inflamm Bowel Dis. 2011;17(3):802-8.

Wei D, Xie L, Zhuang Z, Zhao N, Huang B, Tang Y, Yu S, Zhou Q, Wu Q. Gut Microbiota: A New Strategy to Study the Mechanism of Electroacupuncture and Moxibustion in Treating Ulcerative Colitis. Evid Based Complement Alternat Med. 2019;2019:9730176.

Weir TL, Manter DK, Sheflin AM, Barnett BA, Heuberger AL, Ryan EP. Stool microbiome and metabolome differences between colorectal cancer patients and healthy adults. PLoS One. 2013;8(8):e70803.

West NR, McCuaig S, Franchini F, Powrie F. Emerging cytokine networks in colorectal cancer. Nat Rev Immunol. 2015;15(10):615-29.

Wlodarczyk M, Sobolewska-Wlodarczyk A, Cygankiewicz AI, Jacenik D, Krajewska WM, Stec-Michalska K, Piechota-Polanczyk A, Wisniewska-Jarosinska M, Fichna J. G protein-coupled receptor 55 (GPR55) expresses differently in patients with Crohn's disease and ulcerative colitis. Scand J Gastroenterol. 2017;52(6-7):711-715.

Wong MCS, Huang J, Lok V, Wang J, Fung F, Ding H, Zheng ZJ. Differences in Incidence and Mortality Trends of Colorectal Cancer Worldwide Based on Sex, Age, and Anatomic Location. Clin Gastroenterol Hepatol. 2021;19(5):955-966 e61.

Wu M, Li P, An Y, Ren J, Yan D, Cui J, Li D, Li M, Wang M, Zhong G. Phloretin ameliorates dextran sulfate sodium-induced ulcerative colitis in mice by regulating the gut microbiota. Pharmacol Res. 2019a;150:104489.

Wu TR, Lin CS, Chang CJ, Lin TL, Martel J, Ko YF, Ojcius DM, Lu CC, Young JD, Lai HC. Gut commensal Parabacteroides goldsteinii plays a predominant role in the anti-obesity effects of polysaccharides isolated from Hirsutella sinensis. Gut. 2019b;68(2):248-262.

Xu Q, Kong N, Zhang J, Bai N, Bi J, Li W. Expression of transient receptor potential cation channel subfamily M member 8 in gastric cancer and its clinical significance. Exp Ther Med. 2021a;21(4):377.

Xu Y, Xie L, Zhang Z, Zhang W, Tang J, He X, Zhou J, Peng W. Tremella fuciformis Polysaccharides Inhibited Colonic Inflammation in Dextran Sulfate Sodium-Treated Mice via Foxp3+ T Cells, Gut Microbiota, and Bacterial Metabolites. Front Immunol. 2021b;12:648162.

Yang J, Yang H. Effect of Bifidobacterium breve in Combination With Different Antibiotics on Clostridium difficile. Front Microbiol. 2018;9:2953.

Yang Y, Cai Q, Shu XO, Steinwandel MD, Blot WJ, Zheng W, Long J. Prospective study of oral microbiome and colorectal cancer risk in low-income and African American populations. Int J Cancer. 2019;144(10):2381-2389.

Yang Y, Gharaibeh RZ, Newsome RC, Jobin C. Amending microbiota by targeting intestinal inflammation with TNF blockade attenuates development of colorectal cancer. Nature Cancer. 2020;1(7):723-734.

Yao H, Shi Y, Yuan J, Sa R, Chen W, Wan X. Matrine protects against DSS-induced murine colitis by improving gut barrier integrity, inhibiting the PPAR-alpha signaling pathway, and modulating gut microbiota. Int Immunopharmacol. 2021;100:108091.

Yee NS, Chan AS, Yee JD, Yee RK. TRPM7 and TRPM8 Ion Channels in Pancreatic Adenocarcinoma: Potential Roles as Cancer Biomarkers and Targets. Scientifica (Cairo). 2012;2012:415158.

Yee NS. Roles of TRPM8 Ion Channels in Cancer: Proliferation, Survival, and Invasion. Cancers (Basel). 2015;7(4):2134-46.

Youssef O, Lahti L, Kokkola A, Karla T, Tikkanen M, Ehsan H, Carpelan-Holmstrom M, Koskensalo S, Bohling T, Rautelin H, Puolakkainen P, Knuutila S, Sarhadi V. Stool Microbiota Composition Differs in Patients with Stomach, Colon, and Rectal Neoplasms. Dig Dis Sci. 2018;63(11):2950-2958.

Yu AI, Zhao L, Eaton KA, Ho S, Chen J, Poe S, Becker J, Gonzalez A, McKinstry D, Hasso M, Mendoza-Castrejon J, Whitfield J, Koumpouras C, Schloss PD, Martens EC, Chen GY. Gut Microbiota Modulate CD8 T Cell Responses to Influence Colitis-Associated Tumorigenesis. Cell Rep. 2020;31(1):107471.

Yu YN, Fang JY. Gut Microbiota and Colorectal Cancer. Gastrointest Tumors. 2015;2(1):26-32.

Zhai R, Xue X, Zhang L, Yang X, Zhao L, Zhang C. Strain-Specific Anti-inflammatory Properties of Two Akkermansia muciniphila Strains on Chronic Colitis in Mice. Front Cell Infect Microbiol. 2019a;9:239.

Zhai Z, Zhang F, Cao R, Ni X, Xin Z, Deng J, Wu G, Ren W, Yin Y, Deng B. Cecropin A Alleviates Inflammation Through Modulating the Gut Microbiota of C57BL/6 Mice With DSS-Induced IBD. Front Microbiol. 2019b;10:1595.

Zhang H, Zhang Z, Song G, Tang X, Song H, Deng A, Wang W, Wu L, Qin H. Development of an XBP1 agonist, HLJ2, as a potential therapeutic agent for ulcerative colitis. Eur J Pharm Sci. 2017;109:56-64.

Zhang L, Barritt GJ. Evidence that TRPM8 is an androgen-dependent Ca2+ channel required for the survival of prostate cancer cells. Cancer Res. 2004;64(22):8365-73.

Zhang L, Barritt GJ. TRPM8 in prostate cancer cells: a potential diagnostic and prognostic marker with a secretory function? Endocr Relat Cancer. 2006;13(1):27-38.

Zhang T, Li Q, Cheng L, Buch H, Zhang F. Akkermansia muciniphila is a promising probiotic. Microb Biotechnol. 2019;12(6):1109-1125.

Zhang YZ, Li YY. Inflammatory bowel disease: pathogenesis. World J Gastroenterol. 2014;20(1):91-9.

Zhu W, Gao Y, Wan J, Lan X, Han X, Zhu S, Zang W, Chen X, Ziai W, Hanley DF, Russo SJ, Jorge RE, Wang J. Changes in motor function, cognition, and emotion-related behavior after right hemispheric intracerebral hemorrhage in various brain regions of mouse. Brain Behav Immun. 2018;69:568-581.

Zhu Y, Tang RK, Zhao P, Zhu SS, Li YG, Li JB. Can oral 5-aminosalicylic acid be administered once daily in the treatment of mild-to-moderate ulcerative colitis? A meta-analysis of randomized-controlled trials. Eur J Gastroenterol Hepatol. 2012;24(5):487-94.

Zou S, Kumar U. Cannabinoid Receptors and the Endocannabinoid System: Signaling and Function in the Central Nervous System. Int J Mol Sci. 2018;19(3)

Zou S, Fang L, Lee MH. Dysbiosis of gut microbiota in promoting the development of colorectal cancer. Gastroenterol Rep (Oxf). 2018;6(1):1-12.